UNIVERSIDADE FEDERAL DE SANTA CATARINA
CENTRO TECNOLÓGICO
PROGRAMA DE PÓS-GRADUAÇÃO EM ENGENHARIA QUÍMICA

Jéssica Mulinari

Lipase immobilization on α-alumina membrane for oil fouling control and self-cleaning properties

Florianópolis
2023

Jéssica Mulinari

Lipase immobilization on α-alumina membrane for oil fouling control and self-cleaning properties

Tese submetida ao Programa de Pós-Graduação em Engenharia Química da Universidade Federal de Santa Catarina como requisito parcial para a obtenção do título de Doutora em Engenharia Química.

Orientador: Prof. J. Vladimir Oliveira, Dr.
Coorientadores: Prof. Dachamir Hotza, Dr.
Profa. Qilin Li, Dra.

Florianópolis
2023

Mulinari, Jéssica
Lipase immobilization on ?-alumina membrane for oil fouling control and self-cleaning properties / Jéssica Mulinari ; orientador, José Vladimir de Oliveira, coorientador, Dachamir Hotza, coorientadora, Qilin Li, 2023.
155 p.

Tese (doutorado) - Universidade Federal de Santa Catarina, Centro Tecnológico, Programa de Pós-Graduação em Engenharia Química, Florianópolis, 2023.

Inclui referências.

1. Engenharia Química. 2. Enzyme immobilization. 3. Membrane separation processes. 4. Fouling control. 5. Membrane cleaning. I. Oliveira, José Vladimir de. II. Hotza, Dachamir. III. Li, Qilin IV. Universidade Federal de Santa Catarina. Programa de Pós-Graduação em Engenharia Química. V. Título.

Jéssica Mulinari

Lipase immobilization on α-alumina membrane for oil fouling control and self-cleaning properties

O presente trabalho em nível de Doutorado foi avaliado e aprovado, em 20 de janeiro de 2023, pela banca examinadora composta pelos seguintes membros:

Profa. Isabel Cristina Tessaro, Dra.
Universidade Federal do Rio Grande do Sul

Prof. Cristiano José de Andrade, Dr.
Universidade Federal de Santa Catarina

Guilherme Zin, Dr.
TransferTech Gestão da Inovação

Certificamos que esta é a versão original e final do trabalho de conclusão que foi julgado adequado para obtenção do título de Doutora em Engenharia Química.

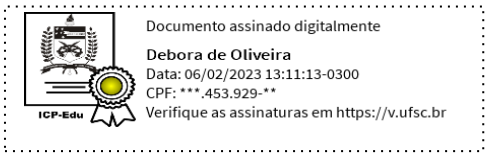

Coordenação do Programa de Pós-Graduação

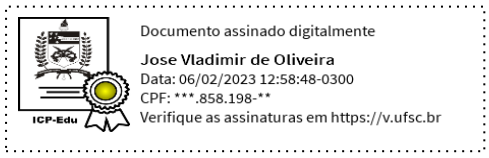

Prof. J. Vladimir de Oliveira, Dr.
Orientador

Florianópolis, 2023.

Aos meus pais, pelo amor, suporte e incentivo.

Aos mestres, por serem exemplo e guiarem o caminho.

AGRADECIMENTOS

Aos meus pais, Maria Ines e Alcemir, e à minha vó, Nilda, por todo amor e apoio para que eu pudesse realizar mais esse sonho. Amo vocês!

Ao meu noivo, Franscisco, pelo amor, companheirismo, cumplicidade e compreensão. Te amo!

Aos professores orientadores oficiais, Prof. Dr. J. Vladimir de Oliveira e Prof. Dr. Dachamir Hotza, por todo suporte e incentivo, e por abrirem portas a excelentes oportunidades. To Dr. Qilin Li, for all the valuable advice and for having me in your group, it was an amazing experience!

Aos professores orientadores não-oficiais, mas não menos importantes, Prof. Dr. Marco Di Luccio e Prof. Dr. Alan Ambrosi, por todo auxilio e por estarem sempre dispostos a ajudar e compartilhar conhecimento.

Aos meus amigos, pelos momentos de descontração, amizade e companheirismo. De modo especial ao Carlos, Éllen, Lisandro, Afonso e Mirele que fizeram uma pandemia ser mais leve, à Monique e Regilene, pelo companheirismo de sempre, ao Bruno e Rueliton, que mesmo longe estiveram sempre presentes, e à Tamires e Carla, que fizeram Houston ser casa.

Aos colegas e amigos do LABSEM, pela colaboração, ajuda e bons momentos compartilhados.

To all the amazing people from Dr. Li's Lab at Rice University, especially Yuren, Xiaochuan, Ze, and Hongchen for all the help with the analyses.

Ao LABSEM e ao ProCer, pela infraestrutura disponibilizada. Ao LINDEN, CA-EQA, LATESC, CERMAT, LABMAT e LCME, pelas análises que tornaram esse trabalho possível. De modo especial ao Leandro G. Nandi, Thiago B. Correia, Aline M. de Borba, Douglas Fabris e Callebe Camelo, pela realização das análises.

To the Shared Equipment Authority at Rice University for making their research infrastructure available for this study.

Aos professores e técnicos do Programa de Pós-Graduação em Engenharia Química, por todo suporte e conhecimento compartilhado.

À CAPES, pelo apoio financeiro. Ao CAPES-Print pela oportunidade de realizar doutorado sanduíche.

À Universidade Federal de Santa Catarina, pelo suporte físico e acadêmico.

A todos que contribuíram para a realização deste trabalho. Muito obrigada!

I am among those who think that science has great beauty.

(Marie Curie)

RESUMO

A imobilização de enzimas em membranas inorgânicas é uma tarefa desafiadora que geralmente necessita várias etapas, usa produtos químicos tóxicos e é feita ex situ (fora do sistema de filtração por membrana). O desenvolvimento de um método de imobilização in situ é essencial para facilitar a ampliação do processo. Assim, esse estudo desenvolveu um método in situ de apenas uma etapa para imobilizar a lipase Eversa Transform 2.0 (ET2) em uma membrana de α-alumina e também avaliou o controle de incrustação de óleo e a capacidade de autolimpeza da membrana após filtração de efluente oleoso. Primeiramente, a tradicional imobilização enzimática em cerâmica por silanização com 3-aminopropiltrietoxisilano (APTES) foi comparada à técnica inovadora de revestimento com polidopamina (PDA). Nesses testes iniciais, a modificação foi feita por imersão da membrana nas soluções (imobilização ex situ). Uma vez que o uso de PDA resultou na maior atividade hidrolítica da membrana em relação a óleo de soja (1845 ± 283 $\mu mol \cdot min^{-1} \cdot m^{-2}$), a abordagem convencional de duas etapas (polimerização de PDA seguida de imobilização enzimática) foi comparada a um método de apenas uma etapa (polimerização e imobilização simultâneas). A estratégia de uma etapa alcançou carga enzimática (3,1 ± 0,1 $g \cdot m^{-2}$), atividade hidrolítica (1986 ± 40 $\mu mol \cdot min^{-1} \cdot m^{-2}$) e atividade específica da enzima (641 ± 18 $\mu mol \cdot min^{-1} \cdot g^{-1}$) semelhantes às do método de duas etapas. O método de uma etapa reduziu o tempo de imobilização em 33%, o consumo de produtos químicos em 25% e a geração de efluentes em 50% em comparação com o método de duas etapas. Usando a abordagem de uma etapa, a ET2 foi imobilizada na membrana in situ, ou seja, através da recirculação da solução de modificação pelo sistema de filtração. A imobilização in situ mostrou-se viável, e otimizando a concentração de cloridrato de dopamina (DA) e ET2 na solução para 0,3 $mg \cdot mL^{-1}$ e 4 $mg \cdot mL^{-1}$, respectivamente, a membrana modificada atingiu uma carga enzimática de 10 $g \cdot m^{-2}$ o que resultou em maior hidrofilicidade e na maior atividade hidrolítica obtida (38 $mmol \cdot min^{-1} \cdot m^{-2}$). O controle de incrustação foi avaliado pela filtração de uma emulsão de óleo de soja, e a membrana modificada mostrou uma forte resistência à incrustação (redução da permeância à água pura de 43% após a filtração) em comparação com a membrana sem modificação (redução de 83%), o que se deve, principalmente, à maior hidrofilicidade após a imobilização da enzima. Depois da filtração, a capacidade de autolimpeza da membrana foi avaliada usando diferentes soluções, temperaturas e tempo. Água deionizada a 40 °C por 6 h resultou em uma recuperação da permeância à água pura de 97%, principalmente devido à hidrólise do óleo incrustado pela ET2 imobilizada. Depois de algum tempo, as enzimas perdem sua atividade e precisam ser substituídas, e como uma das principais vantagens do uso de membranas cerâmicas é sua reusabilidade e resistência química, testou-se também a regeneração da membrana por calcinação e limpeza química. Os resultados mostraram que, após cinco ciclos de modificação-regeneração, não foram observadas alterações morfológicas ou químicas na superfície da membrana. A imobilização enzimática in situ e a regeneração química são grandes vantagens que podem facilitar o aumento de escala do processo. A reutilização da membrana juntamente com a modificação de uma etapa usando PDA pode reduzir custos e tornar o processo mais sustentável.

Palavras-chave: Eversa Transform 2.0; imobilização de enzima; membrana cerâmica; polidopamina; imobilização em uma etapa; imobilização in situ.

RESUMO EXPANDIDO

Introdução

Um grande volume de efluentes líquidos oleosos é gerado por diversas indústrias e diferentes técnicas tradicionais podem ser utilizadas para remoção do óleo. Contudo, esses métodos apresentam limitações para emulsões com gotas de óleo ≤ 20 μm de diâmetro. Nesses casos, processos de separação por membranas têm se mostrado uma boa alternativa. No caso de efluentes oleosos, membranas de materiais hidrofílicos, como cerâmicas, são geralmente menos suscetíveis à incrustação que materiais hidrofóbicos. Além de maior hidrofilicidade, membranas cerâmicas possuem alta estabilidade térmica e química, e permitem o reuso. Para melhorar ainda mais a performance das membranas cerâmicas na filtração de efluente oleoso, diversos processos de modificação superficial podem ser feitos. Entre eles, a imobilização de enzimas ainda é pouco explorada. No tratamento de efluentes oleosos, a imobilização da enzima lipase (triacilglicerol hidrolase, EC 3.1.1.3) pode ser uma opção para diminuir a incrustação de óleo e dar à membrana capacidade de autolimpeza. As lipases imobilizadas na membrana catalisam a hidrólise do óleo, podendo ser uma alternativa ao uso de produtos químicos durante a limpeza da membrana, tornando o processo mais ambientalmente correto. A imobilização de enzimas em membranas inorgânicas é uma tarefa desafiadora que geralmente necessita várias etapas, usa produtos químicos tóxicos e é feita ex situ (fora do sistema de filtração por membrana). O desenvolvimento de um método de imobilização simples e in situ é essencial para facilitar a ampliação do processo. Recentemente, a modificação de superfícies com polidopamina (PDA) tem chamado a atenção já que esse polímero natural consegue facilmente aderir a uma ampla gama de materiais orgânicos e inorgânicos, além de ser menos tóxico que os reagentes normalmente utilizados para imobilização enzimática. Geralmente, a imobilização de enzimas utilizando PDA é feita em duas etapas: polimerização da dopamina no suporte formando um revestimento de PDA seguida pela imobilização da enzima. No entanto, alguns estudos demonstraram que é possível realizar o processo em apenas uma etapa, na qual a polimerização e a imobilização ocorrem simultaneamente. A imobilização em apenas uma etapa pode diminuir o tempo do processo, o consumo de produtos químicos e a geração de efluentes.

Objetivos

O objetivo geral dessa tese foi desenvolver um método in situ de apenas uma etapa para imobilizar a enzima lipase em uma membrana de α-alumina e avaliar o controle de incrustação de óleo e a capacidade de autolimpeza da membrana após filtração de efluente oleoso. Os objetivos específicos foram: comparar a tradicional imobilização enzimática em cerâmica por silanização com a técnica inovadora de revestimento com PDA; comparar os métodos de imobilização em duas etapas e em uma etapa utilizando PDA; avaliar a imobilização in situ da lipase utilizando o método de uma etapa; otimizar o processo de imobilização visando aumentar a atividade hidrolítica da membrana; avaliar a capacidade de controle de incrustação e de autolimpeza das membranas modificadas na filtração de efluente oleoso.

Metodologia

Primeiramente, testou-se três lipases na hidrólise de óleo de soja e a Eversa Transform 2.0 (ET2) foi escolhida para ser imobilizada na membrana devido à sua alta

atividade hidrolítica. Membranas tubulares comerciais de α-alumina foram utilizadas em todos os testes. Inicialmente, a técnica convencional de imobilização enzimática em cerâmica por silanização com 3-aminopropiltrietoxisilano (APTES) seguida de ativação com glutaraldeído foi comparada ao revestimento com PDA utilizando uma solução alcalina de cloridrato de dopamina (DA). Avaliou-se a quantidade de enzima imobilizada, a atividade hidrolítica da membrana em relação ao óleo de soja, e a atividade específica das enzimas imobilizadas. Uma vez que o uso de PDA resultou na maior atividade hidrolítica, a abordagem convencional de duas etapas (polimerização de PDA seguida de imobilização enzimática) foi comparada a um método de apenas uma etapa (polimerização e imobilização simultâneas). Nesses testes iniciais, a modificação foi feita por imersão da membrana nas soluções (imobilização ex-situ) utilizando 2 $mg \cdot mL^{-1}$ de DA e 2 $mg \cdot mL^{-1}$ de ET2. Usando a abordagem de uma etapa, a ET2 foi imobilizada na membrana de forma in situ, ou seja, através da recirculação da solução de modificação pelo sistema de filtração. A atividade hidrolítica da membrana foi otimizada avaliando-se as concentrações iniciais de DA e ET2 na solução de modificação. O controle de incrustação das membranas foi avaliado pela filtração de uma emulsão de óleo de soja, analisando-se a diferença da permeância à água pura antes e após a filtração. Depois da filtração, a capacidade de autolimpeza da membrana foi avaliada usando diferentes soluções (tampão fosfato de sódio 100 mM pH 7 e água deionizada), temperaturas (40 °C e 24 °C) e tempo (3 a 12 h). As membranas foram reutilizadas por três ciclos consecutivos de filtração e limpeza para avaliar a estabilidade da ET2 imobilizada. E, por fim, avaliou-se a possibilidade de regeneração das membranas por calcinação e limpeza química para que uma nova modificação pudesse ser feita quando as enzimas imobilizadas perdessem sua atividade. As membranas foram caracterizadas em relação à hidrofilicidade por adsorção de vapor de água e n-heptano, morfologia superficial por microscopia eletrônica de varredura (MEV), e química superficial por espectroscopia de energia dispersiva de raio-X (EDX), espectroscopia no infravermelho por transformada de Fourier (FTIR) e espectroscopia de fotoelétrons excitados por raios-X (XPS).

Resultados e Discussão

Ao comparar-se a silanização e o uso de PDA em duas etapas para imobilização da lipase, o revestimento com PDA resultou em maior atividade hidrolítica da membrana em relação ao óleo de soja ($1845 \pm 283\ \mu mol \cdot min^{-1} \cdot m^{-2}$) com carga enzimática de $3,2 \pm 0,4\ g \cdot m^{-2}$ e, portanto, atividade especifica da enzima imobilizada de $571 \pm 23\ \mu mol \cdot min^{-1} \cdot g^{-1}$. O uso de PDA é uma técnica mais simples e mais sustentável quando comparada a técnicas tradicionais de imobilização já que usa menos reagentes de menor toxicidade.

A imobilização da enzima utilizando PDA em uma etapa alcançou carga enzimática ($3,1 \pm 0,1\ g \cdot m^{-2}$), atividade hidrolítica ($1986 \pm 40\ \mu mol \cdot min^{-1} \cdot m^{-2}$) e atividade específica da enzima ($641 \pm 18\ \mu mol \cdot min^{-1} \cdot g^{-1}$) semelhantes às do método de duas etapas. O método de uma etapa reduziu o tempo de imobilização em 33%, o consumo de produtos químicos em 25% e a geração de efluentes em 50% em comparação com o método de duas etapas. Além disso, a enzima imobilizada em uma etapa apresentou maior estabilidade ao longo do tempo de reação e em maiores temperaturas (50-60 °C).

A imobilização in situ utilizando o método de uma etapa mostrou-se viável, resultando em uma carga enzimática de $2,5 \pm 0,2\ g \cdot m^{-2}$, atividade hidrolítica de $7200 \pm 300\ \mu mol \cdot min^{-1} \cdot m^{-2}$, e atividade específica da enzima imobilizada de

2900 ± 300 $\mu mol \cdot min^{-1} \cdot g^{-1}$. É importante ressaltar que o método para medir a atividade hidrolítica para os ensaios in situ foi modificado em relação ao método utilizado nos ensaios anteriores, por isso a grande diferença entre os valores. A possibilidade de modificar a membrana in situ representa uma grande vantagem para o aumento de escala do processo.

Depois de verificar a viabilidade da imobilização in situ, otimizou-se a concentração de DA e ET2 na solução para 0,3 $mg \cdot mL^{-1}$ e 4 $mg \cdot mL^{-1}$, respectivamente. Utilizando essas concentrações, a membrana modificada atingiu uma carga enzimática de 10 $g \cdot m^{-2}$, o que resultou em maior hidrofilicidade e na maior atividade hidrolítica obtida (38 $mmol \cdot min^{-1} \cdot m^{-2}$). Com a membrana modificada pelo método otimizado, realizaram-se ensaios de filtração de emulsão de óleo de soja a fim de avaliar a resistência à incrustação e a capacidade de autolimpeza. A membrana modificada mostrou uma forte resistência à incrustação (redução da permeância à água pura de 43% após a filtração) em comparação com a membrana sem modificação (redução de 83%), o que se deve, principalmente, à maior hidrofilicidade após a imobilização da enzima. Os ensaios de limpeza da membrana mostraram que o uso de água deionizada a 40 °C por 6 h resultou em uma recuperação da permeância à água pura de 97%, principalmente devido à hidrólise do óleo incrustado pela ET2 imobilizada. O teste de reuso da mesma membrana por diversos ciclos de filtração e limpeza mostraram que, após três ciclos, a permeância à agua pura da membrana sem modificação reduziu 91% enquanto a da membrana modificada reduziu apenas 17%. A possibilidade de utilizar água como solvente durante a limpeza da membrana representa um grande avanço que, além de facilitar o aumento de escala do processo, também evita o uso de produtos químicos poluentes durante essa etapa.

Os ensaios de regeneração da membrana, tanto por calcinação quanto por limpeza química in situ, mostraram que após cinco ciclos de modificação-regeneração, não foram observadas alterações morfológicas ou químicas na superfície da membrana. Além disso, a permeância à água pura e a atividade hidrolítica da enzima imobilizada se mantiveram as mesmas após cada regeneração. Esses resultados demonstram que a mesma membrana pode ser reutilizada por diversos ciclos após a perda de atividade da enzima. Além disso, a possibilidade de regeneração in situ juntamente com a imobilização in situ favorecem o uso do processo em escalas maiores.

Considerações Finais

Esse trabalho apresenta um método mais simples e sustentável para a imobilização de enzimas em membranas inorgânicas. A utilização de PDA provou-se uma técnica competitiva aos métodos tradicionais de imobilização já que resultou em maior carga enzimática e maior atividade hidrolítica da membrana, além de ser mais simples e mais ambientalmente correta. A estratégia de imobilização em apenas uma etapa mostrou-se uma excelente alternativa ao método de duas etapas, aumentou a estabilidade da enzima imobilizada, é mais rápida, usa menos produtos químicos e gera menos efluente, diminuindo custos e tornando o processo mais sustentável. Além disso, a viabilidade da imobilização enzimática in situ e da regeneração química in situ demonstram que a reutilização da membrana é possível, o que é uma grande vantagem que pode facilitar o aumento de escala do processo e torná-lo ainda mais barato.

Palavras-chave: Eversa Transform 2.0; imobilização de enzima; membrana cerâmica; polidopamina; imobilização em uma etapa; imobilização in situ.

ABSTRACT

Enzyme immobilization on inorganic membranes is a challenging task that generally is multi-step, time-consuming, uses toxic chemicals, and is done ex-situ (outside the membrane filtration system). Developing an in-situ immobilization method is essential to facilitate the scale-up of the process. Therefore, this study aimed to develop a one-step in-situ method to immobilize the lipase Eversa Transform 2.0 (ET2) on an α-alumina membrane and evaluate the membrane oil fouling control and self-cleaning capacity after oil-water emulsion filtration. First, the traditional enzyme immobilization on ceramics by silanization using 3-aminopropyltriethoxysilane (APTES) was compared to the innovative and greener technique of polydopamine coating (PDA). In these first tests, the modification was done by immersing the membrane in the solutions (ex-situ immobilization). Since the use of PDA resulted in the highest membrane hydrolytic activity toward soybean oil (1845 ± 283 $\mu mol \cdot min^{-1} \cdot m^{-2}$), the conventional two-step approach (PDA polymerization followed by enzyme immobilization) was compared to a one-step method (simultaneous polymerization and immobilization). The one-step strategy achieved similar enzyme loading (3.1 ± 0.1 $g \cdot m^{-2}$), membrane hydrolytic activity (1986 ± 40 $\mu mol \cdot min^{-1} \cdot m^{-2}$), and enzyme-specific activity (641 ± 18 $\mu mol \cdot min^{-1} \cdot g^{-1}$) to those of the two-step method. The one-step method reduced the immobilization time by 33%, the chemical consumption by 25%, and the wastewater generation by 50% compared to the two-step method. Using the one-step approach, ET2 was immobilized on the membrane in situ, i.e., by recirculating the modification solution in the filtration system. The in-situ immobilization proved to be feasible, and by optimizing the dopamine hydrochloride (DA) and ET2 concentration in the solution to 0.3 $mg \cdot mL^{-1}$ and 4 $mg \cdot mL^{-1}$, respectively, the modified membrane reached an enzyme loading of 10 $g \cdot m^{-2}$ which resulted in an improved water affinity and in the highest membrane hydrolytic activity (38 $mmol \cdot min^{-1} \cdot m^{-2}$). The membrane fouling control was evaluated by the filtration of a soybean oil in water emulsion, and the modified membrane showed a strong fouling resistance (pure water permeance reduction of 43% after the emulsion filtration) compared to the pristine membrane (reduction of 83%), which is mainly due to the higher hydrophilicity after enzyme immobilization. After oil-water emulsion filtration, the membrane's self-cleaning capacity was evaluated using different cleaning solutions, temperatures, and time. Cleaning with deionized water at 40 °C for 6 h resulted in a pure water permeance recovery of 97%, mainly due to the fouled oil hydrolysis by the immobilized ET2. After some time, the enzymes eventually lose their activity and need to be replaced, and since one of the main advantages of using ceramic membranes is their reusability and chemical resistance, membrane regeneration by calcination and chemical cleaning was also tested. The results showed that, after five modification-regeneration cycles, no morphological or chemical changes were observed in the membrane surface. The in-situ enzyme immobilization and chemical regeneration are huge advantages that can facilitate the scale-up of the process. Reusing the membrane coupled with the one-step modification using PDA can reduce costs and make the process more environmentally friendly.

Keywords: Eversa Transform 2.0; enzyme immobilization; ceramic membrane; polydopamine; one-step immobilization; in-situ immobilization.

LIST OF FIGURES

LIST OF TABLES

CONTENTS

CONCEPTUAL DIAGRAM OF THIS STUDY

Lipase immobilization on α-alumina membrane for oil fouling control and self-cleaning properties

Why?

- Enzymes are an environmentally friendly functionalization
- Lipases can catalyze oil hydrolysis
- Control of membrane fouling during oil-water separation process
- Lower cleaning frequency
- Reduction of the consumption of chemicals during membrane cleaning
- Improved process performance and lower operational costs

Who already did it?

- No reports were found in the literature about Eversa Transform 2.0 lipase immobilization on inorganic supports or membranes
- There are just few reports about immobilized lipases as antifouling and self-cleaning agents, all of them using polymeric membranes

Research hypotheses

- Is it possible to efficiently immobilize lipase on ceramic supports?
- Can the lipase activity and stability be maintained after the immobilization?
- Can the immobilized lipase efficiently act as a fouling-reducing and self-cleaning agent during oil-water separation processes using membranes?

Method

- Lipase immobilization on α-alumina tubular membrane using polydopamine (PDA)
- One-step lipase immobilization on the membrane using PDA as bonding agent;
- In situ enzyme immobilization on the membrane
- Characterization of the control and functionalized membranes by different techniques
- Evaluation of the functionalized membrane during oil-water separation in relation to fouling formation and self-cleaning capacity
- Evaluation of membrane reusability during several filtration steps
- Evaluation of membrane regeneration by thermal and chemical treatments

Main outcomes

- PDA coating method can be an alternative to traditional enzyme immobilization methods on ceramics
- A one-step immobilization protocol can replace the conventional two-step method using PDA
- In-situ immobilization (membrane on the filtration system) is feasible and can replace the ex-situ immobilization
- Enzymatically active membrane has a better performance than the pristine membrane during an oil emulsion filtration in relation to fouling and self-cleaning capacity
- Reusability of the modified membrane during several filtration and cleaning steps
- The membrane can be regenerated using a thermal and a chemical treatment and be recoated by the enzyme and PDA

1 INTRODUCTION

Several industries, such as food processing, metallurgical, petrochemical, and cosmetics, generate oily wastewater in large volumes. When the system is not emulsified, the hydrophobic compounds can be separated using physical methods such as gravity settling, coalescence, skimming, centrifugation, or air flotation. When it is the form of an emulsion, chemical techniques are required (flocculation and coagulation, for example). However, these methods have limitations for emulsions with oil droplets of 20 μm or lower in diameter since the addition of chemicals is necessary to break the emulsion, which requires close control to determine the type and quantity of chemicals in order to achieve an optimal removal (CHERYAN; RAJAGOPALAN, 1998; PORNEA et al., 2020; ZHU et al., 2014). Membrane separation processes have proven to be a good alternative in these cases, presenting advantages such as high oil removal efficiencies, no need for chemical additives, and compact facilities that can be fully automated (ABBASI et al., 2012; KHOUNI et al., 2020).

Even though membrane systems are widely studied, the applicability of these processes in the wastewater treatment still has limitations, mainly related to fouling issues. Fouling causes a permeate flux decline, consequently decreasing the system efficiency, increasing the energy consumption and the frequency of membrane cleaning procedures, which in turn can decrease the membrane lifespan and increase the process costs (TANUDJAJA et al., 2019). Hydrophilic membranes are generally less susceptible to oil fouling than hydrophobic ones. In this sense, ceramic membranes have some advantages since they generally are highly hydrophilic, very stable at high temperatures and pressures, can reach high water fluxes, and have excellent chemical stability, lifespan, reusability, and mechanical resistance during filtration (ABBASI et al., 2012; JEONG et al., 2018). However, although the costs of ceramic membranes have been decreasing over the years with the development of new technologies, it is still a limitation to their use in environmental applications (ISSAOUI; LIMOUSY, 2019). Besides the production costs, fouling also increases the operational expenses of membrane systems, restricting the use of ceramic membranes in low-profit applications even more.

Several strategies were developed, and new ones have been studied to minimize fouling. Lately, polydopamine (PDA) coating has attracted considerable attention for surface modification since it can firmly adhere to a wide range of organic

and inorganic materials (GAO; FAN; XU, 2020; GUO et al., 2020). Surface coating with PDA occurs through the polymerization of dopamine (natural monometer inspired by the adhesive capacity of marine mussels) in a slightly alkaline environment. PDA coating itself can improve the antifouling capacity of the membranes in oil-water emulsions by increasing its hydrophilicity (KASEMSET et al., 2016; LI et al., 2018; ZARGHAMI; MOHAMMADI; SADRZADEH, 2019). Moreover, due to the presence of different reactive groups in the PDA (such as amine, imine, quinone, and catechol), this technique can be used to bond different materials and molecules to the membrane, which can contribute to the enhancement of the fouling control property (CUI et al., 2019; GAO; XU, 2019; MARQUES et al., 2020; PRONER et al., 2020; YANG et al., 2014; ZIN et al., 2019).

Among the molecules that PDA coatings can bind are enzymes (CHEN et al., 2019b; CHENG et al., 2018; LUO et al., 2014; MORTHENSEN et al., 2017; MULINARI et al., 2022; TOUQEER et al., 2019; WANG et al., 2021). The immobilization of enzymes on membranes can aim at the synthesis of products of interest through enzymatic catalysis (LUO et al., 2014; MORTHENSEN et al., 2017; SULAIMAN et al., 2019) and the improvement of the membrane's fouling control property by degrading the fouling layer during the filtration process (KOLESNYK et al., 2019; KOSEOGLU-IMER; DIZGE; KOYUNCU, 2012; NG; WRIGHT; SEAH, 2011). The immobilized enzymes can also promote the hydrolysis of the fouling layer during the cleaning procedure through a simple activation by adjusting the reaction conditions, such as pH and temperature (SCHMIDT et al., 2018; SCHULZE et al., 2017; VANANGAMUDI et al., 2018a). Thus, the immobilized enzymes provide the membrane with a self-cleaning capacity, decreasing or even avoiding chemical cleaning, which makes the process greener and more sustainable.

In the treatment of oily wastewater, the immobilization of the enzyme lipase (triacylglycerol hydrolases, EC 3.1.1.3) on the membrane could be an alternative to improve the fouling control and self-cleaning capacity of the membrane since lipase can catalyze oil hydrolysis. Lipase is one of the most used enzymes due to its high versatility, tolerance to organic solvents, and thermal stability (GOLUNSKI et al., 2017; ITTRAT et al., 2014; JIANG et al., 2017). They can be employed in a variety of applications, such as biodiesel production (SANTIN et al., 2017; WANCURA et al., 2019), as well as in agrochemical (BOROWIECKI; DRANKA, 2019), pharmaceutical (ALMEIDA et al., 2019), cosmetics (HOLZ et al., 2018) and food industries (DE

MENESES et al., 2019), fine chemistry (AGUILLÓN et al., 2019) and oily effluent treatment (MULINARI et al., 2017). In membrane separation processes of oil-water emulsions, lipase immobilized in the membrane can hydrolyze the triacylglycerols of the oil into fatty acids and glycerol, degrading the oil fouling.

The covalent immobilization of enzymes on membranes is a challenging task that generally requires several steps and the use of toxic chemicals, is time-consuming and done ex situ (outside the filtration system, normally by immersing the membranes in the modification solution) (AGHABABAIE et al., 2016; BRISOLA et al., 2022; VASCONCELOS et al., 2020). Few studies have done the modification in situ (membrane inside the filtration module), which can facilitate the scale-up of the process (CHEN et al., 2019b; GUO et al., 2018; MARPANI et al., 2015). Moreover, the enzymes lose their activity after some time and must be replaced. In an in-situ immobilization, to reuse the membrane, both cleaning and modification steps could be performed directly in the filtration setup, so the membrane would not have to be removed and replaced in the system. Therefore, in-situ immobilization can save time and decrease operational costs.

Thus, this study aims to immobilize the enzyme lipase on a ceramic membrane using PDA coating. The main goal is to provide fouling-controlling and self-cleaning properties to the membrane for the treatment of oily wastewater. To the best of our knowledge, there is no previous study in the literature about lipase immobilization in ceramic membranes using PDA coating. Moreover, there are very few studies concerning immobilized enzymes as fouling-controlling and self-cleaning agents on membranes, and only a few using an in-situ immobilization method.

1.1 OBJECTIVES

1.1.1 General objective

The general objective of this work is the immobilization of lipase on α-alumina tubular membranes aiming at fouling-controlling and self-cleaning properties for application in oil-water emulsion filtration.

1.1.2 Specific objectives

- Select a lipase with high hydrolytic activity toward soybean oil;
- Compare the lipase immobilization using PDA coating with traditional immobilization methods on ceramic materials in terms of enzyme loading, membrane hydrolytic activity, and specific immobilized enzyme activity;
- Develop a simple one-step immobilization strategy using the PDA coating and compare it to the conventional two-step method;
- Determine if an in-situ immobilization is viable by comparing it with the ex-situ immobilization;
- Optimize the lipase and dopamine concentrations during the immobilization, considering the membrane hydrolytic activity;
- Evaluate the operational stability of the immobilized lipase to pH, temperature, and reaction time;
- Evaluate the performance of the modified membrane in the process of oil-water emulsion separation in terms of permeate flux and oil retention;
- Evaluate the fouling control and self-cleaning properties of the modified membrane in the filtration of an oil-water emulsion;
- Evaluate the reusability of the modified membrane during several steps of oil-water emulsion filtration and cleaning;
- Assess the regeneration of the membrane by a thermal and a chemical method and evaluate the recoating of the regenerated membrane in terms of pure water permeance and membrane hydrolytic activity for several regeneration-recoating steps.

2 LITERATURE REVIEW

This chapter presents a brief literature review on the relevant topics to this work. Firstly, the main information on oily wastewater generation, potential environmental impacts, and traditional treatment techniques are approached. Then, important aspects of membrane processes for oil-water separation, membrane fouling, fouling reduction techniques and membrane cleaning methods are described with a special emphasis on ceramic membranes. Finally, the main enzyme immobilization techniques are discussed highlighting lipase immobilization on ceramic materials. Lastly, the use of immobilized enzymes as antifouling and self-cleaning agents is addressed.

Part of this chapter was published in Biotechnology Advances as “Lipase immobilization on ceramic supports: an overview on techniques and materials”[1]. Another part was published by Elsevier as the chapter “Catalytic membranes for the treatment of oily wastewater” in the book “Membrane-based hybrid processes for wastewater treatment” edited by Maulin P. Shah and Susane R. Couto[2].

2.1 OILY WASTEWATERS

Oily wastewater is generated in large volumes by different sources such as food processing (slaughterhouse, dairy industries, bakeries, seafood, cooked foods, edible oil processing, animal feed industries), oil and gas, metallurgical, petrochemical, pharmaceutical and cosmetics industries (PADAKI et al., 2015). These wastewaters contain varying concentrations of oil and grease. The discharge of untreated oily wastewater can cause severe environmental and public health issues, and affect entire aquatic ecosystems, since the oil film or droplets can block sunlight, compromising photosynthesis and gaseous exchange. When discharged in the soil, the oil enhances its impermeabilization, hindering water flow and oxygenation (SANTOS; MARANHO, 2018). Additionally, when discarded in the public sewage system, the oil can cause pipe blockage and increase the costs of the treatment since more chemicals are needed (WALLACE et al., 2017). Thus, inadequate treatment of the oily wastewaters

[1] https://doi.org/10.1016/j.biotechadv.2020.107581
[2] https://doi.org/10.1016/B978-0-12-823804-2.00026-4

can compromise drinking water availability, agriculture production, and sewage treatment efficiency.

There are several ways for purifying oily wastewater, including conventional physical, chemical, and biological methods. The degree of dispersion and the stability of the oil droplets in the wastewater are the most important factors regarding the choice of the most suitable technique. These characteristics are governed by the diameter of the droplets: free oil (> 150 μm), dispersed oil (20-150 μm), emulsified oil (< 20 μm) and soluble oil (< 5 μm) (PINTOR et al., 2016). Physical methods (gravity settling and air flotation, for example) are generally used when the oil is not in an emulsion (WANG et al., 2019). When the oil is emulsified, chemical techniques (coagulation and flocculation, for example) are necessary; however, these methods have limitations in treating emulsions with finely dispersed oil droplets. Biological treatment includes activated sludge, biofilter, and stabilization ponds and are generally used in combination with other methods (ALMASI et al., 2019; YU; HAN; HE, 2017).

The conventional techniques have drawbacks such as high cost, use of toxic compounds, large installation facilities, and generation of secondary pollutants (HE et al., 2019; YU; HAN; HE, 2017). Moreover, they cannot efficiently remove oil when it is emulsified, especially when the size of the oil droplets is below 20 μm (PORNEA et al., 2020). The addition of chemicals is necessary to break these fine stable emulsions, which requires close control to determine the type and quantity of chemicals in order to achieve an optimal removal, making the operation very challenging (CHERYAN; RAJAGOPALAN, 1998; ZHU et al., 2014). In these cases, membrane technology has shown great performance, presenting some advantages as high oil removal, compact facilities, low energy consumption, and no need for chemical additives (KHOUNI et al., 2020). Section 2.2 approaches the use of membrane processes as alternatives to traditional techniques for oil-water separation.

2.2 MEMBRANE PROCESSES FOR OIL-WATER SEPARATION

The use of membrane-based processes for the separation of oil-water emulsions has been reported in the literature for decades (SCHNABEL; VAULONT, 1977; JEONG; IHM; WON, 1987; YAO; FANE; POPE, 1997; PAN et al., 2007; CAI et al., 2017; XIE et al., 2023). When studying the use of membranes for the oil removal from wastewaters, some parameters must be carefully analyzed, including permeate

flux, fouling resistance, and rejection coefficient (ABBASI et al., 2012). Microfiltration (MF), ultrafiltration (UF), nanofiltration (NF) and reverse osmosis (RO) can be considered the main membrane separation processes with a pressure-based driving force and are usually classified in terms of their pore size range, which defines their applications (BAKER, 2012). UF, and sometimes MF, are the most effective in treating oily wastewater due to their pore size range that can separate oil even from surfactant stabilized emulsions (MASOUDNIA et al., 2015; ZHU et al., 2014).

Different configurations have been used for oil-water separation, such as flat sheet, tubular, hollow fiber, spiral wound, and capillary membranes, with the flat sheet and tubular being more commonly applied (TANUDJAJA et al., 2019). Flat sheet configurations are mainly used for research purposes at bench-scale experiments since they require relatively simple modules and are of easy operation and control. However, the membrane area per unit of module volume (packing density) is low, which hinders the use of flat sheet membranes at an industrial scale due to the large space required. Hence, flat sheets can be stacked with spacers, rolled and placed inside a cylindrical case, forming a spiral wound membrane module, which offers a much larger membrane area for filtration. However, spiral wound configuration does not allow backflush, while tubular-shaped modules do (FRANK et al., 2001). Tubular, capillary, and hollow fiber membranes have a similar shape but different diameters. There is no consensus in the literature about the tube diameter ranges of the different configurations; the most used ranges were proposed by Mulder (2000): tubular membranes have diameters greater than 10 mm, capillary membranes from 0.5 to 10 mm, and hollow fiber lower than 0.5 mm.

Membrane systems can operate in a dead-end (perpendicular flow) or a cross-flow (tangential flow) mode. Most dead-end filtrations are carried out in batch systems since the membrane fouling causes flux decline and, thus, more frequent membrane cleaning or replacement is necessary, decreasing the membrane lifespan (TANUDJAJA et al., 2019). Batch processing is used mainly when the goal is to recover certain products from the oily wastewater, which means that the retentate is the valuable fraction. Hence, the lower feed volume used in batch systems in comparison to continuous processing allows better control of the retentate quality (TANUDJAJA et al., 2019). Continuous operating mode is more adequate than batch mode when dealing with large quantities of oily wastewater, and the main goal is to discharge this wastewater into water bodies in compliance with environmental regulations.

Continuous systems usually operate under crossflow mode. Besides accepting higher wastewater flow rates, the cross-flow generates a tangential shear at the membrane surface, which helps to decrease membrane fouling, prolonging the lifespan of the membrane (TANUDJAJA et al., 2019).

Regarding the membrane material, polymers, ceramics, and mixed matrices have been studied for oil-water separation. Among the polymers, the most common are polyacrylonitrile (PAN), polyvinylidene fluoride (PVDF), polyethersulfone (PES), polyurethane (PU), polystyrene (PS), polyvinyl chloride (PVC), and cellulose acetate (CA) (AL-HUSAINI et al., 2019; DIAO et al., 2017; KIM et al., 2019; NADJAFI; REYHANI; AL ARNI, 2018; PENG et al., 2017; WANG et al., 2020; YANG et al., 2020). Polymeric membranes have shown high efficiency and low energy requirements to remove dispersed and emulsified oil, having a lower cost than ceramic membranes (PADAKI et al., 2015). However, due to the hydrophobic character of most of the polymeric materials, polymeric membranes are more susceptible to fouling, particularly when treating oily wastewater, which results in flux decline and, consequently, short operation times and low lifespan (ZUO et al., 2018). Consequently, surface modification, polymer-blending, and incorporation of nanoparticles are strategies being developed to improve the membrane hydrophilicity (IKHSAN et al., 2018; ZIN et al., 2019; ZUO et al., 2018).

Due to the high chemical resistance, the ceramic membranes have presented longer operation times and lifespan. Also, they have greater resistance to high concentrations of oil and good antifouling capacity since they are more hydrophilic than most of the polymeric membranes. Alumina (Al_2O_3), zirconia (ZrO_2), titania (TiO_2) and silicon carbide (SiC) are examples of materials being used in the fabrication of the ceramic membranes (FRAGA et al., 2017; ŠEREŠ et al., 2016; WESCHENFELDER; BORGES; CAMPOS, 2015; ZHANG et al., 2018a). Although presenting advantages over polymeric membranes, the high cost of manufacturing and materials used to produce ceramic membranes have limited their utilization in environmental applications, including wastewater treatment. Cheaper precursors such as mullite, bentonite, kaolinite and inorganic waste materials may be an alternative to produce ceramic membranes (ABBASI et al., 2012; EOM et al., 2015; KUMAR; GHOSHAL; PUGAZHENTHI, 2015; ZHU et al., 2016; ZHU; CHEN, 2017). Even though ceramic materials are more hydrophilic than the polymeric, ceramic membranes are still susceptible to fouling and, thus, surface modifications and different formulations have

been tested to improve the membranes' antifouling capacity (FARD et al., 2018; HU et al., 2015; ZHANG et al., 2018a). Therefore, there are still many possibilities to improve the characteristics of ceramic membranes, reduce manufacturing costs, and refine the ability to treat wastewater, including oily effluents.

Mixed-matrix membranes are made of two or more materials of different classes (CHEN et al., 2019c; IKHSAN et al., 2018; QADIR; MUKHTAR; KEONG, 2017). The goal is to combine the advantages of the materials, developing better membranes in terms of performance, fouling, permeate quality, and longevity (ISMAIL et al., 2020; QADIR; MUKHTAR; KEONG, 2017). Generally, mixed-matrix membranes are made of a continuous phase (usually polymeric) filled with a dispersed phase (ceramic, zeolite, carbon, etc.). Thus, the resulting membrane can have the physicochemical stability of ceramic material and the ease of manufacture of polymers. According to Qadir et al. (2017), the polymer matrix has a major influence on permeability, whereas the inorganic filler controls the selectivity of the membrane.

Several combinations of membrane materials, configurations and operation modes can be used. Each application requires different characteristics. The membrane process for the treatment of oily wastewater depends on the oil concentration, oil form (free, dispersed, or in an emulsion), effluent volume, and presence of salts and other contaminants. Commercial membranes are already available for oil-water separation processes. Table 1 presents some of the membranes offered in the market.

Although membranes are already being used for many applications, including oil-water separations, some problems still hinder their use in environmental applications. Among these issues, membrane fouling is a major drawback that compromises performance and increases operational costs of membrane separation processes. Section 2.3 describes the main consequences of fouling on the membrane process performance and some strategies developed to minimize fouling formation.

Table 1 - Examples of commercially available membranes designed for oil-water separation applications, including oily wastewater treatment

Manufacturer	Material	Filtration type	Nominal pore size / MWCO[1]	Configuration	Membrane area per element (m^2)
Osmonics (USA)	Modified PAN	UF	10 nm	Spiral wound	24
Filtration Solution, Inc. (USA)	Modified PAN	UF	10 nm	Spiral wound	26
Pall (USA)	PVDF	MF	100 nm	Hollow fiber	-
Pall (USA)	α-alumina	MF	100-1400 nm	Tubular	0.24-0.47
Pall (USA)	Zirconia	UF	20-100 nm	Tubular	0.24-0.47
Clean Water Tech PTE, Ltd (Singapore)	Hydrophilic PAN	UF	10-100 nm	Hollow fiber	30
TriTech (China)	PVDF, PS, PVC, PAN	UF	10-80 nm	Hollow fiber	8-48
Koch (USA)	Polysulfone	UF	50 kDa	Hollow fiber	25
Veolia Water Technologies (France)	Al_2O_3/TiO_2	UF	100 nm	Tubular	10.7
Hydranautics (USA)	Composite polyamide	RO	-	Spiral wound	37

[1]MWCO: Molecular weight cutoff.
Source: Adapted from Tanudjaja et al. (2019) and Yu et al. (2020)

2.3 MEMBRANE FOULING: FORMATION AND MINIMIZATION STRATEGIES

A decrease in the permeate flux over the filtration time is a characteristic behavior in membrane separation processes, representing one of the main limitations of its use at a large scale. In theory, the flux is the driving force (in the case of oil-water separation, transmembrane pressure) divided by the fluid viscosity and the total resistance that the fluid faces when passing through the membrane (MULDER, 2000). The total resistance is composed of a series of resistances, as shown in Figure 1.

Figure 1 – Schematic representation of the various resistances towards mass transport across a membrane in pressure-driven systems

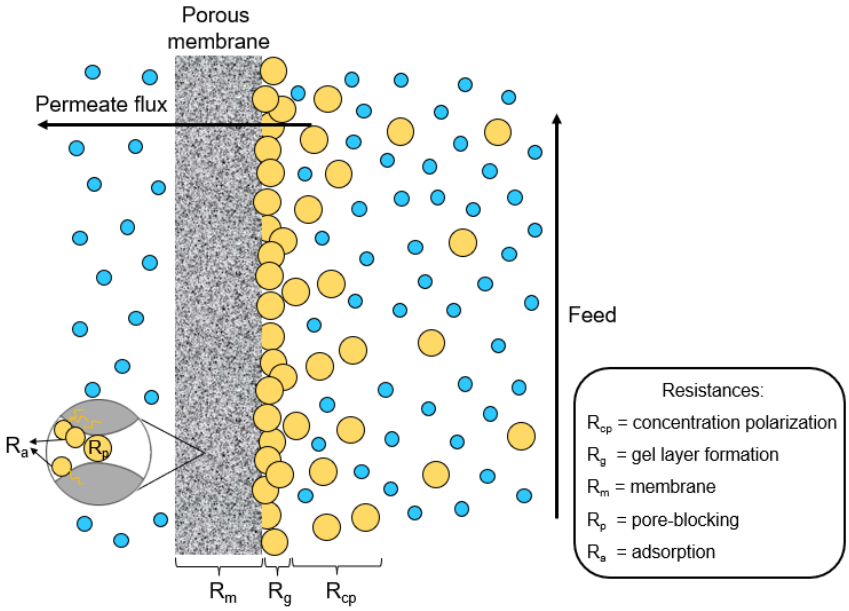

Note: yellow spheres represent the solute to be retained and blue spheres represent the permeate.
Source: adapted from Mulder (2000)

In ideal cases, the only resistance faced by the fluid is the intrinsic resistance of the membrane (R_m). However, in real cases, due to solute retention, there is an accumulation of solutes close to the membrane surface, resulting in a highly concentrated layer that ends up offering a resistance to the flow, which is the resistance due to the concentration polarization (R_{pc}) (MULDER, 2000). The concentration of the accumulated solutes can become so high that some of them can form a gel layer that will also offer resistance to flow (R_g). Besides, some solutes may penetrate the pores of the membrane, blocking them, leading to a resistance caused by the clogging of the pores (R_p). Moreover, certain components of the solution can adsorb to both the surface and the pores of the membrane, giving rise to a resistance caused by adsorption (R_a) (MULDER, 2000).

The concentration polarization is a reversible phenomenon that can be minimized by increasing the flow rate and the turbulence by using a crossflow system. According to Huang et al. (2018), in water-oil separation systems, the oil droplets forming the cake layer are thermodynamically unstable and tend to coalesce, forming larger oil droplets that are easier removed by cross-flow. Thus, both tangential shear and coalescence of the oil droplets help to decrease membrane fouling in crossflow systems.

The other resistances form what is known as fouling, which is defined as the deposition of particles, colloids, emulsions, suspensions, macromolecules, salts, among others on the membrane surface and pores by physical and chemical interactions or mechanical action (LIU et al., 2019; MULDER, 2000). Fouling is one of the main problems that prevent a broader application of membrane processes, since, by causing a decrease in permeate flux over time, it consequently decreases the efficiency of the process, increasing energy consumption and the required frequency of membrane cleaning, which can reduce the durability of the membrane and ends up increasing the overall costs of the process (AL-AMOUDI; LOVITT, 2007). According to Lin and Rutledge (2018), in dead-end filtration, the fouling occurs mainly due to electrostatic interactions between membrane and oil droplets. In contrast, in crossflow filtration, the adsorption of surfactant molecules at the membrane interface by hydrophobic/hydrophilic interactions is the principal factor influencing fouling.

There are several methods to minimize fouling, such as the pretreatment of the feed solution, changes in membrane properties, and changes in process conditions. Some pre-treatment methods include heat treatment, pH adjustment (especially for protein fouling), the addition of complexing agents, such as ethylenediaminetetraacetic acid (EDTA) for example, chlorination (mainly for biofouling), among others (MULDER, 2000).

Another strategy that has been widely studied is the change in membrane properties that affect the interaction with the solute, such as hydrophilicity and surface charge. Several studies have been carried out with the objective of making membranes, mainly polymeric ones, more hydrophilic to reduce the fouling of proteins, oils, biopolymers, etc. (SHAHKARAMIPOUR et al., 2017). For this, membranes have been grafted or coated with some key hydrophilic materials, such as poly(ethylene glycol) (PEG) (ILYAS et al., 2019), polyethyleneimine (PEI) (ZIN et al., 2019) and zwitterions (LEE et al., 2019b). Together with hydrophilicity, the surface charge of the membrane can also be modified to cause repulsion of solutes that cause fouling since it plays a significant role in controlling the surface tension as demonstrated by Wang et al. (2016).

Recently, membrane modification using compounds inspired by the adhesive secretions of marine mussels has attracted great attention. These secretions can form a strong adhesive layer in different substrates, permitting mussels to adhere to several materials such as rocks and ships (BURZIO; WAITE, 2000; YAN et al., 2020).

According to Dalsin et al. (2003), L-3,4-dihydroxyphenylalanine (L-DOPA) and its derivative dopamine (DA) are critical compounds for the adhesive capacity of the mussel secretions. Thus, DA has been successfully used for the modification of several organic and inorganic materials by forming thin polydopamine (PDA) layers (GAO; XU, 2019; KASEMSET et al., 2016; LI et al., 2018; XIANG; LIU; XUE, 2015). The adhesion mechanism is not clearly elucidated yet, but it has been generally accepted that the presence of catechol and amino groups is critical to the strong adhesion of PDA. PDA can be used to co-deposit several compounds in the material surface through co-polymerization or can be used as an interface layer for post-modification through hydrogen bonds, electrostatic attraction and covalent bonds (WANG et al., 2019b; YAN et al., 2020). The functional groups present in the PDA layer (such as quinone, catechol, and amino groups) allow the deposition of several compounds on the functionalized material. Compounds containing thiols and amines, for example, can covalently react with the PDA layer via Michael addition or Schiff base reaction (HUANG et al., 2015). These reactions are simple and do not require any harsh conditions or complicated instruments (YAN et al., 2020).

PDA has been used to modify membranes by co-polymerization with hydrophilic compounds such as PEI (PRONER et al., 2020; ZIN et al., 2019), diglycolamine (DGA) (GAO; FAN; XU, 2020), tetraethoxysilane (TEOS) (WANG et al., 2015), poly(sulfobetaine methacrylate) (PSBMA) (ZHOU et al., 2014), PEG (AN et al., 2020), etc. Post-modifications of PDA-coated membranes have also been evaluated, such as grafting polymeric membranes with inorganic nanoparticles (CUI et al., 2019; GUO et al., 2020) or hydrophilic polymers (HE et al., 2017; LI et al., 2014). Generally, the goal is to increase membrane hydrophilicity and decrease fouling formation.

Although fouling minimization methods reduce it to a certain extent, cleaning the membrane will always be necessary after a period of operation so that the membrane regains most of its permeability. This cleaning can be done physically through backwashing, ultrasound, electric fields, pneumatic cleaning or mechanical processes, for example, and/or chemically, which is the most used method for reducing fouling (LIN; LEE; HUANG, 2010). For chemical cleaning, several products can be used depending on the type of fouling, such as acids (phosphoric acid, citric acid), bases (NaOH), detergents, enzymes, complexing agents (EDTA), disinfectants (H_2O_2), among others (CHARCOSSET, 2012). Chemical cleaning must effectively remove or dissolve the fouling without compromising the mechanical strength and chemical

characteristics of the membrane. The cleaning step has a significant impact on the commercial viability of membrane processes as it greatly influences the performance and costs of the process (CHARCOSSET, 2012).

A relatively new technique is the development of “active” membranes, which, while promoting the separation of components from the solution, also degrade the fouling formed during the process, besides presenting self-cleaning properties. For this purpose, catalysts are generally incorporated on the membrane surface, such as photocatalysts (in this case, a UV light source is necessary for the activation of the membrane) or enzymes that degrade the fouling component when the system operates under conditions that promote their catalytic activity, mainly pH and temperature. Section 2.4 summarizes the main applied techniques to immobilize enzymes on solid supports, such as membrane surfaces.

2.4 ENZYME IMMOBILIZATION TECHNIQUES

Immobilized enzymes can be defined as enzymes that are physically confined in a certain region or bonded to an inert or insoluble support matrix (BILAL et al., 2018). The main goal of enzyme immobilization is to develop a stable biocatalyst that can be reused several times with little loss of activity (FACIN et al., 2019). Several immobilization techniques have arisen, and many benefits have been reported as higher stability, selectivity, specificity and/or activity, as well as the improvement of performance and feasibility of industrial processes (BARBOSA et al., 2015; BILAL et al., 2018).

Enzymes can be immobilized by physical or chemical methods, as summarized in Figure 2. Physical methods include adsorption, entrapment, and encapsulation, in which the enzyme is confined within the support or there are weak interactions between support and enzyme, such as hydrogen bonds, van der Waals forces, hydrophobic interactions, ionic bonding or affinity binding (MOHAMAD et al., 2015). Chemical immobilization can be achieved by covalent bonding between enzyme and support or cross-linking. More than one technique can be used in combination to improve the characteristics of the immobilized enzyme.

Figure 2 – Most used enzyme immobilization techniques

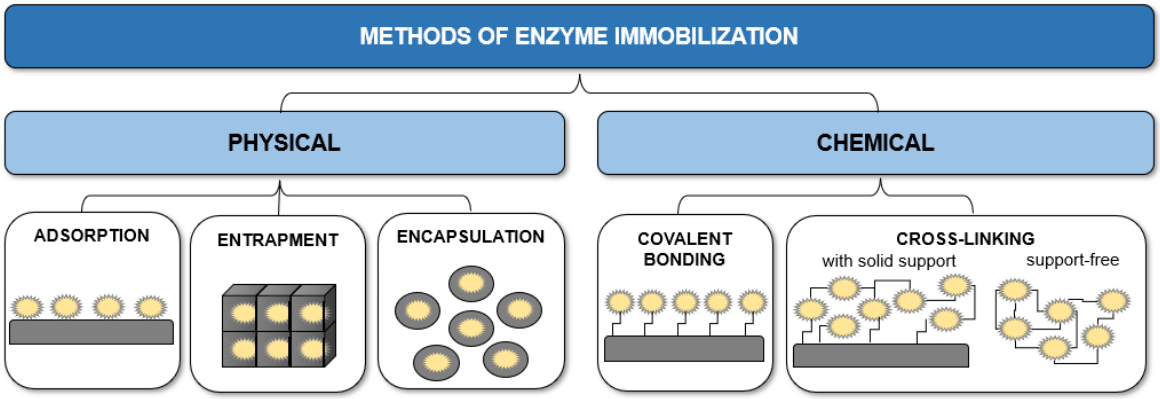

Source: Author

Physical adsorption (or physisorption) is the simplest and less expensive immobilization method. It generally occurs due to non-specific weak forces, such as van der Waals forces, hydrogen bonds, electrostatic or hydrophobic interactions (CHAKRABORTY et al., 2016; FACIN et al., 2019). Because this method relies on a weak interaction between the enzyme and the support, the biocatalyst can easily desorb during the reaction due to changes in pH, ionic strength, temperature, pressure, etc. However, the weak interactions generally do not alter the native structure of the enzyme, preserving the active sites and, thus, maintaining its catalytic activity (JESIONOWSKI; ZDARTA; KRAJEWSKA, 2014).

The entrapment and the encapsulation techniques are based on the irreversible immobilization of the enzyme inside the support material by physical confinement. Generally, there is no chemical interaction between the enzyme and the support, so the enzyme structure is not modified. However, sometimes the contact between the enzyme and the substrate becomes more difficult due to mass transfer limitations (CHAKRABORTY et al., 2016; MOHAMAD et al., 2015). Nevertheless, entrapment and encapsulation techniques generally improve mechanical stability and prevent the enzyme leakage (DATTA; CHRISTENA; RAJARAM, 2013; MOHAMAD et al., 2015.

The covalent bonding technique is used when strong interactions between the enzyme and the support are required (AN et al., 2015; FACIN et al., 2019). Generally, enzyme side-chain amino acids (lysine, cysteine, aspartic acid, glutamic acid) play a key role in the covalent interactions, as well as several functional groups (carboxyl, sulfhydryl, hydroxyl, imidazole, amino, epoxy, indole, thiol, and phenolic groups) (CHAKRABORTY et al., 2016; FACIN et al., 2019). Covalent immobilization generally

results in improvements in enzyme stability and reusability, when compared to other methods, since it promotes a strong link between enzyme and support, preventing enzyme leakage (BERNAL; RODRÍGUEZ; MARTÍNEZ, 2018). Covalent bonding causes chemical modifications in the enzyme, which can be both beneficial and detrimental to catalytic activity. The catalytic activity can be maintained or improved if the amino acid residues involved in the covalent bond do not integrate the active site or substrate-binding site of the enzyme (ELDIN et al., 2011). In this case, beneficial conformational changes that specifically modify the enzyme specificity and selectivity can occur, increasing the catalytic activity (ANTINK et al., 2019). However, covalent immobilization can also cause denaturation, loss of enzyme motility, detrimental conformational changes, blockage of the active site, and/or mass transfer limitations. Therefore, some studies report increases (KUMAR et al., 2019; LI et al., 2019) while others point decreases in the catalytic activity when a covalent bonding method is applied (AGHABABAIE et al., 2016; VILA-COSTA et al., 2017). Although sometimes there is a loss in the enzymatic activity, the gains on reusability and thermal, chemical, and mechanical stability can compensate it and should be taken into account to establish the feasibility of the method.

The cross-linking technique uses a bi- or multifunctional agent to make intermolecular bonds between enzymes or between enzymes and support (MOHAMAD et al., 2015; SHELDON; VAN PELT, 2013). This method is usually applied in combination with other methods, such as adsorption, to minimize enzyme leakage (FACIN et al., 2019). The extensively used Novozym® 435, for example, consists of lipase immobilized by hydrophobic interactions on a macroporous polymer based on butyl and methyl methacrylic esters with divinylbenzene as a cross-linking agent to minimize the desorption (PÄIVIÖ; PERKIÖ; KANERVA, 2012). The main advantage of cross-linking is that, since covalent bonds are formed during cross-linking, enzymes are tightly immobilized, which considerably improves its stability and reusability (LIU; CHEN; SHI, 2018). However, there is the possibility of activity losses due to mass transfer limitations and/or modifications in the enzyme conformation and in the active site during the cross-linking process (CUI; JIA, 2015).

Table 2 summarizes the pros and cons of each immobilization method discussed above. The selection of an adequate technique is a crucial step in the immobilization process as it has a huge influence on the activity and stability of the immobilized enzyme. A wrong choice can lead to structural transformations in the

enzyme and block its active site, causing great losses in the catalytic activity and even the inactivation of the enzyme. Physical methods are indicated when the principal purposes of the immobilization are to maintain the catalytic activity and permit easy separation of the enzyme at the end of the process. Chemical methods, on the other hand, should be used when enhanced stability and reusability are the main goals. The combination of physical and chemical methods (adsorption and cross-linking, for example) can be an interesting strategy to produce immobilized enzymes with both high catalytic activity and stability (LIU; CHEN; SHI, 2018) (LIU; CHEN; SHI, 2018).

Table 2 – Comparison between the most used immobilization techniques

Immobilization technique	**Interaction nature**	**Advantages**	**Disadvantages**
Adsorption	Weak bonds	• Simple and easy • Little or no loss of activity	• Desorption • Non-specific adsorption
Entrapment/ encapsulation	Incorporation of the enzyme inside the support	• No chemical modifications in the enzyme • Support production and enzyme immobilization in a single step • Little or no desorption	• Diffusion barrier • Irreversible
Covalent bonding	Strong chemical bonds	• Little or no desorption • Good reusability • No diffusion barrier	• Irreversible (in most cases) • Can cause chemical modification in the enzyme
Cross-linking	Intramolecular bonds	• Simple • Little or no desorption	• High enzyme activity loss • Diffusion barrier • Irreversible

Source: Author

Several support materials from different origins can be used for enzyme immobilization. An adequate material should preserve the three-dimensional structure of the enzyme when unfavorable reaction conditions occur, maintaining or promoting the catalytic activity and stability, as well as preventing enzyme leakage (BILAL et al., 2018). Support materials can be organic or inorganic. Although organic materials have a better affinity with enzymes since they naturally have reactive groups in their surfaces which facilitate the immobilization, inorganic materials have important advantages, such as better thermal, chemical and mechanical resistances and increased reusability (SIGURDARDÓTTIR et al., 2018; ZUCCA; SANJUST, 2014). Additionally, inorganic

support rigidity ensures that no variance in pore diameter or pore volume will occur during the process (ZUCCA; SANJUST, 2014). Zeolites, metals, and ceramic oxides have already been successfully used as supports for enzyme immobilization (HOLLERMANN et al., 2017). Among inorganic materials, ceramics have a relatively long service life and are relatively less expensive (GOLDSTEIN; MANECKE, 1976; SIGURDARDÓTTIR et al., 2018). Moreover, ceramic membranes are the most used ones among inorganic membranes for oil-water emulsion separation processes. Based on this, the use of ceramic materials for lipase immobilization is highlighted in Section 2.5.

2.5 LIPASE IMMOBILIZATION ON CERAMIC MATERIALS

Lipases are hydrolytic enzymes whose natural function is to hydrolyze the ester bonds present in triacylglycerols (ADLERCREUTZ, 2013). They are very chemoselective, regioselective and stereoselective enzymes that can catalyze a wide range of reactions, including hydrolysis and synthesis by esterification or transesterification (interesterification, alcoholysis, and acidolysis) (GUPTA; BHATTACHARYA; MURTHY, 2013). Lipases can be produced from plants, animals, and microorganisms. Microbial lipases are the most used ones since they can be easily extracted in high yields (JOSHI; SHARMA; KUILA, 2019; PEREIRA; FONTES-SANT'ANA; AMARAL, 2019; TREICHEL et al., 2016).

Lipases have α-β hydrolase fold and a catalytic triad formed by the amino acids serine, histidine, and aspartic acid/glutamic acid. The lipase structure contains four substrate-binding pockets: an oxyanion hole and three pockets. The pockets are used to hold the fatty acids of the substrate at sn-1, sn-2, and sn-3 positions. The active site is protected by an amphiphilic α-helix peptide sequence lid structure (KAPOOR; GUPTA, 2012). When in contact with a hydrophobic surface, hydrophobic residues are exposed and hydrophilic ones are hidden inside, forming an electrophilic region (oxyanion hole) around the serine residues. As can be seen in Figure 3, carboxylic side chains are located at the periphery of the external hydrophobic region. When near a hydrophobic surface, the lid opens, and the catalytic triad becomes accessible for the substrate, which is known as lipase interfacial activation (GUPTA; BHATTACHARYA; MURTHY, 2013).

Because of the interfacial activation of lipases, hydrophobic materials are the most applied for lipase immobilization since they can improve the catalytic activity by rearranging the enzyme conformational structure to its open form (AGHABABAIE et al., 2016). Therefore, when working with ceramic supports for lipase immobilization, it may be necessary to modify the material surface to obtain a suitable hydrophobicity to favor physical adsorption of the enzyme by hydrophobic interactions. The use of silane coupling agents containing hydrophobic groups, the promotion of phenyl (GAMA et al., 2019; GAO et al., 2018), octadecyl (JIN et al., 2018) and octyl (MACHADO et al., 2019; VESCOVI et al., 2016) groups, for example, can be strategies to enhance the support hydrophobicity, favoring the physical adsorption of the lipases.

Figure 3 – Schematic representation of the closed and the open form of a lipase

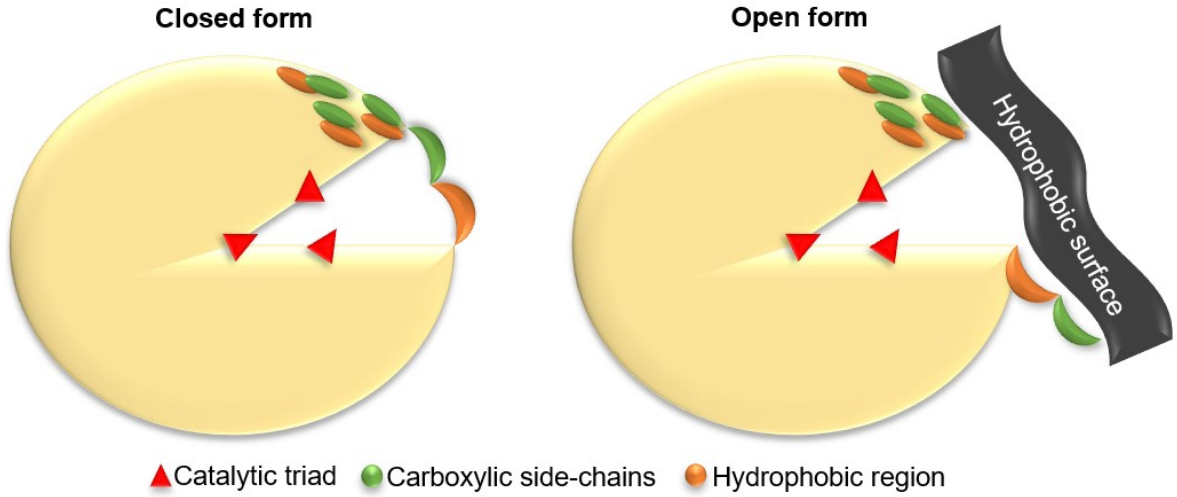

Source: Author

However, the low wettability of hydrophobic materials may hinder the contact between substrate and enzyme and, in the case of oil-water separation, can decrease the oil rejection coefficient of the membrane (AGHABABAIE et al., 2016). Thus, it is possible to use hydrophilic supports promoting covalent bonds between the enzyme and the material. The use of hydrophilic inorganic surfaces can be advantageous since, according to Adlercreutz (2013), it might be interesting to perform lipase immobilization under conditions favoring its closed form to protect the active site and then, after immobilization, change it to its open form.

When using a hydrophilic material, the support surface must have reactive groups able to bond with the lipase. Different from most inorganic surfaces, which naturally present a high degree of hydroxylation, ceramic materials commonly need

activation and functionalization before the immobilization itself (SIGURDARDÓTTIR et al., 2018). Common functionalizing agents are organic compounds such as carbon or silicon-based polymers. Polymers are generally used to coat the support material (instead of forming covalent bonds with it) to promote amino groups. The most commonly used carbon-based polymers are gelatin (AMEUR et al., 2014), PEI (KHAN et al., 2019b; KHOOBI et al., 2015) and PEG (YANG et al., 2010). Recently, PDA coating has also been studied for enzyme immobilization on inorganic materials such as Fe_3O_4 nanoparticles (REN et al., 2011), halloysite nanotubes (CHAO et al., 2013), TiO_2 nanoparticles (CHENG et al., 2018) and monolithic macroporous SiO_2 (CHENG et al., 2019). The amino groups located at the side chain amino acids of the enzyme can react with the quinone groups of the PDA coating through Michael addition or Schiff base reaction, covalently bonding the enzyme to the inorganic surfaces, as shown in Figure 4.

Figure 4 – Examples of enzyme immobilization on ceramic materials through PDA coating: (a) halloysite nanotubes, (b) silica monolith, and (c) Fe_3O_4 nanoparticles

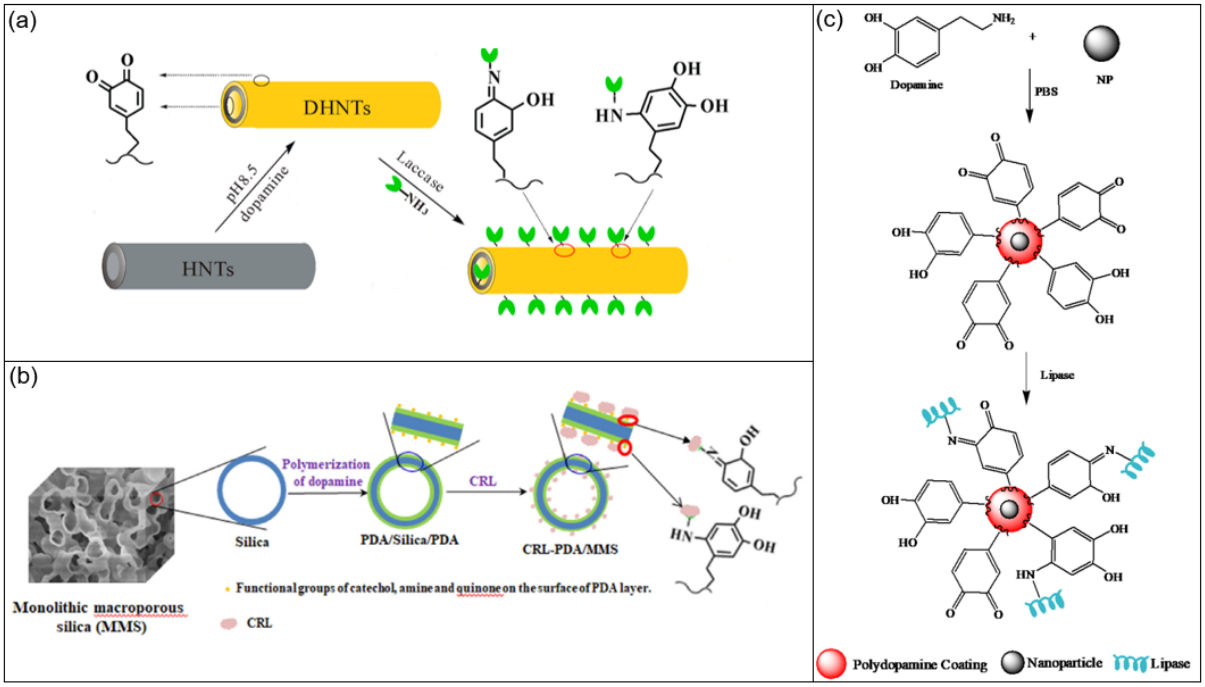

Source: Chao et al. (2013), Cheng et al. (2019) and Touqeer et al. (2019)

Silicon-based polymers, such as organosilanes, usually functionalize the support material by forming covalent bonds between the surface and the silanes, letting an organic functional group extending into the liquid media (SIGURDARDÓTTIR et al., 2018). 3-aminopropyltriethoxysilane (APTES) (CHEN et al., 2019a; FATHI et al.,

2018), TEOS (GUSTAFSSON et al., 2012) and 3-mercaptopropyltrimethoxysilane (MPTMS) (THANGARAJ et al., 2019) are examples of organosilanes used for enzyme immobilization. One possible strategy is to add amino groups on the material surface and then treat it with glutaraldehyde, generating aldehyde groups that will also bond with the amino groups of the enzyme (LYU et al., 2019; MIAO et al., 2018). For example, APTES can be used to create amino groups in the ceramic material (the silane group bonds to the hydroxyl groups of the support leaving an amino group free) and then glutaraldehyde is used to bond both support and enzyme amino groups, as shown on Figure 5. The use of APTES and glutaraldehyde is the most common technique to covalently immobilize enzymes on ceramic materials (SIGURDARDÓTTIR et al., 2018; ZHOU et al., 2019). Table 3 shows examples of ceramic supports (mostly membranes) used for lipase immobilization, summarizing some information about the material physical properties and immobilization techniques.

Figure 5 – Lipase immobilization on ceramic support using APTES and glutaraldehyde as functionalizing agents: (a) hydroxylation, (b) silanization, (c) binding between glutaraldehyde and amino-group of silanized support; (d) enzyme covalent binding

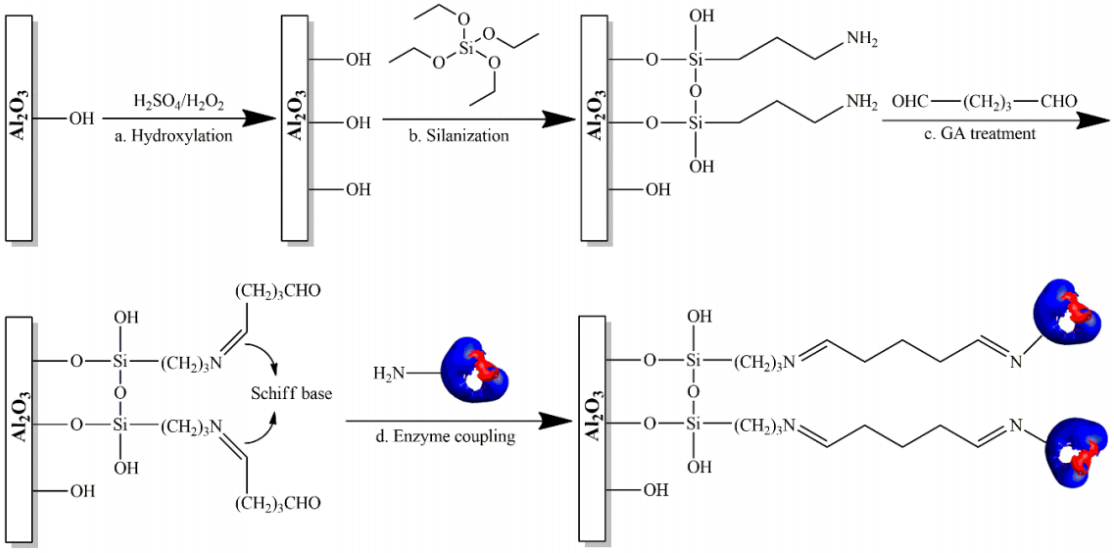

Source: Ranieri et al. (2016)

Table 3 – Examples of ceramic materials used for lipase immobilization, as reported in literature

Material	Physical properties	Enzyme	Immobilization method	Functionalizing agents	Application	Reference
SiO_2 spheres	Surface area: 157.6 m^2/g Pore volume: 0.08 cm^3/g Pore size: 2.42 nm	*Thermomyces lanuginosus* lipase (TLL)	Physical adsorption	PEI	Hydrolysis of p-nitrophenyl butyrate and synthesis of ethyl and methyl valerate	Khoobi et al. (2014)
SiO_2 spheres	Surface area: 157.6 m^2/g Pore volume: 0.08 cm^3/g Pore size: 2.42 nm	TLL	Covalent bonding	PEI and glutaraldehyde (GLU)	Hydrolysis and synthesis of ethyl and methyl valerate	Khoobi et al. (2014)
SiO_2 monolith	Pore volume: 5.25 cm^3/g Pore diameter: 0.34 μm	*Candida rugosa* lipase (CRL)	Covalent bonding	Polydopamine (PDA)	Hydrolysis of *p*-nitrophenyl laurate	Cheng et al. (2019)
Al_2O_3 macroporous material	Surface area: 338.1 m^2/g Pore size: 4.8 nm Pore volume: 0.40 cm^3/g	*Candida antarctica* lipase B (CALB)	Covalent bonding	APTES and GLU	Synthesis of palmitic acid	Zhou et al. (2019)
Al_2O_3 tubular membrane	Pore size: 0.8 μm Hydraulic diameter: 7×10^{-3} m Effective surface: 2.86×10^{-3} m^2	CALB	Covalent bonding	Gelatin and GLU	Hydrolysis of butyl acetate	Ameur et al. (2014)
Al_2O_3 hollow fiber membrane	Outer diameter: 1830 μm Internal diameter: 920 μm Pore volume: 0.34 cm^3/g	CRL	Covalent bonding	APTES and GLU	Hydrolysis of olive oil	Ranieri et al. (2016)
Fe_3O_4 nanoparticles	Particle size: 24.18 nm	*Aspergillus terreus* lipase	Covalent bonding	PDA	Biodiesel production	Touqeer et al. (2019)
Fe_3O_4 and SiO_2 nanocomposite membranes	Roughness: 62 nm Nanoparticles size: 40 nm	CRL	Covalent bonding	APTES and GLU	Hydrolysis	Aghababaie et al. (2016)
TiO_2 tubular membrane	Pore size: 0.8 μm Hydraulic diameter: 2×10^{-3} m Effective surface: 6.5×10^{-3} m^2 Length: 0.13 m	CALB	Covalent bonding	Gelatin and GLU	Hydrolysis of butyl acetate	Ameur et al. (2014)

2.6 IMMOBILIZED ENZYMES AS ANTIFOULING AND SELF-CLEANING AGENTS

As aforementioned, enzymes can be used as catalysts on “active” membranes and are also used in the cleaning solutions of membranes. The use of enzymatic solutions to clean organic fouling of membranes is a well-known environmentally friendly and effective technique introduced in 1996 by Muñoz-Aguado, Wiley and Fane (1996) and Maartens, Swart and Jacobs (1996) that is still in use. However, a great amount of highly active enzymes is wasted at the end of each cleaning step. Thus, the enzyme immobilization on the membrane itself is a way of reuse these enzymes, lowering resource consumption and, also, improving enzyme stability (SCHMIDT et al., 2018). Besides the self-cleaning capacity, the immobilization of certain enzymes in the membrane also provides antifouling ability against some compounds. According to Schmidt et al. (2018), the immobilization of digestive enzymes (proteases, lipases, and amylases, for example) on the membrane surface allows the contact between enzymes and fouling substances adsorbed on the surface during filtration. Therefore, the fouling layer can be degraded by the enzymes during the filtration (antifouling property) or by activating the enzymes through the adjustment of ambient conditions, such as pH and temperature, during the cleaning procedure (self-cleaning capacity), as schematized in Figure 6. The main goal is to reduce the costs of membrane separation processes, making them more attractive to the industry, mainly for low-profit applications such as wastewater treatments.

Although there are several studies in the literature regarding enzyme immobilization on membranes for the synthesis of valuable compounds (CHEN et al., 2019b; RANIERI et al., 2016; YUJUN et al., 2008; ZARE et al., 2019), there is just a few focusing on the use of immobilized enzymes for enhancing the performance of membrane separation processes. The first studied found on the literature after searching *Portal de Periódicos CAPES* (which includes several databases such as Science Direct, Scopus, Web of Science, Scielo, among many others) regarding the use of immobilized enzymes as antifouling and self-cleaning agents in membranes is from 1977 and approaches the use of immobilized proteases in polysulfone membrane used for the ultrafiltration of cheddar cheese whey (VELICANGIL; HOWELL, 1977). The authors noticed a lower flux decline when the active membranes were used. Six more works were published in the ‘80s after that: four using proteases to minimize

protein fouling in polymeric ultrafiltration membranes used in food industry processes (HOWELL; VELICANGIL, 1980, 1982; VELICANGIL; HOWELL, 1981; WANG et al., 1980), one using pectolytic enzymes and proteases for the ultrafiltration of raw sewage (first to focus on wastewater treatment) (JENQ; WANG; DAVIDSON, 1980), and one using immobilized pectinase in a metallic membrane as an antifouling agent in the clarification of apple juice (first using an inorganic membrane) (THOMAS; MCKAMY; SPENCER, 1989).

Figure 6 – Schematic degradation of the fouling layer by the enzymatic membrane during filtration (a) and cleaning (b)

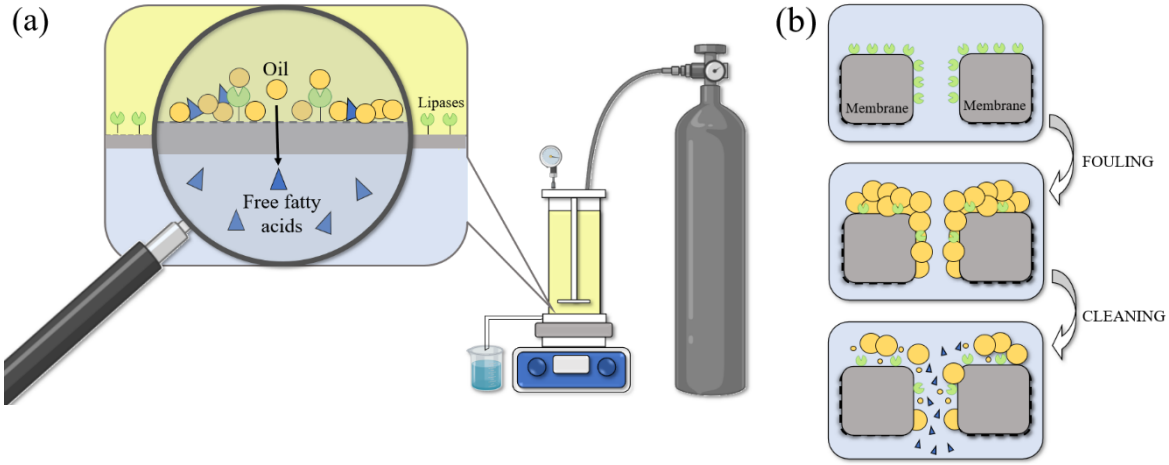

Source: Author

Until 1998, only proteases and pectinases had been evaluated as antifouling agents, mainly in food industry processes (CHEN; WANG; ZHU, 1992; SZANIAWSKI; SPENCER, 1996, 1997; WANG et al., 1994). But then came the work of Giorno et al. (1998) who immobilized commercial enzyme mixtures (containing pectinase, cellulase and hemicellulase) in polyamide capillary membranes for apple juice clarification. The authors noticed that the permeate flux was higher when the enzymes were immobilized on the membrane when compared to the use of free enzymes directly added to the feed. In 2002, Edwards, Leukes and Bezuidenhout (2002) published the second study approaching immobilized enzymes in membranes as antifouling and self-cleaning agents for wastewater treatment. They immobilized peroxidase and laccase on polysulfone membranes for the treatment of petrochemical industry wastewater by ultrafiltration. They achieved a 25% increase in flow when using the membrane with the immobilized enzymes. In 2009, a study was published with urease immobilization on cellulose acetate membranes for use in hemodialysis (MAHLICLI; ALTINKAYA,

2009). The immobilization of urease improved the mass transfer and the biocompatibility of the membrane, demonstrating the diversity of applications in which enzymes can be used as antifouling agents.

From then on, several enzymes were evaluated as antifouling and self-cleaning agents in membrane separation processes for the various purposes: acylase, protease, lysozyme, pectinase, lipase, and amylase to mitigate biofouling (DU PLESSIS et al., 2013; KEHAIL; BRIGHAM, 2018; KIM et al., 2011, 2018; LAN; HIEBNER; CASEY, 2021; LEE et al., 2019a; LIU et al., 2015; MEHRABI et al., 2020; SAEKI et al., 2013; SUN et al., 2016; VILLA et al., 2015; ZHAO et al., 2015), proteases for protein fouling (CHEN et al., 2021; KOSEOGLU-IMER; DIZGE; KOYUNCU, 2012; SCHULZE et al., 2015; SHI et al., 2011; VANANGAMUDI et al., 2018a, 2018b; YUREKLI, 2020), pectinase for olive mill wastewater filtration (GEBREYOHANNES et al., 2013), polygalacturonase for the treatment of vegetation wastewater and xylanase for the treatment of bio-ethanol production, brewery and bakery wastewaters (GEBREYOHANNES et al., 2015), proteases, lipases, and amylases for anaerobic membrane bioreactors (WONG; LEE; TEO, 2015), pectinase to mitigate pectin fouling (GEBREYOHANNES et al., 2016, 2017), alginate lyase for alginate fouling (MESHRAM et al., 2016), cellulolytic enzymes for glucose production from cellulose (GEBREYOHANNES et al., 2018), transglutaminase for the separation of proteins from cheese whey (WANG et al., 2018b), α-amylase for ultrafiltration of starch (KOLESNYK et al., 2019, 2020), laccase for dyeing wastewater treatment (ZHU et al., 2020), and peroxidase for the filtration of micropollutants (ZHANG et al., 2021b).

Specifically for oil-water separation, membranes with immobilized lipases stand-out since lipases can catalyze triacylglycerol hydrolysis, generating free fatty acids and glycerol. Schulze et al. (2017) covalently immobilized pancreatin (a mixture of lipase, protease, and amylase) in polyethersulphone flat sheet membranes for the microfiltration of linseed oil solution. The “active” membrane showed 33% less permeance reduction than the unmodified membrane during the separation process and a recovery of 75% of water flux after self-cleaning (using phosphate-buffered saline at pH 8 and 37 ºC overnight). Schmidt et al. (2018) covalently immobilized *Candida rugosa* lipase (CRL), α-amylase and porcine pancreatin on PVDF flat sheet membranes for the treatment of a linseed oil emulsion, a mixture of linseed oil, alginate, and albumin (simulating a more complex wastewater), and real household sewage. Figure 7 shows the results for water permeance after fouling and self-cleaning for the

untreated and “active” membranes. It can be noticed that the enzyme immobilization on the membrane improved the performance of the separation process for all the simulated and real wastewater tested. Recently, the same research group immobilized lipases on PVDF flat sheet membranes using electron beam irradiation aiming at self-cleaning capacity (SCHMIDT et al., 2022). The lipolytic membrane was tested in the filtration of olive oil emulsion and showed a 100% regeneration of filtration performance after 3 h of cleaning in an aqueous buffer pH 8 at 37 °C and 95% regeneration after three consecutive filtration steps.

Figure 7 – Results obtained by Schmidt et al. (2018) when using lipase, α-amylase and pancreatin immobilized on a PVDF membrane as antifouling and self-cleaning agents for the filtration of (a) linseed oil emulsion, (b) linseed oil, alginate and albumin mixture, and (c) household sewage (pristine membrane in black and enzymatic membrane in blue)

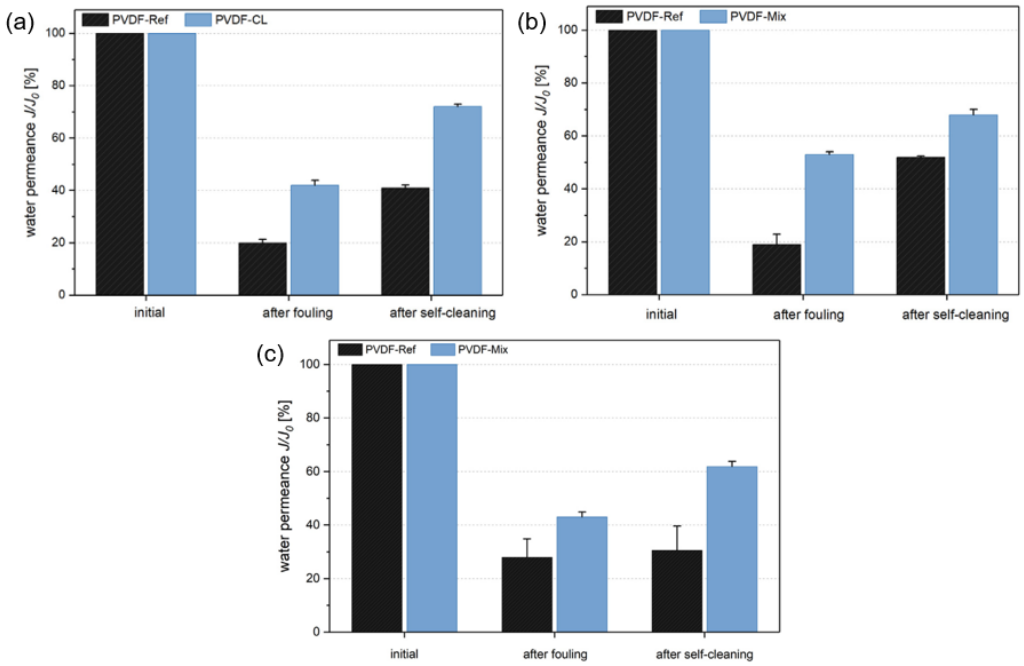

Source: adapted from Schmidt et al. (2018)

So far, most of the studies focused on biofouling control or protease immobilization for protein fouling mitigation, flat sheet polymeric membranes are the most evaluated, and food industry processes are the most studied. Thus, it is noted that the use of enzymes as antifouling and self-cleaning agents in membranes is a relatively unexplored area due to the huge variety of enzymes, membranes, and membrane separation processes that can be improved using immobilized enzymes. These processes can be both the synthesis of commercial products and the treatment

of wastewaters, whether industrial or domestic and even the treatment of drinking water. The use of enzymes as antifouling and self-cleaning agents is a technology that can offer several economic, operational, and environmental advantages, mainly due to the increase in membrane lifespan and the reduction in the use of chemicals.

2.7 CLOSING REMARKS

The development of self-cleaning and antifouling membranes through enzyme immobilization can be an efficient and environmentally friendly alternative to be used in wastewater treatment. The immobilized enzymes can improve the membrane permeation performance by reducing fouling and, consequently, decreasing the frequency of cleaning procedures. When the cleaning is necessary, the immobilized enzymes can degrade the fouling by just immersing the membrane in a buffer solution with adequate pH and temperature, avoiding extensive chemical cleaning steps. This can increase the membrane lifespan, besides reducing waste generation and energy consumption, turning the process more sustainable.

However, to be used at an industrial level (especially for low-profit applications such as wastewater treatment), this technology requires a breakthrough, mainly related to the reduction of the biocatalysts' costs, membrane lifespan and immobilization protocols. Regarding lifespan, ceramic membranes are promising alternatives due to their high resistance to chemicals, temperature, pH and mechanical stress, as well as the ease of being regenerated and reused. As discussed, lipases can be successfully immobilized on ceramic materials using different techniques. A successful immobilization protocol must guarantee a good enzymatic activity and stability over the process conditions and must allow the reuse of the active membrane for several cycles. Thus, lipase immobilization on ceramic membranes using an adequate method can be a potential solution to the development of a robust antifouling and self-cleaning membrane to be applied in wastewater treatment.

3 COMPARISON BETWEEN APTES AND PDA AS IMMOBILIZATION AGENTS

This chapter shows the screening between different lipase immobilization methods using ceramics as support. The main objective was to compare the traditional method of silanization using 3-aminopropyltriethoxysilane (APTES) with the innovative technique of polydopamine coating (PDA) for lipase immobilization on α-alumina membranes. The activation with glutaraldehyde (GA) was also tested for both protocols. Three lipases were tested, and Eversa Transform 2.0 (ET2) was chosen to be immobilized in the membrane due to its high hydrolytic activity towards soybean oil. Polydopamine deposition with and without glutaraldehyde activation presented the highest membrane hydrolytic activities (1.55 ± 0.21 and 1.85 ± 0.28 $mmol \cdot min^{-1} \cdot m^{-2}$, respectively). The membrane without activation maintained 41.1 ± 1.7 % of the free enzyme activity while the one with glutaraldehyde preserved only 23.9 ± 1.0 %. When tested in oil-water separation using a soybean oil-water emulsion, the membranes with ET2 immobilized by PDA showed water permeance 2-fold higher than the nonactive membranes (300 ± 12 and 156 ± 4 $L \cdot h^{-1} \cdot m^{-2} \cdot bar$, respectively), showing good fouling-degrading capacity. They also presented self-cleaning properties when activated through the use of proper pH and temperature. The water permeance recovery for the pristine membrane was 34% while the membranes with immobilized ET2 by PDA and APTES showed recoveries of 69% and 49%, respectively. Permeance recovery for ET2 immobilized by silanization was similar to the PDA-coated membrane with no enzyme (45%). The results of this chapter were published in the paper “Lipase immobilization on alumina membranes using a traditional and a nature-inspired method for active degradation of oil fouling” at Separation and Purification Technology[3].

3.1 INTRODUCTION

Many traditional physical and chemical techniques are used to remove oil from wastewaters, such as gravity settling, coalescence, skimming, air flotation, flocculation, and coagulation. However, these methods have limitations when the wastewater contains emulsified oil with droplet diameter of 20 μm or less (PORNEA et al., 2020).

[3] https://doi.org/10.1016/j.seppur.2022.120527

Membrane separation processes have proven to be a good alternative in such cases, presenting advantages such as high oil removal efficiencies, no need for chemical additives, and compact facilities that can be fully automated (ABBASI et al., 2012; KHOUNI et al., 2020).

Even though membrane systems are widely studied, the applicability of these processes in the treatment of oily wastewaters still has limitations, mainly related to fouling issues. Fouling causes a permeate flux decline, consequently decreasing the system efficiency, increasing the energy consumption and the frequency of membrane cleaning procedures, which in turn can decrease the membrane lifespan and increase the process costs (TANUDJAJA et al., 2019). Membranes made of hydrophilic materials are generally less susceptible to oil fouling than hydrophobic ones. In this sense, ceramic membranes have some advantages, since they generally are highly hydrophilic, very stable at high temperatures and pressures, can reach high water flux, have great chemical stability, lifespan, reusability, and mechanical resistance during filtration (ABBASI et al., 2012; JEONG et al., 2018). However, even though the production costs of ceramic membranes have been decreasing over the years with the development of new technologies, they still limit the use of ceramic membranes in environmental applications (ISSAOUI; LIMOUSY, 2019). Besides the production costs, fouling is still a problem that increases the operational expenses of membrane systems, restricting even more the use of ceramic membranes in low-profit applications.

Several strategies have continuously been developed to minimize fouling such as the immobilization of enzymes on the membrane surface in an attempt to develop an “active” membrane capable of degrading fouling during the separation process (KIM et al., 2021; KOLESNYK et al., 2019; KOSEOGLU-IMER; DIZGE; KOYUNCU, 2012; LAN; HIEBNER; CASEY, 2021; NG; WRIGHT; SEAH, 2011). Besides improving the membrane system performance, the immobilized enzymes can also provide the membrane with a self-cleaning capacity, reducing the consumption of chemicals during the cleaning step (SCHMIDT et al., 2018; SCHULZE et al., 2017; VANANGAMUDI et al., 2018a).

The most common technique to immobilize enzymes in inorganic supports, such as ceramic membranes, is the silanization of the material followed by activation with glutaraldehyde (DOS SANTOS et al., 2021; SIGURDARDÓTTIR et al., 2018; ZHOU et al., 2019). Nevertheless, it is a time-consuming method since three steps are

required: silanization, activation, and immobilization. Moreover, the toxicity of the reagents used in this protocol is a concern to the environment and public health (BEAUCHAMP et al., 1992; NAKASHIMA et al., 1998; TAKIGAWA; ENDO, 2006; VAN BIRGELEN et al., 2000). Thus, the search for simple and less hazardous immobilization protocols is essential to develop a more economic, competitive, safer, and environmentally friendly process.

Lately, polydopamine (PDA) coatings have attracted noteworthy attention for surface modification (GAO; FAN; XU, 2020; MAVUKKANDY et al., 2022). The development of PDA coatings was inspired by the secretions of marine mussels that can form a strong adhesive layer in different substrates (BURZIO; WAITE, 2000; YAN et al., 2020). According to Dalsin et al. (2003), L-3,4-dihydroxyphenylalanine (L-DOPA) and its derivative dopamine are critical compounds for this adhesive capacity. Thus, several organic and inorganic materials have been successfully modified by dopamine polymerization forming thin PDA layers (GAO; XU, 2019; KASEMSET et al., 2016; XIANG; LIU; XUE, 2015). PDA coating itself can improve the antifouling capacity of the membranes in oil-water emulsions by increasing its hydrophilicity (KASEMSET et al., 2016; ZARGHAMI; MOHAMMADI; SADRZADEH, 2019; ZIN et al., 2019). Moreover, due to the presence of different reactive groups (such as amine, imine, and catechol) in the PDA layer, this technique can be used to bond several materials and molecules to the membrane, including enzymes (CHENG et al., 2018, 2019; LUO et al., 2014; MORTHENSEN et al., 2017; TOUQEER et al., 2019).

The immobilization of lipase (triacylglycerol hydrolases, EC 3.1.1.3) in the membrane could be an alternative to improve the fouling-degrading and self-cleaning capacity of the membrane in the treatment of oily wastewater. Lipase can catalyze fouled oil hydrolysis, degrading the triacylglycerols of the oil into fatty acids and glycerol (TREICHEL et al., 2016). Moreover, the lipase present in the membrane can be an alternative to the use of chemicals during membrane cleaning, making the process more environmentally friendly.

This study aims to immobilize the lipase Eversa Transform 2.0 (ET2) in α-alumina tubular membranes through PDA coating and compare this technique with the traditional silanization protocol. The main objective is to show that it is possible to immobilize the enzyme in ceramic supports using simple and less hazardous functionalizing agents. Also, the development of an “active” ceramic membrane capable of degrading the oil fouling during the filtration process (decreasing the

frequency of cleaning) and with self-cleaning properties (decreasing the consumption of harsh chemicals) is evaluated. This is a first step in the development of an active membrane to be used in the food industry, for example, as well as in its wastewater treatment facilities. To the best of our knowledge, there is no study in the literature about lipase immobilization in ceramic membranes using PDA coatings. Only a few studies proposed the use of immobilized enzymes as fouling-degrading and self-cleaning agents, but no one has tested the lipase Eversa Transform 2.0. Furthermore, no study was found comparing silane and PDA functionalization for enzyme immobilization with the same support material and under controlled reaction conditions.

3.2 MATERIAL AND METHODS

3.2.1 Chemicals and materials

Three different lipases liquid solutions were supplied by Novozymes (Denmark): Eversa Transform 2.0 (ET2) (produced by a genetically modified strain of *Aspergillus oryzae*), Lipozyme TL 100L (produced by a *Thermomyces lanuginosus* strain), and Lipozyme CALB (produced by *Candida antarctica*).

α-Alumina porous tubes were custom-made (Tecnicer, Brazil) (Figure 8). According to the manufacturer, the tubes were extruded and sintered at 1180 °C. Their dimensions are 25 cm in length, 1.2 cm of outer diameter, and 0.8 cm of inner diameter. The average pore size and the total porosity, determined by mercury intrusion porosimetry, are 290 nm and 42.65%, respectively. The pore size distribution is shown in Figure 9.

The following chemicals were used: dopamine hydrochloride (DA, $C_8H_{11}NO_2$.HCl, Sigma-Aldrich), glutaraldehyde 25% (GA, $C_5H_8O_2$, Vetec), 3-aminopropyltriethoxysilane 99% (APTES, $C_9H_{23}NO_3Si$, Sigma-Aldrich), sodium dodecyl sulfate 90% (SDS, $C_{12}H_{25}SO_4Na$, Synth), polyvinyl alcohol (PVA, $(C_2H_4O)_x$, Neon), sodium hydroxide (NaOH, Neon), ethanol (C_2H_6O, Neon), and phenolphthalein ($C_{20}H_{14}O_4$, Sigma-Aldrich). For the Tris-HCl buffer preparation, tris(hydroxymethyl)aminomethane ($C_4H_{11}NO_3$, Neon) and hydrochloric acid 37% (HCl, Neon) were used. The sodium phosphate buffer was prepared using sodium phosphate monobasic (NaH_2PO_4, Neon) and sodium phosphate dibasic (Na_2HPO_4,

Neon). All chemicals were analytical grade and used without further purification. Refined soybean oil (Soya, Brazil) was purchased from a local market.

Figure 8 – α-Alumina porous tubes custom-made by Tecnicer (Brazil) and used as membranes

Source: Author

Figure 9 – Pore size distribution of the α-alumina membranes

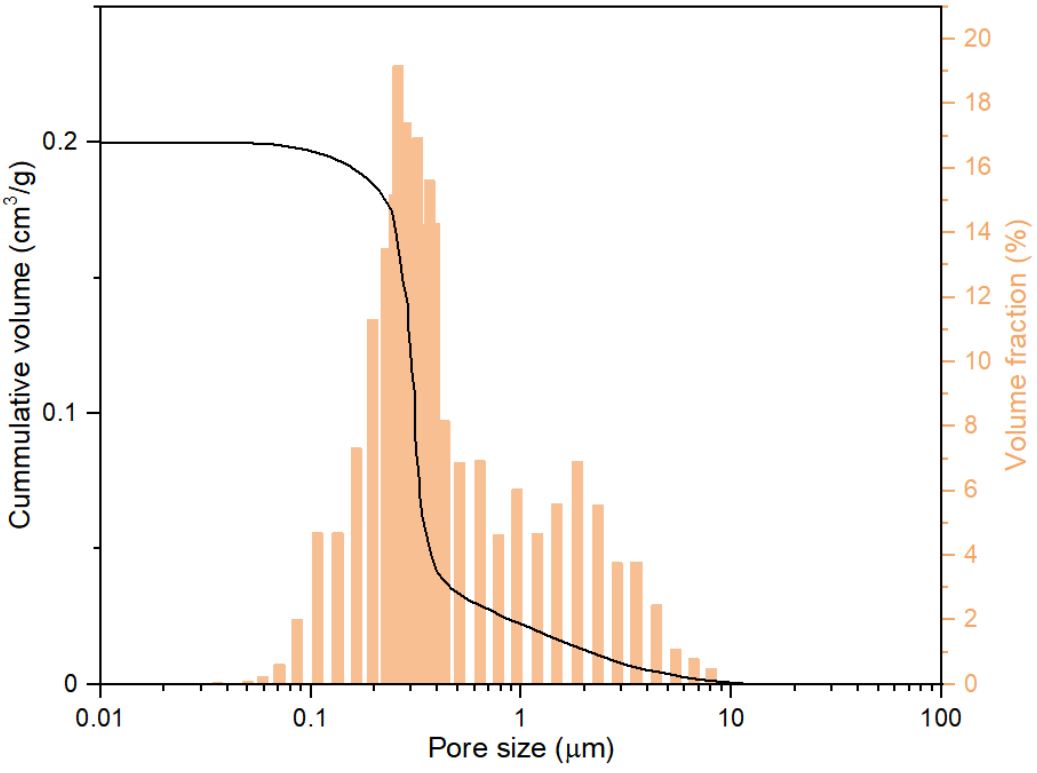

Source: Author

3.2.2 Lipase selection

The choice of the lipase to be immobilized on the membrane was based on the enzyme hydrolytic activity using soybean oil as substrate. For this purpose, soybean oil (25% v/v) was emulsified in an aqueous solution of PVA 2% (m/v) using a magnetic stirrer at 1500 rpm for 10 min according to the method proposed by Fu et al. (1995). Then, 4 mL of the emulsion was added to 5 mL of sodium phosphate buffer 0.1 mol·L^{-1} pH 7.0 and 1 mL of each lipase solution (ET2, TL 100L, and CALB). After incubation for 30 min at 45 °C and agitation of 160 rpm, the reaction was interrupted through the addition of 15 mL of ethanol. The concentration of fatty acids liberated during the reaction was determined by titration using NaOH 0.1 mol·L^{-1} and phenolphthalein as a pH indicator. Control assays were carried out by adding ethanol right after the addition of the enzyme. The hydrolytic activity (*HA*) was calculated using Eq. 1. All tests were performed in triplicate.

$$HA\ (mmol \cdot min^{-1} \cdot mL^{-1}) = \frac{(V_s - V_c) \times M}{t \times V} \quad (1)$$

in which V_s is the NaOH volume used to titrate the sample (mL), V_c is the NaOH volume used to titrate the control assay (mL), M is NaOH molarity (mol·L^{-1}), t is the reaction time (min), and V is the volume of enzymatic solution added to the reaction media (mL).

3.2.3 Enzyme preparation

Dialysis using sodium phosphate buffer 50 mmol·L^{-1} pH 6.0 for 120 h was performed to remove impurities and stabilizers from the commercial solution and concentrate the chosen lipase. After the dialysis, the purified enzyme solution was frozen at -20 °C and lyophilized for 48 h (Liotop model L101n). The resulting powder was stored at 4 °C until use.

The hydrolytic activity of the lyophilized lipase was determined using the method described in Section 3.2.2 with minor modifications: 4 mL of the emulsion was added to 6 mL of sodium phosphate buffer 0.1 mol·L^{-1} pH 7.0 containing 1 mg·mL^{-1} of the lyophilized enzyme (this solution was stirred at 300 rpm for 1 h before the test). To compare the lipase activity before and after purification and lyophilization, the specific

hydrolytic activity (HA_s) was calculated based on the total protein present in each test using Eq. 2. The tests were performed in triplicate.

$$HA_s\ (mmol \cdot min^{-1} \cdot g^{-1}) = \frac{(V_s - V_c) \times M}{t \times V \times PC} \quad (2)$$

in which V_s is the NaOH volume used to titrate the sample (mL), V_c is the NaOH volume used to titrate the control assay (mL), M is NaOH molarity (mol·L^{-1}), t is the reaction time (min), V is the volume of enzymatic solution added to the reaction media (mL), and PC is the protein content of the enzymatic solution (g·mL^{-1}) determined by the Bradford method using bovine serum albumin as a standard (BRADFORD, 1976).

3.2.4 Lipase immobilization

The traditional immobilization protocol using 3-aminopropyltriethoxysilane (APTES) and glutaraldehyde (GA) was compared to the polydopamine (PDA) coating technique with and without glutaraldehyde activation. The lipase was immobilized in the membrane by simple adsorption as a control assay (membrane with no modification), and functionalization of the membrane using only glutaraldehyde was also evaluated. The next sections describe the immobilization methods in detail.

Before each test, the membrane extremities were sealed with a thermoplastic adhesive to functionalize only the external surface. Then, they were immersed in ultrapure water for 2 h and dried in an air-circulation oven for 12 h at 30 °C. After the functionalization, the membranes were rinsed with ultrapure water to eliminate the excess of the solutions. Then, they were immersed in a 2 mg·mL^{-1} lipase solution at sodium phosphate buffer 100 mmol·L^{-1} pH 7 for 12 h at room temperature using an agitation table at 40 rpm (the enzymatic solution was stirred at 300 rpm for 1 h before the test). The membranes were then rinsed several times with sodium phosphate buffer 100 mmol·L^{-1} pH 7 for 10 min at 40 rpm to remove the weakly bound enzymes until no protein was detected using the Bradford method. All immobilization protocols were tested in triplicate.

The amount of immobilized enzyme was determined with the Bradford method in the solution before and after immobilization, also considering the protein removed by the rinsing steps. Enzyme loading (EL) was obtained using Eq. 3.

$$EL\ (g \cdot m^{-2}) = \frac{(C_o - C_f) \times V - M_r}{A} \quad (3)$$

in which C_0 is the initial protein content in the solution (before the immobilization) (g·mL^{-1}), C_f is the final protein content (after the immobilization) (g·mL^{-1}), V is the volume of enzyme solution used in the test (mL), M_r is the amount of weakly bound protein removed by the rinsing step (g), and A is the membrane external area (m^2).

The hydrolytic activity of the immobilized lipase was evaluated by immersing the membrane in 50 mL of emulsion (prepared as described in item 3.2.2) and 75 mL of sodium phosphate buffer 0.1 mol·L^{-1} pH 7 using rectangular glass vessels. The vessels were incubated for 30 min at 40 rpm and 35 °C. Then, a homogenized sample of 10 mL was withdrawn from the solution and titrated with NaOH 0.1 mol·L^{-1} to determine the amount of free fatty acids liberated. A control assay was performed to each condition tested using a membrane with the functionalizing agents but without the enzyme. The membrane hydrolytic activity (*MHA*) was calculated according to Eq. 4.

$$MHA\ (mmol \cdot min^{-1} \cdot m^{-2}) = \frac{(V_s - V_c) \times M \times (V_t/V)}{t \times A} \quad (4)$$

in which V_s is the NaOH volume used to titrate the sample (mL), V_c is the NaOH volume used to titrate the control assay (mL), M is NaOH molarity (mol·L^{-1}), V_t is the total volume of emulsion used in the test (mL), V is the volume of the emulsion sample titrated (mL), t is the reaction time (min), and A is the membrane external area (m^2).

Depending on the immobilization method, the enzymatic activity can decrease, increase, or stay the same. Thus, the specific hydrolytic activities of the free lipase (Eq. 2) and immobilized lipase (MHA_s) (Eq. 5) were determined. Residual activity was calculated by Eq. 6 to estimate the effect of the immobilization protocol on the enzyme activity.

$$MHA_s\ (mmol \cdot min^{-1} \cdot g^{-1}) = \frac{(V_s - V_c) \times M \times (V_t/V)}{t \times A \times EL} \quad (5)$$

in which V_s is the NaOH volume used to titrate the sample (mL), V_c is the NaOH volume used to titrate the control assay (mL), M is NaOH molarity (mol·L^{-1}), V_t is the total

volume of emulsion used in the test (mL), *V* is the volume of the emulsion sample titrated (mL), *t* is the reaction time (min), *A* is the membrane external area (m^2), and *EL* is the protein loading immobilized in the membrane ($g \cdot m^{-2}$).

$$Residual\ activity\ (\%) = 100 \times \frac{MHA_S}{HA_S} \quad (6)$$

The statistical difference between the immobilization protocols for protein loading, membrane hydrolytic activity, and specific hydrolytic activity were determined through analysis of variance (ANOVA) followed by Tukey's test with a confidence level of 95% ($p < 0.05$).

3.2.4.1 Silanization and activation

Since it is the most used method for enzyme immobilization on ceramic materials, APTES functionalization followed by glutaraldehyde activation was used as a standard procedure. The method used was adapted from Ranieri et al. (2016). A solution containing APTES (5% v/v), ultrapure water (5% v/v), and ethanol (90% v/v) was prepared and its pH was adjusted to 5.0 using acetic acid. The membrane was immersed in the solution and, after 6 h at 40 rpm and room temperature, the membrane was rinsed with ethanol and ultrapure water and used in the activation step. The membrane was immersed in an aqueous solution of glutaraldehyde (2.5 % v/v) for 2 h at 40 rpm and room temperature, based on the method used by Asmat et al. (2019). A membrane with no functionalization was also activated using glutaraldehyde for comparison.

3.2.4.2 Polydopamine coating

PDA deposition was performed by air oxidation, according to a method adapted from Proner et al. (2020) and Gao and Xu (2019). The membrane was immersed in a solution of dopamine hydrochloride (DA) (2 $mg \cdot mL^{-1}$) dissolved in Tris-HCl buffer (pH 8.5, 50 $mmol \cdot mL^{-1}$) for 6 h at 40 rpm and room temperature (25 °C). The membrane was then rinsed with ultrapure water and used in the next

functionalization/immobilization steps. The PDA-coated membranes were tested with and without glutaraldehyde activation (described in section 3.2.4.1).

3.2.5 Optimum operating temperature and pH of the free and immobilized lipase

The effects of pH and temperature on the free and immobilized ET2 were investigated during oil hydrolysis. Both free and immobilized lipase activities were determined using different temperatures (20 – 60 °C) and pH values (4 – 10). Free ET2 activity was determined as described in section 3.2.3 and immobilized ET2 activity as described in section 3.2.4; however, instead of phenolphthalein as an indicator, titration was performed until pH 11 due to the different pH values used as the method described by Treichel et al. (2016).

3.2.6 Preliminary fouling and cleaning assays

Oil-water emulsion filtration was performed using a membrane modified with the best immobilization procedure (the one that resulted in the higher membrane hydrolytic activity) to assess if the immobilized lipase could resist a pressure-driven filtration and act as a fouling-degrading and self-cleaning agent. The membrane without modification and the functionalized membranes with and without the enzyme were tested in triplicate.

An emulsion of 1 $g \cdot L^{-1}$ of refined soybean oil in an aqueous solution of SDS 2 $mmol \cdot L^{-1}$ (emulsifier) was prepared and used as feed in the separation system. A coarse emulsion was prepared by magnetic stirring at 1000 rpm for 5 min, followed by probe sonication (DES5000, Unique) at 100 W for 5 min. The emulsion pH was 6.3 ± 0.5. The size of the oil droplets was determined by dynamic light scattering (Zetasizer Nano ZS3600, Malvern).

Fouling experiments were conducted based on the procedures described by Schmidt et al. (2018) and Proner et al. (2020). Firstly, distilled water was filtered to determine the initial water permeance. Then, two filtration steps using the oil-water emulsion were performed. Every 15 min, approximately 5 mL of the permeate was collected and weighed in a semi-analytical balance to calculate the permeate flux. The oil concentration in the sample was measured using a UV–visible spectrophotometer at a wavelength of 240 nm (Q898U2M5, Quimis) (ZIN et al., 2019). At the end of each

filtration step, a backwash was carried out using distilled water to remove weakly bound fouling layers. After the final backwash, water permeance was determined again to evaluate the residual degree of fouling. The experiments were performed using a stainless-steel single-channel module (15 mm of internal diameter) in crossflow and total reflux operating mode as represented in Figure 10. A transmembrane pressure of 1 bar, a retentate flow rate of 1 $L \cdot min^{-1}$, and a crossflow velocity of 0.20 $m \cdot s^{-1}$ were used. Sealing rings were fixated after 1 cm in length in both extremities of the membrane, providing a useful membrane length of 23 cm and a flow area of 79.5 cm^2. All the tests were performed at room temperature (23 ºC).

After the fouling experiments, the self-cleaning capacity of the membranes was evaluated and expressed as the increase in pure water permeance after cleaning (Eq. 8). The membranes were immersed in sodium phosphate buffer 100 $mmol \cdot L^{-1}$ pH 7 for 12 h at 40 rpm and 40 °C to activate the enzymes. Finally, the membranes were washed with distilled water and the water permeance was measured.

Figure 10 – Schematic representation of the crossflow permeation system used in the fouling experiments

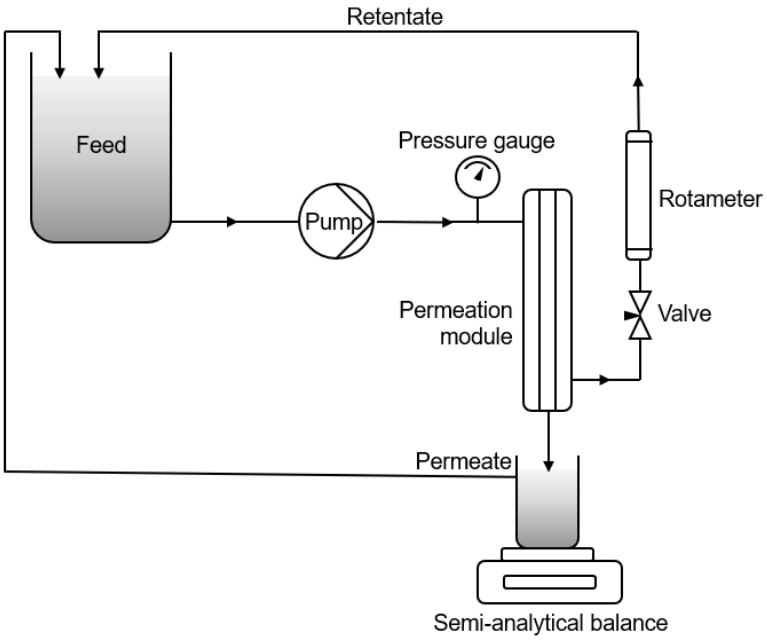

Source: Author

To investigate the reusability of membranes in long-term applications, repetitive cycles of filtration and cleaning were performed (cycles 1–3). The number of filtration steps within each cycle was two. The emulsion was prepared as described above as well as the filtration and self-cleaning experiments.

3.2.7 Membrane characterization

Membrane microstructure was characterized by Scanning Electron Microscopy (SEM, TM 3030, Hitachi) at 15 kV coupled with Electron Dispersion X-ray (EDX, Quantax 70, Bruker) for a qualitative analysis of the chemical elements present in the membrane surface. EDX was performed in three regions of 26.4 μm^2 for each of the scanned images. The crystallinity of the α-alumina membranes was determined using X-ray Diffractometry (XRD, MiniFlex600, Rigaku) in the 2θ range of 10° to 140°, speed of 2.4°·min^{-1} and a step size of 0.02°. The crystallinity index (CI, Eq. 7) of the membrane surfaces was calculated according to Navarro-Pardo et al. (2013) and Khan et al. (2019a) since the presence of the functionalizing agents and the enzyme can cause a loss of crystallinity in the material's surface and then be detected by the XRD analysis.

$$CI\ (\%) = \frac{A_c}{A_c + A_a} \times 100 \quad (7)$$

where A_c is the integrated area underneath the crystalline peaks and A_a is the integrated area of the amorphous phase.

Membrane wettability was investigated using water and n-heptane vapor adsorption measurements which were performed by placing glass vessels with approximately 0.2 g of crushed membrane samples (with particle size ≤ 300 μm) inside closed Erlenmeyer flasks containing water or n-heptane at 23 °C (NISHIHORA et al., 2018; PRENZEL et al., 2014). The samples were weighed at the beginning of the test and after 24 h to determine the vapor uptake. The analysis was performed in triplicate. Apparent density, apparent porosity, and water absorption were determined by the Archimedes principle using distilled water, according to ASTM C20 (2000). The total density of the pristine membrane was also determined by helium pycnometry. The apparent density determined by the Archimedes principle was used to calculate the total porosity and the closed porosity of the membrane. The surface chemistry of the pristine and modified membranes were characterized by X-ray Photoelectron Spectroscopy (XPS, PHI Quantera, MN, USA) using monochromatic Al Kα X-rays. The membranes and the lyophilized ET2 were also analyzed by attenuated total reflectance

Fourier transform infrared spectroscopy (ATR-FTIR, Cary 660, Agilent Technologies, CA, USA).

3.3 RESULTS AND DISCUSSION

3.3.1 Lipase selection and preparation

Figure 11 shows the hydrolytic activity of lipases CALB, ET2, and TL 100L towards soybean oil. The lipase ET2 showed the highest activity (0.046 ± 0.002 mmol·min^{-1}·mL^{-1}) and therefore was selected to be immobilized on the membrane.

Figure 11 – Hydrolytic activity of the lipases CALB, ET2, and TL 100L towards soybean oil at 45ºC, pH 7, and 160 rpm for 30 min (1 mL of enzyme solution in 4 mL of 25% v/v oil-water emulsion and 5 mL of sodium phosphate buffer pH 7)

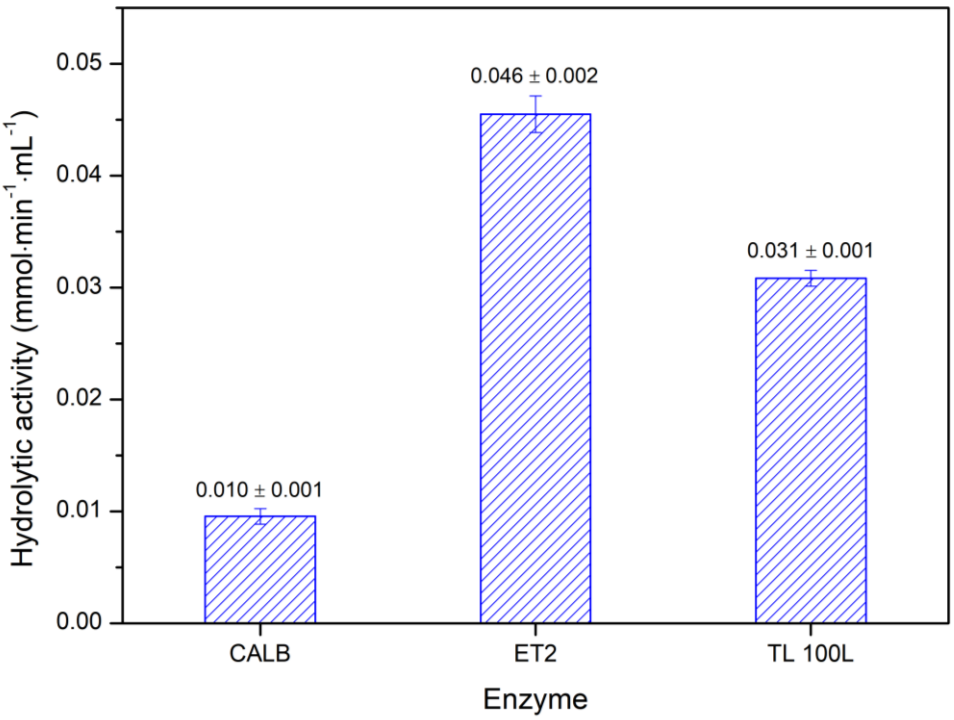

Source: Author

Arana-Peña et al. (2018) compared the hydrolytic activity of CALB and ET2 towards p-nitrophenyl butyrate (p-NPB), and ET2 showed an activity more than six times higher than CALB at pH 7. Bresolin et al. (2020) also reported an activity nine times higher for the hydrolysis of p-nitrophenyl palmitate (p-NPP) using ET2 when

compared to CALB. Furthermore, Martínez-Sanchez et al. (2020) obtained a hydrolytic activity almost two times higher for the lipase ET2 when compared to TL 100 L in the hydrolysis of p-NPB, and slightly higher activity of ET2 in the hydrolysis of triacetin. These results corroborate with the ones found in this work, indicating that ET2 has greater performance in the hydrolysis of triacylglycerols.

The soluble ET2 was dialyzed and lyophilized to remove stabilizers and possible impurities of the crude enzyme solution and concentrate the enzyme. The protein content of the crude solution was 28.6 ± 0.3 $mg \cdot g^{-1}$ while the lyophilized enzyme presented a protein content of 425.0 ± 1.6 $mg \cdot g^{-1}$ (which means purity of approximately 42%), showing that the concentration was successful. The specific hydrolytic activities of the soluble and lyophilized ET2 were 1.32 ± 0.01 $mmol \cdot min^{-1} \cdot g^{-1}$ and 1.39 ± 0.01 $mmol \cdot min^{-1} \cdot g^{-1}$, which shows that the dialysis and lyophilization processes did not cause any inhibition or deactivation of the enzyme.

3.3.2 Lipase immobilization

Table 4 summarizes the results obtained for enzyme loading (*EL*), membrane hydrolytic activity (*MHA*), specific hydrolytic activity of the immobilized lipase (MHA_s), and residual activity considering that the free ET2 has a specific activity of 1.39 ± 0.01 $mmol \cdot min^{-1} \cdot g^{-1}$.

The immobilization by adsorption (i.e., using the membrane with no functionalization or activating agent) provided a low protein loading in the membrane (0.9 $g \cdot m^{-2}$), which resulted in a low membrane hydrolytic activity (0.69 $mmol \cdot min^{-1} \cdot m^{-2}$) when compared to the other immobilization protocols used. As expected, the specific activity (0.72 $mmol \cdot min^{-1} \cdot g^{-1}$) was the highest since the immobilization by adsorption does not cause changes in the native structure of the enzyme, preserving the active sites (JESIONOWSKI; ZDARTA; KRAJEWSKA, 2014). However, because of the weak forces involved, the biocatalyst can easily desorb from the membrane during the separation process due to changes in pH, ionic strength, pressure, etc. Despite having the highest residual activity among the tests, the activity maintained by the adsorption method was only around 52% when compared to the free enzyme, which may be due to problems of mass transfer during the hydrolysis reaction.

The use of glutaraldehyde alone increased the protein loading of the membrane (1.8 $g \cdot m^{-2}$) when compared to the adsorption method (0.9 $g \cdot m^{-2}$) but

decreased the specific activity of the immobilized lipase from 0.72 $mmol \cdot min^{-1} \cdot g^{-1}$ (adsorption) to 0.25 $mmol \cdot min^{-1} \cdot g^{-1}$, reducing the overall membrane hydrolytic activity from 0.69 to 0.45 $mmol \cdot min^{-1} \cdot m^{-2}$. This behavior can be due to the nature of the bonding formed between the aldehyde group and the enzyme (represented in Figure 12a), which may have made the active site less accessible to the substrate or may have caused changes in the enzyme conformation, maintaining only 18% of the free enzyme specific activity (SIGURDARDÓTTIR et al., 2018; ZHOU et al., 2019).

Table 4 – Enzyme loadings and hydrolytic activities of the α-alumina membranes with ET2 immobilized by the different protocols

Immobilization method	**EL ($g \cdot m^{-2}$)**	**MHA ($mmol \cdot min^{-1} \cdot m^{-2}$)**	**MHA_s ($mmol \cdot min^{-1} \cdot g^{-1}$)**	**Residual activity (%)**
Adsorption	0.9 ± 0.2^{a}	0.69 ± 0.13^{a}	0.72 ± 0.02^{a}	52.1 ± 1.5
GA	1.8 ± 0.3^{a}	0.45 ± 0.05^{a}	0.25 ± 0.02^{b}	18.0 ± 1.2
APTES + GA	3.1 ± 0.5^{b}	0.38 ± 0.10^{a}	0.13 ± 0.01^{c}	9.0 ± 0.7
PDA	3.2 ± 0.4^{b}	1.85 ± 0.28^{b}	0.57 ± 0.02^{d}	41.1 ± 1.7
PDA+GA	4.7 ± 0.6^{c}	1.55 ± 0.21^{b}	0.33 ± 0.01^{e}	23.9 ± 1.0

The values are means of triplicates and their respective standard deviations. Different superscript letters in the same column indicate statistically significant differences according to Tukey's test ($p < 0.05$).
Source: Author

The use of APTES as functionalizing agent and glutaraldehyde as an activating agent was also tested since there are several reports on the literature demonstrating the effectiveness of this method in the immobilization of other enzymes on ceramic supports (AGHABABAIE et al., 2016; RANIERI et al., 2016; YI et al., 2017; ZHOU et al., 2019). However, the results obtained in the present study show that, although the protein loading (3.1 $g \cdot m^{-2}$) increased in relation to adsorption (0.9 $g \cdot m^{-2}$) and glutaraldehyde activation (1.8 $g \cdot m^{-2}$), the hydrolytic activity of the immobilized lipases by APTES+GA decreased in comparison to the use of glutaraldehyde alone, providing a low specific activity. Massive changes in the enzyme structure, enzyme deactivation, blockage of the active site, and decreased mobility due to the formation of covalent bonds can be possible explanations for this result (Figure 12b) (SIGURDARDÓTTIR et al., 2018). Furthermore, the higher enzyme loading using APTES+GA could have caused some protein-protein interactions, inhibiting the flexible stretching of enzyme conformation, which could have resulted in steric hindrance. With that, the enzyme would have difficulty modulating its most suitable conformation for

catching the substrate and releasing the product (HU et al., 2009; ZHANG; YUWEN; PENG, 2013). Similar behavior was observed by Aghababaie et al. (2016) when comparing adsorption with covalent bonding (also using APTES and glutaraldehyde) for the immobilization of *Candida rugosa* lipase in composite membranes. The authors noticed that the immobilization by covalent bonding provided a higher enzyme loading but a lower specific activity when compared to the adsorption method.

The use of polydopamine (PDA) as a functionalizing agent is a relatively new technique for enzyme immobilization. The presence of catechol, quinone, primary amines and secondary amines in the PDA coating allows the immobilization of molecules containing thiols or amino groups (such as enzymes) via Michael addition or Schiff base reaction (Figure 12c) (REN et al., 2011; TOUQEER et al., 2019; YAN et al., 2020). Table 4 shows that PDA as functionalizing agent increased the protein loading in the membrane to a similar value to that found using APTES and glutaraldehyde. Furthermore, the membrane hydrolytic activity was significantly higher, demonstrating that the specific activity of the enzyme was less affected by the immobilization protocol (a residual activity of 41.1% was achieved).

The immobilization protocol using polydopamine and glutaraldehyde showed the highest protein loading in the membrane (4.7 $g \cdot m^{-2}$). The glutaraldehyde forms covalent bonds between the amino groups of the polydopamine and the amino groups present in the enzyme (as represented in Figure 12d) (ASMAT; ANWER; HUSAIN, 2019). However, the higher amount of immobilized protein did not significantly increase the membrane hydrolytic activity compared to the tests using PDA functionalization with and without glutaraldehyde activation. The covalent bonds formed between the aldehyde and the amino groups of the enzyme possibly changed the enzyme's 3D structure or partially blocked the active site, resulting in lower specific activity. Similar results were found by Zhang et al. (2018b) when immobilizing lipase in a polymeric membrane using PDA coating and glutaraldehyde: the enzyme loading was higher but the catalytic activity was lower than electrostatic attraction and hydrophobic adsorption.

Figure 12 – Possible immobilization mechanisms for the tested protocols: (a) GA, (b) APTES and GA, (c) PDA, and (d) PDA and GA

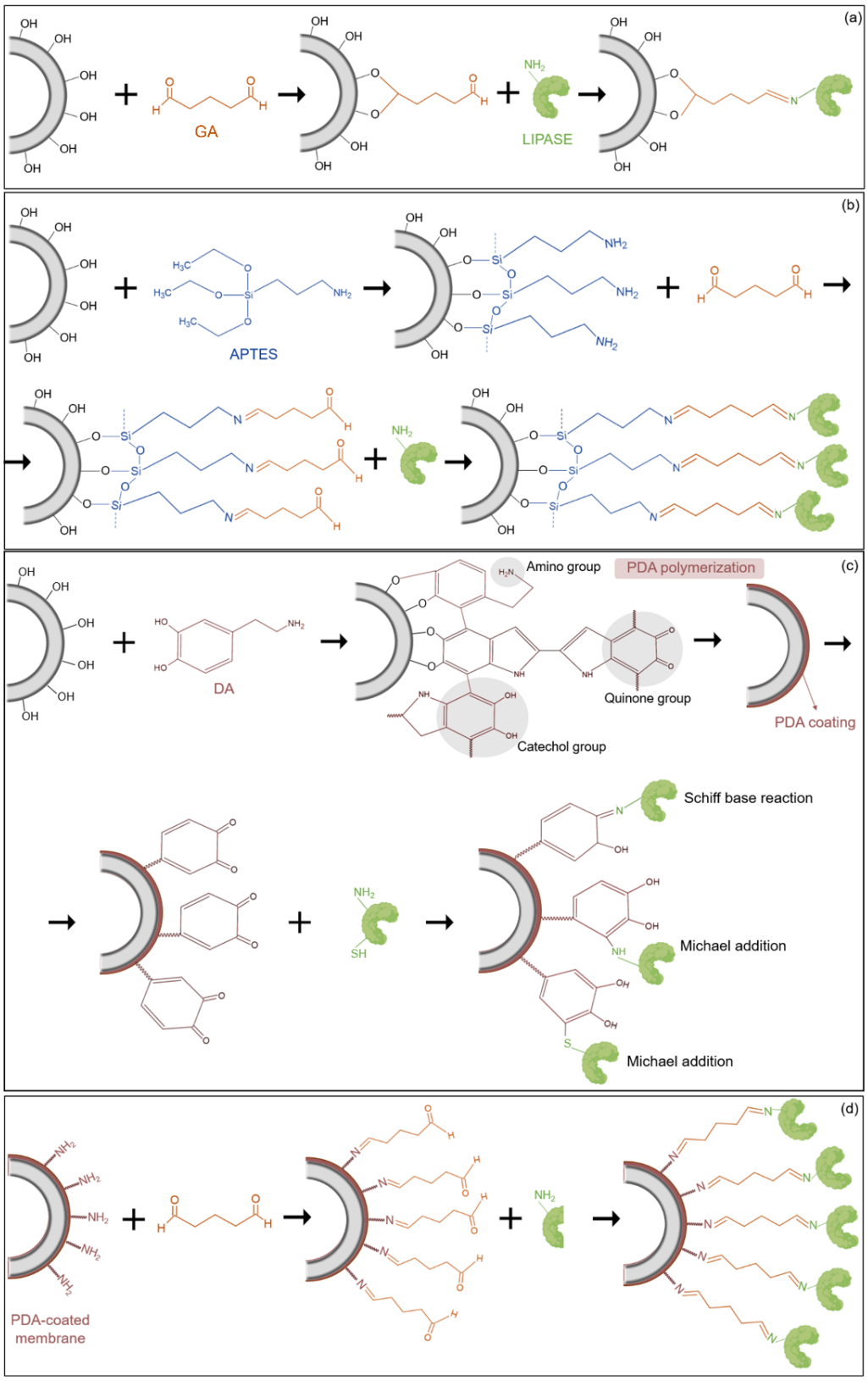

Source: Author

The immobilization protocol using PDA as the functionalizing agent was then selected to test the lipase ET2 performance as a fouling-degrading and self-cleaning agent in oil-water emulsion filtration. The results are promising and are consistent with the search for simple immobilization methods. The use of dopamine as a functionalizing agent requires the coating and the immobilizations steps, while the traditional silanization method needs one more step for activation. Moreover, the use of PDA represents a more environmentally friendly immobilization technique since dopamine presents lower toxicity than APTES and glutaraldehyde according to available literature data (APTES, glutaraldehyde, and dopamine average lethal doses – LD50 – are shown in Table 5) (KISO TO RINSHO, 1974; LEWIS, 2004; SMYTH et al., 1962). APTES and glutaraldehyde present the lowest average lethal doses (LD50), which means they are the most toxic compounds for the tested organism (rats).

Table 5 – Literature data for the toxicity of the functionalizing agents used in this work applied by oral route in rats

Functionalizing agent	**LD_{50} ($mg \cdot kg^{-1}$)**	**Reference**
APTES	1780	(Smyth et al., 1962)
GA	134 - 2390	(Lewis, 2004)
DA	2859	(Kiso to Rinsho, 1974)

Source: Author

3.3.3 Optimum operating temperature and pH of the free and immobilized ET2

Optimum temperature and pH of free and immobilized ET2 by PDA coating were evaluated (Figure 13). The immobilization did not change the enzyme optimal operating temperature range (around 40 °C) but increased the lipase activity over other temperatures, mainly at higher temperatures (Figure 13a). This improved thermostability can be due to the covalent bonding between the enzyme and the PDA layer, which may have resulted in a more stable enzyme conformation with higher resistance to increased temperatures when compared to the free enzyme (BAHARFAR; MOHAJER, 2016; TOUQEER et al., 2019).

Figure 13 – Optimum operating temperature (a) and pH (b) of the free and immobilized ET2 by PDA coating

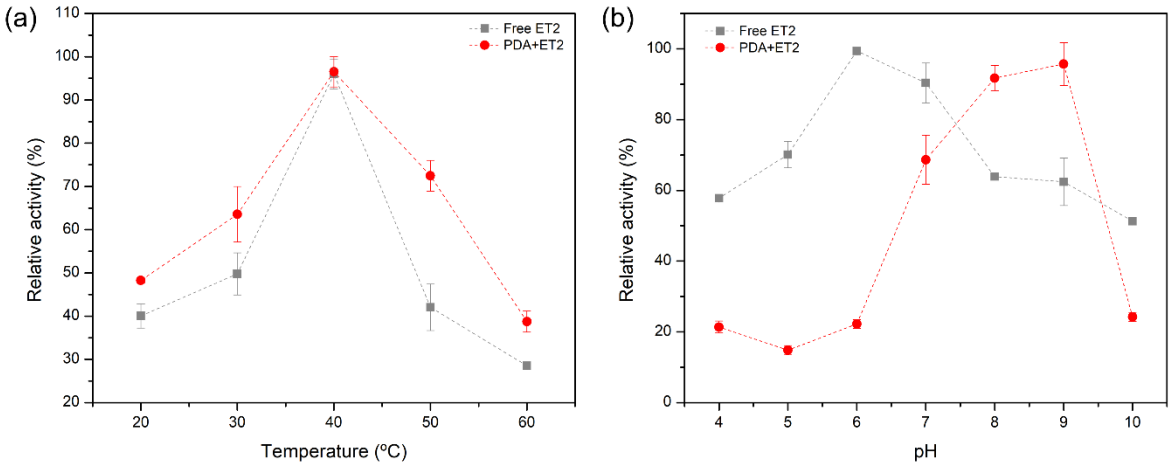

Source: Author

As shown in Figure 13b, the immobilization of ET2 by PDA coating changed the enzyme optimum operating pH to more alkaline ones: from pH 6 for the free enzyme to pH 9 for the PDA-immobilized enzymes. It can be noticed that the immobilization decreased the enzyme activity at lower pH values (4 - 7) and pH 10, while increasing it over slightly alkali pH (8 - 9). The same behavior was observed by Touqeer et al. (2019) after immobilization of *Aspergillus terreus* lipase in PDA-coated iron oxide nanoparticles and Cheng et al. (2019) after immobilization of *Candida rugosa* lipase in PDA-coated silica monoliths: the maximum enzyme activities were obtained with more alkaline pH values after immobilization.

3.3.4 Membrane characterization

Figure 14 shows the SEM images of the membrane before (Figure 14a) and after ET2 immobilization (Figures 14c and 14d). The presence of some clusters on the membrane surface can be noticed for both APTES + glutaraldehyde immobilization method and PDA coating. However, the PDA-coated membrane presents larger clusters along the surface, which suggests a more effective functionalization. The occurrence of agglomeration can be attributed to the formation of PDA aggregates on top of the uniform PDA layer, as reported by Ding et al. (2014) and Teng et al. (2021). Figure 14b shows a cross-section of the membrane, which reveals a symmetric porous structure. As expected, EDX analysis showed an increase in the carbon content of the

membrane surface for both immobilization protocols and an increase in oxygen content for the membranes with ET2 immobilized by PDA coating. The silicon present in the membrane surface treated with APTES+GA indicates a successful modification of the membrane with APTES.

Figure 14 – SEM images and EDX analysis of the (a) pristine membrane external surface and (b) cross-section, (c) membrane with ET2 immobilized by APTES and GA, and (d) membrane with ET2 immobilized by PDA coating

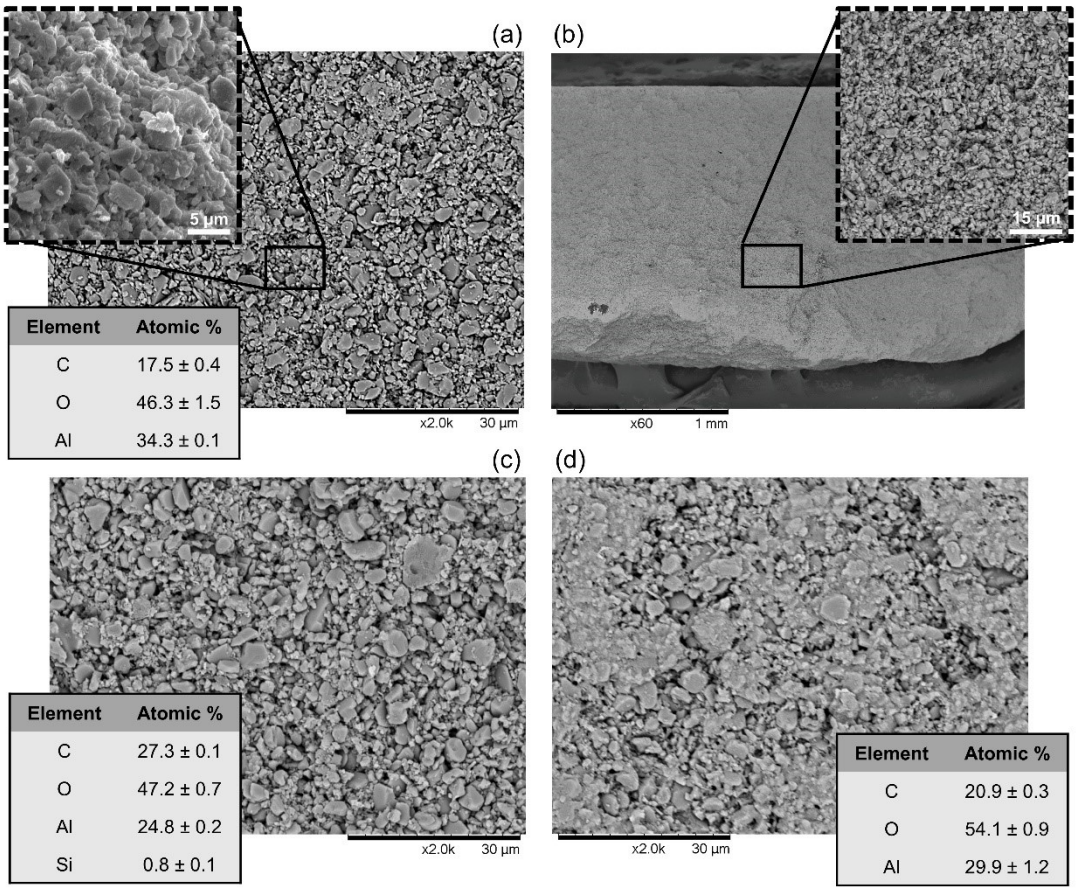

Source: Author

The pristine membrane apparent porosity, water absorption ratio, and apparent density were 39.9 ± 3.1 vol%, 17.4 ± 2.4 wt%, and 2.3 ± 0.1 g·cm^{-3}, respectively. These parameters for the modified membranes were not significantly different from the pristine according to the Tukey test (p < 0.05) (Table 6), demonstrating that the enzyme immobilization on the membrane did not affect these physical characteristics. Based on the apparent density and considering the total density determined by helium pycnometry (3.99 ± 0.01 g·cm^{-3}), it was possible to estimate the total porosity of the membrane as 42.5 ± 3.2 vol% and, thus, a closed

porosity of approximately 2.6 ± 0.1 vol%. The porosity determined by the Archimedes principle and the helium pycnometry analysis is similar to the one obtained by mercury intrusion (42.65%).

Table 6 – Water absorption, apparent porosity, apparent density, total porosity and closed porosity determined by the Archimedes method

Membrane	Water absorption (wt%)	Apparent porosity (vol%)	Apparent density ($g \cdot cm^{-3}$)	Total porosity (vol%)	Closed porosity (vol%)
Pristine	17.4 ± 2.4	39.9 ± 3.1	2.3 ± 0.1	42.5 ± 3.2	6.47 ± 0.2
Adsorption	16.8 ± 1.3	38.6 ± 2.0	2.3 ± 0.1	42.5 ± 1.6	10.1 ± 2.5
GLU	16.8 ± 1.4	39.0 ± 1.9	2.3 ± 0.1	41.9 ± 2.1	7.4 ± 0.3
GLU+ET2	15.7 ± 0.4	37.0 ± 0.8	2.3 ± 0.1	41.0 ± 0.7	10.8 ± 2.3
APTES+GLU	16.6 ± 1.7	38.5 ± 2.4	2.3 ± 0.1	41.7 ± 2.2	8.5 ± 1.3
APTES+GLU+ET2	15.6 ± 0.5	37.2 ± 0.8	2.4 ± 0.1	40.3 ± 0.5	8.5 ± 1.2
PDA	16.4 ± 1.1	37.9 ± 2.1	2.3 ± 0.1	42.2 ± 1.9	7.1 ± 1.1
PDA+ET2	16.8 ± 0.2	39.1 ± 0.2	2.3 ± 0.1	41.8 ± 0.7	6.9 ± 1.6
PDA+GLU	16.6 ± 1.7	38.0 ± 2.2	2.3 ± 0.1	42.6 ± 2.8	11.9 ± 3.7
PDA+GLU+ET2	17.0 ± 1.0	39.2 ± 1.2	2.3 ± 0.1	42.5 ± 1.6	8.3 ± 0.9

Source: Author

Well-defined peaks of typical α-alumina (ICDD 00-010-0173) can be identified in the XRD spectrogram of the pristine membrane (Figure 15). Interestingly, the membranes with immobilized ET2 show peaks with lower intensities than the functionalized membranes with no enzyme, which is indicative that the enzyme covers the membrane surface, decreasing the crystallinity detected by the method. The crystallinity indexes also show the loss of crystalline structure after membrane functionalization with both APTES+GA and PDA. The loss of crystallinity was more intense when PDA was used, which is in accordance with the SEM results shown in Figure 14. Similar results were obtained by Khan et al. (2019b) when immobilizing lipase on ZnO nanoparticles. PDA-modified membranes also present a broad XRD reflection peak at 22.1°, which can be attributed to the diffraction of amorphous PDA layers. The same broad peak was also identified by Luo et al. (2015) when using PDA to modify ceramic surfaces. According to Yeroslavsky et al. (2013) and Han et al. (2019), this diffraction peak can be ascribed to π-stacked structures of PDA.

Figure 15 – XRD spectra and crystallinity index (CI) of the pristine and modified membranes

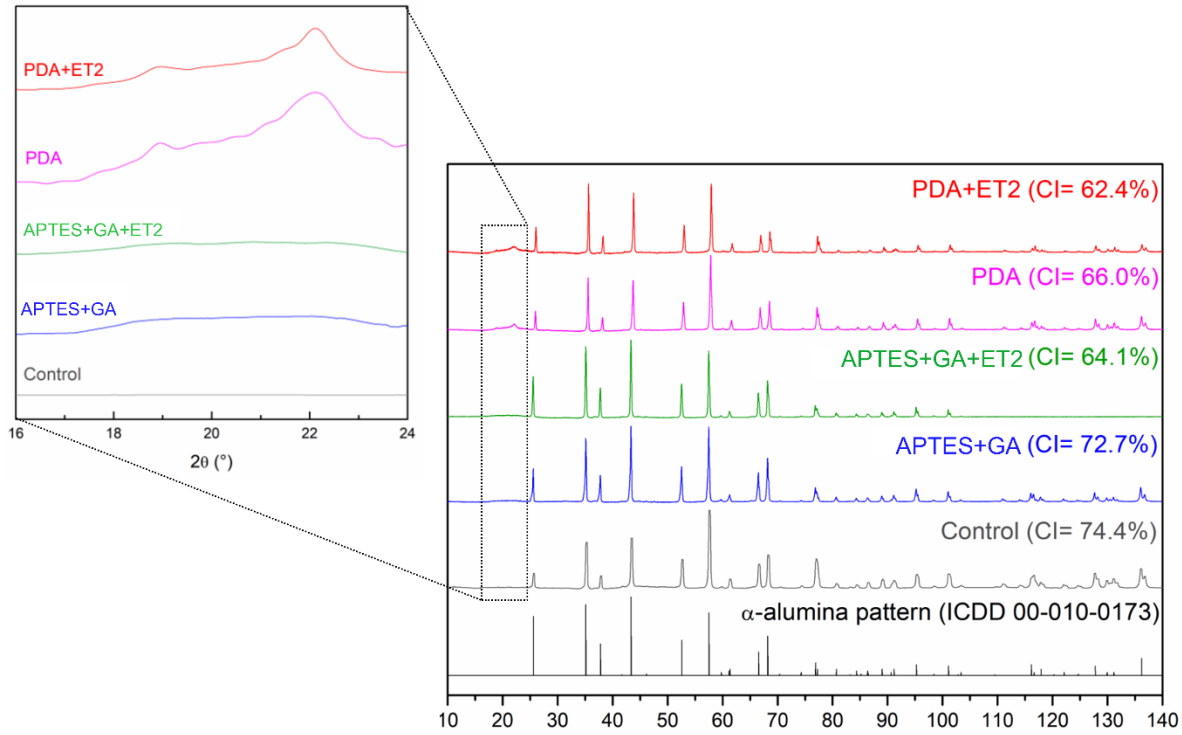

Source: Author

Figure 16 shows the hydrophilic and hydrophobic characteristics of the membranes analyzed through the vapor adsorption of a polar (water) and a non-polar (n-heptane) solvent. As expected, water vapor is adsorbed more efficiently than n-heptane vapor in the pristine membrane due to the hydrophilic nature of alumina. All modified membranes showed this characteristic but with some changes in the quantity of adsorbed vapor. The activation of the membrane with GA and the functionalization with PDA+GA did not significantly change the hydrophilicity of the membrane, while the silanization followed by activation with glutaraldehyde (APTES+GA) decreased the adsorption of water vapor. Some researches show that the silanization of ceramic surfaces using APTES can increase the hydrophobicity of the surface due to the introduction of propyl groups and reduction of free hydroxyl groups (BOURKAIB et al., 2021; SHAH et al., 2008; XIE et al., 2021). The PDA-coated membrane showed a decrease in the adsorption of both water and n-heptane vapor. The decline of n-heptane vapor uptake was more intense than water, yielding a higher water/n-heptane ratio. The decrease in n-heptane adsorption was expected since polydopamine coating contains several hydrophilic groups such as amine and hydroxyl (WANG et al., 2018a; ZARGHAMI; MOHAMMADI; SADRZADEH, 2019).

The enzyme immobilization significantly increased the adsorption of both water and n-heptane vapor in the membrane, though water vapor uptake was more pronounced. Kujawa et al. (2021) also reported increased hydrophilicity of functionalized alumina supports after CALB immobilization using different functionalization agents. The amphiphilic character of the enzyme, which has both hydrophobic and hydrophilic regions, can be a possible explanation for the increased adsorption of both water and n-heptane (KAPOOR; GUPTA, 2012).

Figure 16 – Water and n-heptane vapor adsorption at 23 °C (left axis) and the ratio of water and n-heptane adsorption (right axis) for the pristine membrane, functionalized membranes (GA, APTES+GA, PDA, and PDA+GA) and membranes with immobilized lipase ET2

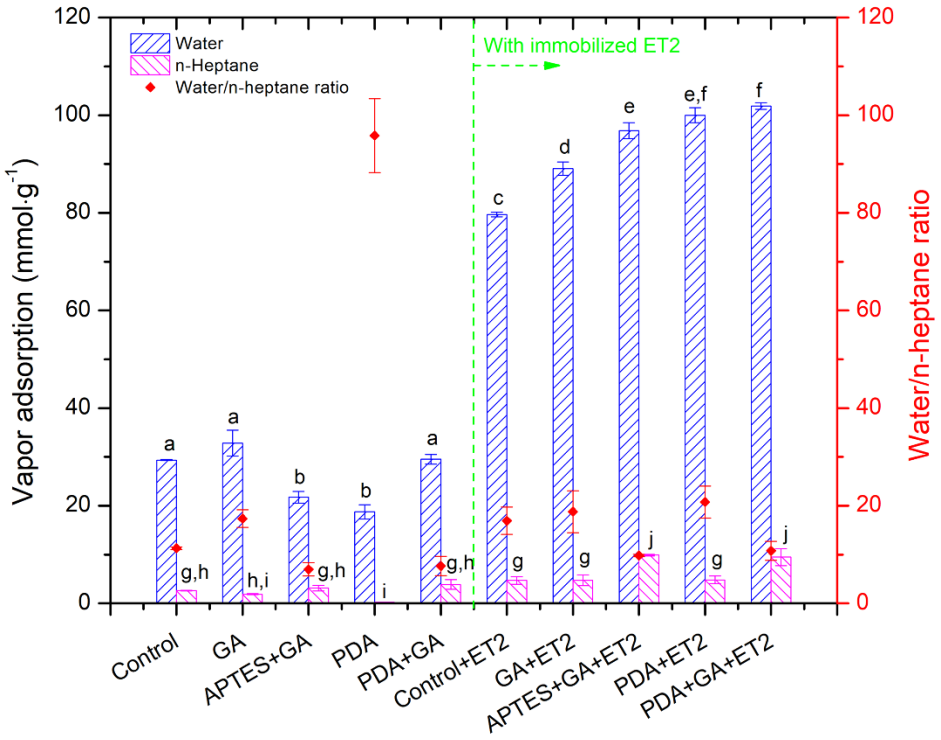

The values are means of triplicates and their respective standard deviations. Bars with different letters are significantly different according to Tukey's test ($p < 0.05$)
Source: Author

The pristine and PDA-modified membranes as well as the free and immobilized ET2 were characterized by FTIR (Figure 17a). In the free lyophilized ET2 spectra, it is possible to observe broad peaks at 3440 cm^{-1} (O–H stretching from hydroxyls), 3380 cm^{-1} (primary amine –NH_2– aliphatic stretching), and 3131 cm^{-1} (O-H stretching from carboxylic acid functional groups). Other peaks centered at around 1540 cm^{-1} can correspond to C=O stretching of secondary amides and the signal around 1660 cm^{-1} is characteristic of the α-helix secondary assignment, common in

the secondary structure of proteins (BRESOLIN et al., 2020; KONG; YU, 2007). Peaks at 1069 and 1190 cm^{-1} can correspond to C-N stretching of amines, and the peak at 1260 cm^{-1} can be due to C-N stretching or N-H bending of tertiary amides (KONG; YU, 2007). The PDA-modified membrane shows peaks at 1650 cm^{-1} (overlap of C=C stretching from the aromatic rings and the N-H bending of the amines), 1510 cm^{-1} (C=O from amide groups), and 1084 cm^{-1} (C-N stretching from amines) as well as a broad band between 3100 and 3500 cm^{-1} that corresponds to the stretching vibrations of –NH and –OH (CHEN et al., 2015; DONG et al., 2018; YANG; DUAN; RAN, 2017). The membrane with immobilized ET2, besides the peaks corresponding to the PDA layer (1650 and 1084 cm^{-1}) also presents peaks suggesting the presence of ET2 (1540 and 1260 cm^{-1}). The spectra also show peaks at 3276 cm^{-1} (O-H stretching), around 2920 cm^{-1} (combination of N-H stretching from amine groups and C-H stretching from alkenes), 1089 cm^{-1} (C-N stretching from amines and/or C-O stretching), and 795 cm^{-1} (C=C bending from alkenes). This indicates the successful immobilization of the lipase in the PDA-coated membranes.

Figure 17b shows the membranes' surface chemical composition obtained by XPS analysis. The pristine membrane shows only O, C, and Al peaks. The small amount of carbon present in the pristine sample must be due to organic impurities from the environment. In the PDA-coated membrane, an N peak appears and the C peak intensifies while the Al peaks decrease, confirming the deposition of PDA in the membrane surface. Similar results were obtained by Gao and Xu (2019) after modifying an alumina membrane with PDA. The intensity of the N peak in the membrane with immobilized ET2 increases considerably in comparison to the PDA-coated membrane. Table 7 summarizes the relative abundance of the elements detected. The N/C atomic ratio of the PDA-coated membrane was 0.12, which is similar to the theoretical ratio (0.125) of dopamine and other PDA coatings reported in the literature (BI et al., 2017; ZIN et al., 2019). After ET2 immobilization, the N/C atomic ratio increased to 0.18, proving the presence of the enzyme on the membrane surface.

Figure 17 – (a) ATR-FTIR of the lyophilized ET2, pristine membrane, and membranes modified by PDA and PDA+ET2 and (b) XPS spectra of the pristine and modified membranes

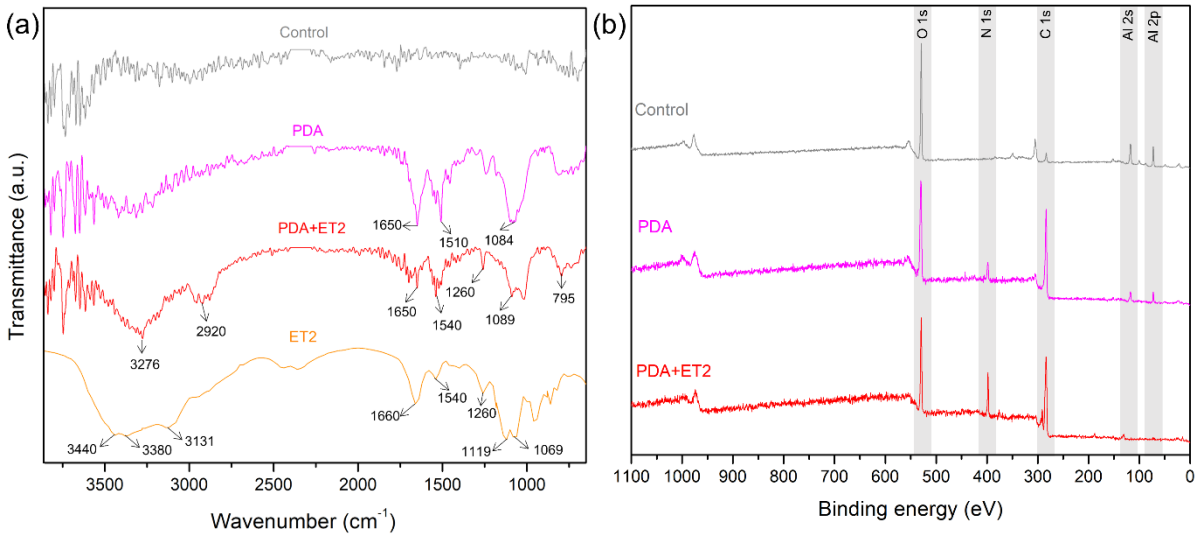

Source: Author

Table 7 – Elemental composition and atomic ratio of the pristine membrane, PDA modified membrane, and membrane with immobilized ET2 analyzed by XPS

Sample	Atomic composition (%)			
	C	N	O	Al
Pristine	17.78 ± 3.27	-	62.83 ± 3.24	19.39 ± 0.03
PDA	64.05 ± 3.60	7.56 ± 0.13	26.41 ± 2.60	1.99 ± 1.13
PDA+ET2	63.94 ± 4.21	11.34 ± 1.28	24.21 ± 3.19	0.53 ± 0.26

Source: Author

3.3.5 Oil-water emulsion filtration

Figure 18 shows pure water permeances before and after emulsion filtration, after the cleaning procedure, and the normalized permeate flux during emulsion filtration. The membrane functionalized with PDA presented a slight reduction (6%) in the initial pure water permeance compared to the pristine membrane. This reduction can be caused by the decreased hydrophilicity as shown in Figure 16 and a possible decrease in the membrane pore size due to the polymerization of PDA inside the pores. Proner et al. (2020) also detected pore blockage after co-polymerization of PDA and PEI in polyethersulphone ultrafiltration membranes. After lipase immobilization, the initial pure water permeance increased, possibly due to the increased membrane hydrophilicity (SCHMIDT et al., 2018). This finding is consistent with the results shown in Figure 16. The increased hydrophilicity can also explain the increase in initial water

permeance observed for the silanized membrane with immobilized ET2. Generally, after enzyme immobilization on membranes, the water permeance decreases due to additional hydraulic resistance (CAO et al., 2018; ZHANG et al., 2019). However, based on the results, the increased hydraulic resistance caused by the PDA coating was mitigated by the increase in the membrane hydrophilicity caused by the enzyme immobilization. Rasouli et al. (2021) showed that when using high PDA-PEI deposition times (9 h), the higher hydrophilicity of the modified membranes can increase the water permeance despite the pore size reduction, which corroborates the results obtained in the present study.

After the emulsion filtration and final backwash, the membranes with no immobilized enzyme showed stronger fouling (permeance reduction of approximately 74% compared to the initial permeation) than the membranes with immobilized ET2 (permeance reduction of 53% for the PDA-coated membrane and 64% for the APTES-functionalized and GA-activated membrane). After the filtration experiments, there was no difference in water permeance between the pristine and the PDA-coated membranes, suggesting the immobilized ET2 is responsible for the lower fouling degree. The higher water permeance after filtration presented by both enzyme-active membranes can be due to the increased hydrophilicity after ET2 immobilization and to fouled oil hydrolysis.

The pristine membrane showed a water permeance recovery of approximately 39% after the cleaning procedure. On the other hand, the water permeance recovery for the PDA-coated, immobilized ET2 by APTES+GA, and ET2 immobilized by PDA membranes were 45%, 49%, and 69%, respectively. The self-cleaning experiments were performed using only sodium phosphate buffer pH 7 and a temperature of 40 °C to activate the enzymes. Thus, no traditional cleaning agents such as acids or bases were used. Then, besides decreasing membrane fouling and increasing permeance recovery, the immobilization of ET2 in the membranes can potentially minimize the use of chemicals during the cleanings.

Figure 18 – Performance of pristine and modified α-alumina membranes in the filtration of soybean oil-water emulsion (1 g·L^{-1}): (a) water permeance before the emulsion filtration (initial), after the final backwash (after fouling), and after the cleaning procedure; (b) normalized permeate flux of the oil-water emulsion filtration

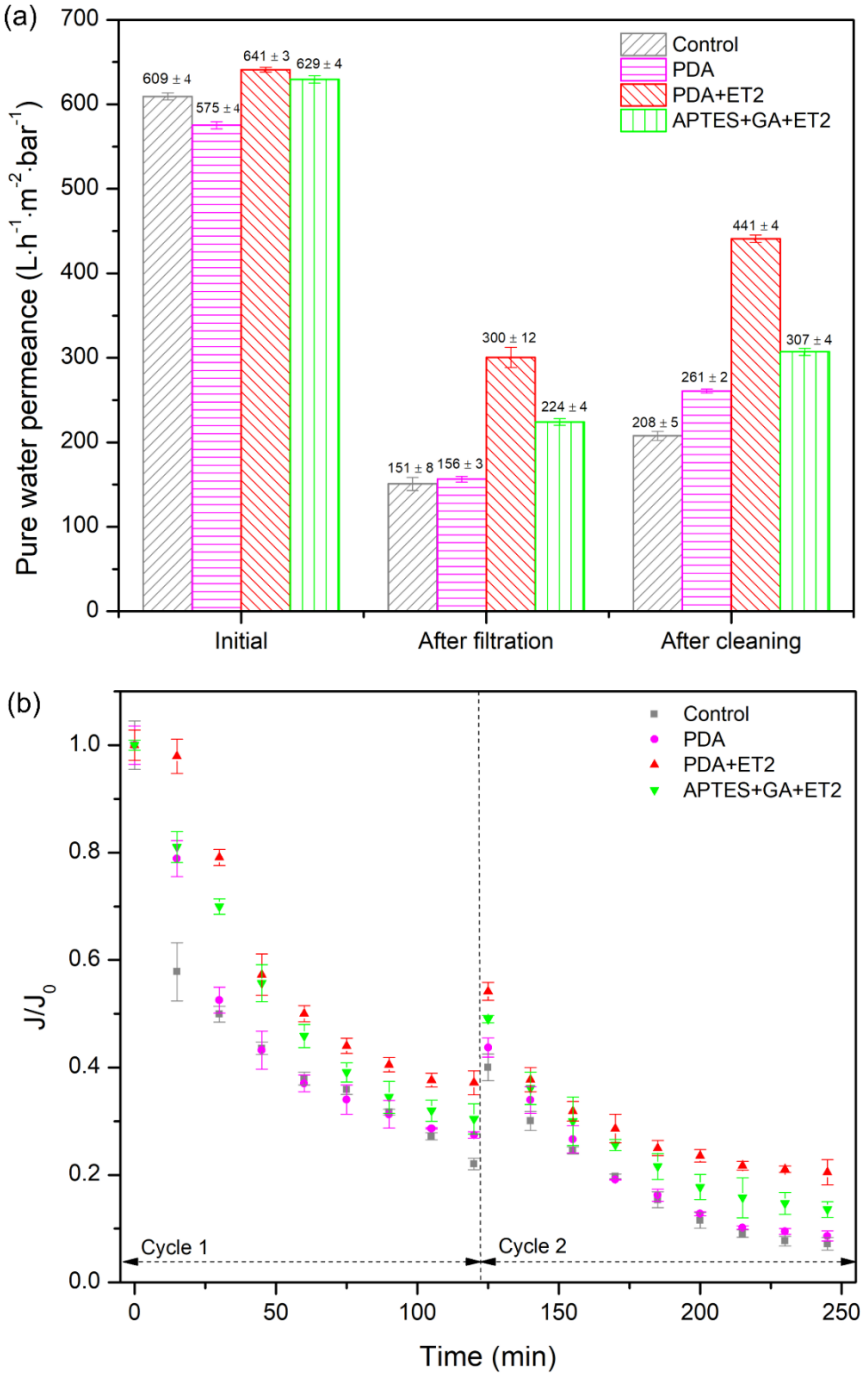

Source: Author

The mean oil droplet diameter of the soybean oil-water emulsion used in the filtration tests was 240 ± 18 nm. Membrane modification of any kind did not change membrane oil retention (p > 0.05), which was above 90% throughout the experiments.

As shown in Figure 19, after three filtration and cleaning cycles, the pristine membrane showed a reduction in pure water permeance of 78%. In comparison, the active membrane with immobilized ET2 by PDA coating showed a reduction of water permeance of only 41%. The combined fouling-degrading and self-cleaning capacity led to a regeneration of water permeance of 84% after cycle 1 (49% for the pristine). After cycle 3, total self-cleaning capacity is reduced to 19%, which is possibly caused by the formation of a thicker fouling layer resulting in a final water permeance recovery of 59% compared to 22% of the pristine.

Figure 19 – Results of repeated filtration and cleaning experiments for the pristine membrane and active membrane with immobilized ET2 by PDA coating

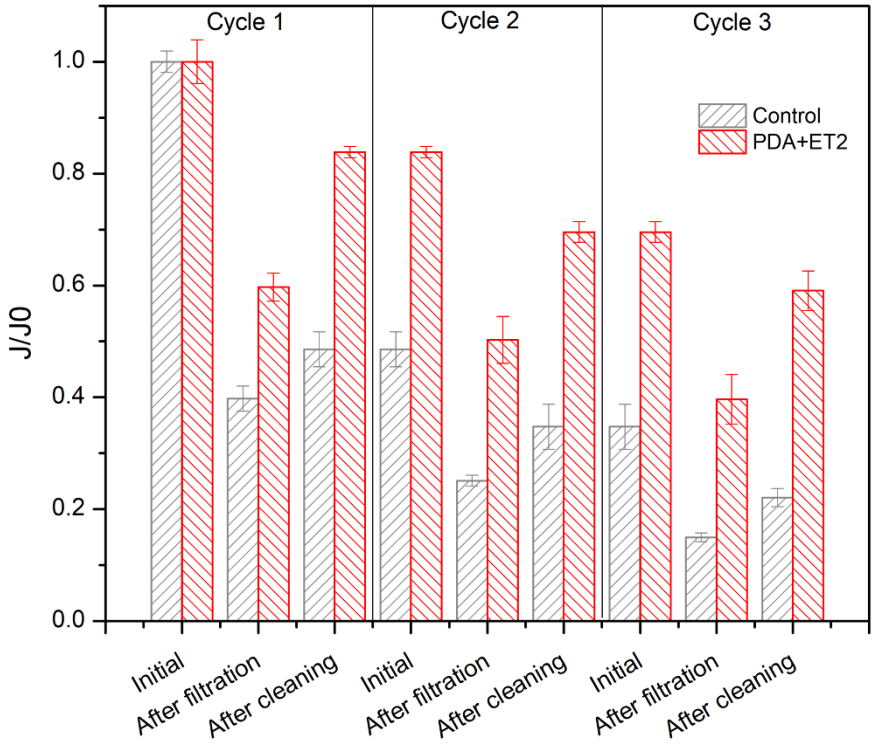

Source: Author

3.4 CONCLUSION

The use of polydopamine coating for lipase immobilization on an inorganic membrane can be a competitive method for the broadly used silanization technique. The functionalization of the membrane with polydopamine resulted in enhanced immobilization performance in terms of protein loading and membrane hydrolytic activity compared to the traditional immobilization protocol. Moreover, the use of

dopamine represents a simple and more environmentally friendly immobilization technique than silanization since it does not require an activation step and has lower toxicity. Also, the immobilized Eversa Transform 2.0 showed potential as a fouling-degrading and self-cleaning agent, resulting in an enzymatically active ceramic membrane with enhanced performance in oil-water emulsion filtration. The simple cleaning procedure applied resulted in good water permeance recovery for the active membranes and can represent an alternative to minimize the consumption of cleaning agents and wastewater generation. There is no report in the literature on the use of polydopamine to immobilize lipase on ceramic membranes. The use of Eversa Transform 2.0 as an antifouling and self-cleaning agent in membranes is also not reported. Therefore, this study may contribute to the development of technologies for the functionalization of inorganic membranes to minimize fouling formation and, consequently, improve the performance of membrane separation processes.

4 POLYDOPAMINE-ASSISTED ONE-STEP IMMOBILIZATION

Covalent enzyme immobilization is generally a time-consuming and multistep procedure that uses toxic solvents and requires more than one chemical, making industrial upscaling unattractive. Using an aqueous polydopamine (PDA) solution for enzyme immobilization is a greener and effective alternative to conventional methods, such as the use of APTES and glutaraldehyde, as shown on Chapter 3. Usually, enzyme immobilization using PDA is performed in two steps: dopamine polymerization on the material surface followed by enzyme immobilization. A few recent studies applied a one-step strategy by mixing dopamine and enzyme in the coating solution, reducing the immobilization time, chemical consumption, and wastewater generation (WANG et al., 2021). Therefore, this chapter compares the two-step and one-step approaches to immobilizing the lipase Eversa Transform 2.0 (ET2) on the α-alumina membrane. The one-step immobilization method achieved similar enzyme loading, membrane hydrolytic activity, and enzyme-specific activity to those of the two-step method. The ET2 immobilized using both strategies showed excellent fouling resistance and self-cleaning performance in oil-water emulsion filtration. The membrane modified by the one-step approach exhibited a lower reduction in pure water permeance after oil fouling (35%) and a higher permeance recovery (90%) than the one modified by the two-step method (40% and 74%, respectively). This better performance can be due to the higher hydrophilicity of the modified membrane and higher stability over reaction time shown by the enzyme immobilized by the one-step strategy. The higher stability can be attributed to more attachment points between the enzyme and PDA, increasing the enzyme rigidity and preventing conformational changes. The results of this chapter are submitted to the Chemical Engineering Journal as “Polydopamine-assisted one-step immobilization of lipase on α-alumina membrane for fouling control in the treatment of oily wastewater”.

4.1 INTRODUCTION

Enzymes are used in a variety of applications as catalysts (CHAPMAN; ISMAIL; DINU, 2018; FACIN et al., 2019). Because enzymes are water-soluble macromolecules, additional separation and purification processes are needed to recover and reuse the enzymes, which increase the complexity of the system and

raises the cost. One strategy is to immobilize enzymes on solid supports, allowing their reuse in multiple reaction cycles. Furthermore, enzyme immobilization enables continuous operation and, in some cases, increases enzymatic stability and activity, improving the process's economics (AGHABABAIE et al., 2016; BARBOSA et al., 2013; FRAAS; FRANZREB, 2017).

Enzymes have been immobilized on different materials. Polymeric materials are most often used as they possess reactive surface functional groups that can bond to the enzymes (RODRIGUEZ-ABETXUKO et al., 2020; ZDARTA et al., 2018). However, inorganic materials have important advantages as a support, including better mechanical, chemical, and thermal stability (SIGURDARDÓTTIR et al., 2018; ZUCCA; SANJUST, 2014). Among inorganic materials, ceramics stand out for their relatively low cost and long service life (GOLDSTEIN; MANECKE, 1976; SIGURDARDÓTTIR et al., 2018).

However, ceramics lack reactive surface functional groups and must be functionalized to allow covalent bonding with enzymes. Silicon-based polymers, such as organosilanes, are typically used to functionalize the ceramic. The organosilane reacts with the hydroxyl functional groups on the ceramic surface, generating organic functional groups available for further reactions with the enzyme [8]. The most common chemicals used to covalently immobilize enzymes on ceramic materials are 3-aminopropyltriethoxysilane (APTES) as a functionalization agent and glutaraldehyde as an activating agent (SIGURDARDÓTTIR et al., 2018; ZHOU et al., 2019). Nevertheless, the immobilization procedures, generally requiring various chemicals and multiple steps, are time-consuming and involve toxic solvents, making industrial upscaling unattractive.

Therefore, simpler immobilization protocols using fewer chemicals are essential to make ceramic materials more competitive as enzyme supports. Polydopamine (PDA) can strongly adhere to different materials (GAO; FAN; XU, 2020; GUO et al., 2020) and has therefore been used for enzyme immobilization. Due to the presence of a large number of reactive functional groups (e.g., amine, imine, quinone, and catechol), PDA coating can bond enzymes to ceramic materials (CHAO et al., 2013; CHENG et al., 2018, 2019; MULINARI et al., 2022; REN et al., 2011). For example, the amino groups located at the side chain amino acids of the enzyme can react with the quinone groups of the PDA coating through the Michael addition or Schiff base reaction, covalently bonding the enzyme to the ceramic surface. Similar to the

conventional method, enzyme immobilization using PDA is usually performed in two steps: dopamine polymerization on the material surface in an alkaline environment, followed by enzyme immobilization using standard buffers. Our previous study compared the PDA coating method on ceramic membranes with traditional enzyme immobilization techniques such as silanization (MULINARI et al., 2022). The PDA coating method resulted in a higher enzyme loading and membrane hydrolytic activity than the traditional salinization method.

Although the use of nature-inspired PDA represents an environmentally friendly and simpler alternative to conventional immobilization agents, it is still a time-consuming multistep method that generates a large volume of wastewater. Here, we adopted a one-step coating strategy to reduce the immobilization time, chemical usage, water consumption and wastewater generation. Therefore, if the one-step method using PDA proves to be a good alternative to the two-step approach, besides being a greener technique and easier to scale up, the costs of the immobilization process can be lower, making it more industrially attractive than the traditional immobilization protocols. Membrane industries can benefit from this technology as well as research institutions, since, due to the non-specificity of the PDA coating, this simpler immobilization technique can be used to modify a wide range of materials using different enzymes.

In the case of oily wastewater treatment, the enzyme lipase is a good candidate to be immobilized on the membrane since they can break the triacylglycerols of the oil into free fatty acids and glycerol. Therefore, when the biocatalytic membrane is used to filtrate oily wastewater, the immobilized lipases can degrade the oil fouling during the filtration and cleaning procedure. Only three studies were found in the literature about lipase immobilization on membranes to develop oil fouling-controlling and self-cleaning abilities: Schulze et al. (2017), Schmidt et al. (2018), and Schmidt et al. (2022). The results presented by these studies are promising, with the biocatalytic membrane showing permeance reductions after emulsion filtration as low as 40% (the pristine membrane had a 60% reduction) and permeance recoveries as high as 100% after cleaning just using a buffer at proper pH and temperature. However, all three studies used polymeric flat-sheet membranes. So far, most of the works using immobilized enzymes to decrease membrane fouling focused on biofouling control (LAN; HIEBNER; CASEY, 2021; LEE et al., 2019a; MEHRABI et al., 2020) or protein fouling mitigation (CHEN et al., 2021; VANANGAMUDI et al., 2018a; YUREKLI, 2020).

Thus, it is noted that the use of enzymes as antifouling and self-cleaning agents in membranes is a relatively unexplored area due to the huge variety of enzymes, membranes, and membrane separation processes that the use of immobilized enzymes can improve.

Compared to other membrane modification methods to decrease fouling, using immobilized enzymes is the simplest way to provide the membrane with a self-cleaning capacity as well. Photocatalytic membranes can also degrade the fouling during the cleaning; however, the performance is limited on how much light reaches the membrane surface. Usually, a UV light source is required since photocatalysis is limited under visible light, which increases the energy demand (ZHANG et al., 2021a). Electrocatalysis is also an alternative in which the membrane acts as an anode or cathode; however, a current source is necessary, also increasing the energy demand (YANG et al., 2012). Fenton-like processes by immobilizing iron on the membrane are also possible, but they require hydrogen peroxide to achieve improved performances (CHEN et al., 2018). Moreover, photocatalysis, electrocatalysis, and Fenton-like processes are not specific and can promote several side reactions, which is not a problem when enzymes are used due to their high specificity (SATYAWALI; VANBROEKHOVEN; DEJONGHE, 2017).

Therefore, besides developing a one-step method to immobilize the lipase on the membrane, this study also aimed to develop a catalytic membrane with fouling control and self-cleaning properties to be applied in the filtration of oily wastewater. If successful, the lipase-active membranes can be applied in the wastewater treatment of various food industries (from the production of poultry, beef, and fish, to dairy, cheese, edible oils, and prepared food).

4.2 MATERIALS AND METHODS

4.2.1 Materials and chemicals

Purified and concentrated lipase Eversa Transform 2.0 (ET2) produced by a genetically modified strain of *Aspergillus oryzae* was used (Novozymes, Denmark). The commercial enzymatic solution was dialyzed for 120 h using a cellulose membrane (12-14 kDa) and sodium phosphate buffer at 50 mmol·L^{-1} and pH 6.0. The buffer was replaced every 12 h. The purified enzyme solution was frozen at -50 °C and lyophilized

for 48 h (Liotop model L101n, Brazil). The resulting powder was stored at 4 °C until use.

Tubular α-alumina membranes were custom-made (Tecnicer, Brazil). They are 25 cm in length, 1.2 cm in outer diameter, and 0.8 cm in inner diameter. The total porosity of the membranes is 30 ± 2 % and it was calculated using the apparent density (2.8 ± 0.1 $g \cdot cm^{-3}$) determined by Archimedes' principle using deionized water (ASTM, 2000) and the absolute density (4.0 ± 0.1 $g \cdot cm^{-3}$) determined by helium pycnometry (Quantachrome Ultra pycnometer 1000, USA). It is important to highlight that the membranes used in this chapter are from a different batch than the membranes used in chapter 3 and, although produced using the same method, they present a lower porosity and, therefore, lower permeances.

Analytical grade dopamine hydrochloride (DA, 98%, $C_8H_{11}NO_2$.HCl, Sigma-Aldrich, USA), sodium dodecyl sulfate (SDS, ≥90%, $C_{12}H_{25}SO_4Na$, Synth, Brazil), polyvinyl alcohol (PVA, 98%, $(C_2H_4O)_n$, M_w = 104.5 kg/mol, NEON, Brazil), sodium hydroxide (≥97%, NaOH, NEON, Brazil), ethanol (99.5%, C_2H_6O, NEON, Brazil), and phenolphthalein (99%, $C_{20}H_{14}O_4$, Sigma-Aldrich, USA) were used as purchased. Tris(hydroxymethyl)aminomethane (≥99.5%, $C_4H_{11}NO_3$, NEON, Brazil) and hydrochloric acid (37%, HCl, NEON, Brazil) were used to prepare the 50 mM Tris-HCl buffer (pH 8.5) and 100 mM Tris-HCl buffers (pH 9 and 10). The 100 mM sodium phosphate buffers (pH 6, 7, and 8) were prepared using sodium phosphate monobasic (98%, NaH_2PO_4, NEON, Brazil) and sodium phosphate dibasic (P.A., Na_2HPO_4, NEON, Brazil). The 100 mM potassium acetate buffers (pH 4 and 5) were prepared using glacial acetic acid (99.8%, CH_3CO_2H, NEON, Brazil) and potassium acetate (≥98.5%, CH_3CO_2K, NEON, Brazil). Refined soybean oil (Soya®) was purchased from a local market.

4.2.2 ET2 hydrolytic activity

The ET2 hydrolytic activity was determined using soybean oil as the substrate. Soybean oil in water emulsion (25% $v \cdot v^{-1}$) was prepared immediately before each experiment by emulsifying soybean oil in a 2% ($m \cdot m^{-1}$) aqueous solution of PVA using a magnetic stirrer at 1500 rpm for 10 min according to the method proposed by Fu et al. (1995). Then, 4 mL of the soybean emulsion was added to 6 mL of sodium phosphate buffer (100 $mmol \cdot L^{-1}$, pH 7) with 1 $mg \cdot mL^{-1}$ of the lyophilized ET2 (volume

ratio soybean oil emulsion:buffer of 2:3, resulting in a soybean oil concentration of 90 g·L^{-1}). The buffer solution with ET2 was stirred at 300 rpm for 1 h before being mixed with the soybean oil emulsion. After incubation for 30 min at 40 °C and agitation at 160 rpm, the reaction was interrupted by adding 15 mL of ethanol. The quantity of fatty acids liberated during the reaction was determined by titration using NaOH 0.05 mol·L^{-1} and phenolphthalein. Control assays were carried out by adding ethanol right before the addition of the enzyme. The specific hydrolytic activity (HA_S) was calculated using Eq. 8. All tests were performed in triplicate.

$$HA_S\ (mmol \cdot min^{-1}.g^{-1}) = \frac{(V_s - V_c) \times M}{t \times V \times PC} \quad (8)$$

where V_s is the NaOH volume used to titrate the sample (mL), V_c is the NaOH volume used to titrate the control assay (mL), M is NaOH molarity (mol·L^{-1}), t is the reaction time (min), V is the volume of enzymatic solution added to the reaction media (mL), and PC is the protein content of the enzymatic solution (g·mL^{-1}) determined by the Bradford method using bovine serum albumin as a standard (BRADFORD, 1976).

4.2.3 ET2 immobilization

Before each test, the ends of each membrane were sealed with a thermoplastic adhesive to prevent the solution from entering the inside of the tubular membrane. PDA deposition was performed by air oxidation (GAO; XU, 2019; MULINARI et al., 2022; PRONER et al., 2020). For the two-step approach (Figure 20a), the membrane was immersed in a solution of dopamine hydrochloride (DA) (2 mg·mL^{-1}) in Tris-HCl buffer (pH 8.5, 50 mmol·L^{-1}) for 6 h at room temperature with gentle stirring at 40 rpm. Then, the membrane was rinsed with deionized water and immersed in a 2 mg·mL^{-1} ET2 solution in Tris-HCl buffer (pH 8.5, 50 mmol·L^{-1}) at 40 rpm for 12 h. Before the immobilization, the ET2 solution was stirred for 1 h at 300 rpm to break possible enzyme agglomerates. For the one-step strategy (Figure 20b), a solution of 2 mg·mL^{-1} of ET2 in Tris-HCl buffer (50 mmol·L^{-1} pH 8.5) was stirred for 1 h, and then 2 mg·mL^{-1} of DA was added to the solution. The membrane was immersed in the DA/ET2 solution for 12 h at 40 rpm. Adsorption of ET2 on a pristine membrane (Figure 20c) was also tested by immersing the membrane in a 2 mg·mL^{-1} ET2 solution in Tris-HCl

buffer for 12 h. After all the immobilization procedures, the membranes were washed with sodium phosphate buffer (100 mmol·L^{-1} pH 7) to remove loosely bound enzymes until no protein was detected using the Bradford method. Triplicate samples were prepared using each immobilization method.

Figure 20 – Schematic representation of the immobilization methods tested in this study: (a) two-step immobilization, (b) one-step immobilization, and (c) adsorption

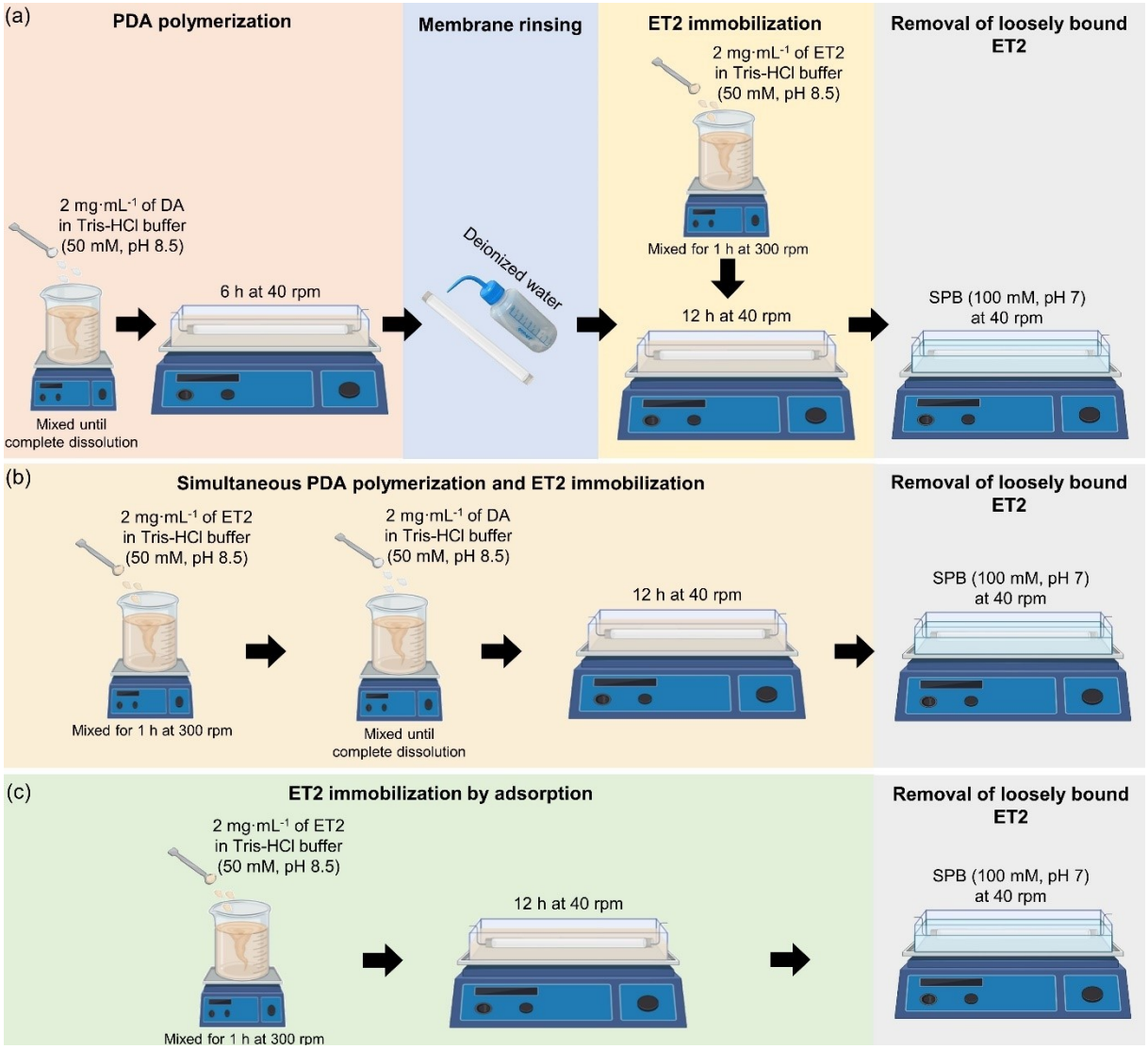

The amount of enzyme immobilized on the membrane was determined by the change in ET2 concentration in the solution before and after the immobilization, as measured by the Bradford method, also accounting for the enzyme removed during the rinsing step. Enzyme loading (EL) was calculated according to Eq. 9.

$$EL\ (g \cdot m^{-2}) = \frac{(C_o - C_f) \times V - M_r}{A} \quad (9)$$

where C_0 is the initial enzyme concentration in the solution (before the immobilization) (g·mL^{-1}), C_f is the final protein content (after the immobilization) (g·mL^{-1}), V is the volume of enzyme solution used in the test (mL), M_r is the amount of loosely bound enzyme removed by the rinsing step (g), and A is the membrane projected external area (m^2).

The hydrolytic activity of the immobilized ET2 was evaluated by the same method used to determine the free ET2 activity. For this, a test solution was prepared using the same soybean oil emulsion:buffer volume ratio of 2:3 and final soybean oil concentration of 90 g·L^{-1} (specifically, 50 mL of soybean emulsion was mixed with 75 mL of sodium phosphate buffer (100 mmol·L^{-1} pH 7)). The membranes were immersed in the test solution and incubated at 40 °C for 30 min with gentle mixing at 40 rpm. Then, a homogenized sample of 10 mL was withdrawn from the solution and titrated with 0.05 mol·L^{-1} NaOH to determine the amount of free fatty acids formed from the hydrolysis reactions. Control assays were performed under the same conditions using membranes subjected to the same immobilization protocols but without the ET2 enzyme. The membrane hydrolytic activity (*MHA*) and the specific hydrolytic activity of the immobilized ET2 (MHA_S) were determined according to Eq. 10 and 11, respectively.

$$MHA\ (mmol \cdot min^{-1}.m^{-2}) = \frac{(V_s - V_c) \times M \times (V_t/V)}{t \times A} \quad (10)$$

$$MHA_S\ (mmol \cdot min^{-1}.g^{-1}) = \frac{(V_s - V_c) \times M \times (V_t/V)}{t \times A \times EL} \quad (11)$$

where V_s is the NaOH volume used to titrate the sample (mL), V_c is the NaOH volume used to titrate the control assay (mL), M is NaOH molarity (mol·L^{-1}), V_t is the total volume of emulsion used in the test (mL), V is the volume of the emulsion sample titrated (mL), t is the reaction time (min), A is the membrane projected external area (m^2), and EL is the enzyme loading on the membrane (g·m^{-2}).

Residual activity, as defined by Eq. 12, was used to estimate the effect of immobilization on enzyme activity.

$$Residual\ activity\ (\%) = 100 \times \frac{MHA_S}{HA_S} \quad (12)$$

Analysis of variance (ANOVA) and Tukey's test ($p < 0.05$) were performed on enzyme loading, membrane hydrolytic activity, and specific hydrolytic activity. Table 8 compares the two-step and one-step immobilization methods regarding immobilization time, consumption of chemicals, and wastewater generation per membrane area. If successful, the one-step strategy can be less time-consuming (-33%) and have a lower generation of wastewater (-50%) and consumption of chemicals (-25%).

Table 8 – Comparative of the two-step and the one-step methods for ET2 immobilization on the ceramic membrane using PDA (approximate values based on the modification methods used in this study)

Method	**Modification time (h)**	**Chemicals usage**		**Wastewater generation ($L \cdot m^{-2}$)**
		DA ($g \cdot m^{-2}$)	**Tris-HCl 100 mM pH 8.5 ($L \cdot m^{-2}$)**	
Two-step	18	30	30	30
One-step	12	30	15	15

Source: Author

4.2.4 Operational stability of the immobilized and free ET2

The effects of pH, temperature and reaction time on the free and immobilized ET2 were investigated during oil hydrolysis. Both free and immobilized ET2 activities were determined at different temperatures (20 – 60 °C) and pH (4 – 10). The hydrolysis activity was then evaluated for 24 h using the optimal temperature and pH. Free and immobilized ET2 activities were determined as described in sections 4.2.2 and 4.2.3, respectively; however, due to the different pH values used, instead of phenolphthalein as an indicator, titration was performed until pH 11, and control assays were performed for each pH (TREICHEL et al., 2016). The effect of pH, temperature, and reaction time were evaluated according to a relative activity (%), calculated by normalizing the obtained activities by the highest one.

4.2.5 Membrane characterization

The surface morphology and elemental composition of the pristine and modified membranes were characterized by Scanning Electron Microscopy (SEM, FEI Helios NanoLab 660 Dual, USA) coupled with Electron Dispersion X-ray (EDX). Membrane hydrophilicity/hydrophobicity was determined using water and n-heptane vapor adsorption measurements as described by Mulinari et al. (2022) and adapted from Nishihora et al. (2018) and Prenzel et al. (2014). Membrane surface chemistry was characterized by X-ray Photoelectron Spectroscopy (XPS, PHI Quantera, MN, USA) using monochromatic Al Kα X-rays. Since alumina is an insulating material, the spectra of all samples were charged correctly by shifting all peaks to the adventitious C 1s spectral component (C-C, C-H) at 284.8 eV. The membranes and the lyophilized ET2 were also analyzed by attenuated total reflectance Fourier transform infrared spectroscopy (ATR-FTIR, Cary 660, Agilent Technologies, CA, USA).

4.2.6 Oil-water emulsion filtration tests

The ET2-immobilized membranes were tested for their fouling resistance and self-cleaning function in the filtration of a soybean oil in water emulsion following previously reported protocols (MULINARI et al., 2022; PRONER et al., 2020; SCHMIDT et al., 2018). Since the immobilization was carried out on the membrane's outer surface, the filtration was performed outside-in. To prepare the test solution, soybean oil (1 $g \cdot L^{-1}$) was emulsified in a 2 $mmol \cdot L^{-1}$ SDS aqueous solution by magnetic stirring at 1000 rpm for 5 min followed by probe sonication (Unique® model DES5000, Brazil) at 100 W for 5 min. In the filtration experiment, deionized water was first filtered at 1 bar and 1 $L \cdot min^{-1}$ of retentate flow rate to determine the initial pure water permeance of the membrane (p_1). Then, two filtration steps of 2 h each were performed using the soybean oil emulsion. At the end of each filtration step, a backwash was carried out for 5 min at 1 bar and 1 $L \cdot min^{-1}$ of retentate flow rate using deionized water. After the final backwash, pure water permeance (p_2) was measured again to evaluate the degree of fouling calculated by the decrease in pure water permeance (Eq. 13). All the steps of the experiment were performed in crossflow mode with complete recirculation of the retentate back to the feed reservoir. The transmembrane pressure used was 1 bar, the retentate flow rate was 1 $L \cdot min^{-1}$, and the crossflow velocity was

0.20 m·s^{-1}. Sealing rings were fixed at 1 cm from each end of the membrane, resulting in an effective membrane length of 23 cm with an effective area of 79.5 cm^2. After the filtration experiments, the membranes were immersed in sodium phosphate buffer (100 mmol·L^{-1} pH 7) for 12 h at 40 °C with stirring at 40 rpm to evaluate the membrane's self-cleaning capacity. Finally, the membranes were rinsed with deionized water, and the water permeance (p_3) was measured again. The overall permeance recovery was calculated by Eq. 14. The pristine membrane and membranes functionalized with and without the enzyme were tested in triplicate. Oil concentration in the feed and permeate was monitored throughout the experiment using a UV-visible spectrophotometer (Shimadzu model UV-2550, Japan) at a wavelength of 240 nm.

$$PWP\ reduction\ after\ filtration\ (\%) = 100 \times \frac{(p_1 - p_2)}{p_1} \quad (13)$$

$$Overall\ PWP\ recovery\ (\%) = 100 \times \frac{p_3}{p_1} \quad (14)$$

where p_1 is the initial pure water permeance (L·h^{-1}·m^{-2}·bar^{-1}), p_2 is the pure water permeance after emulsion filtrations and final backwash (L·h^{-1}·m^{-2}·bar^{-1}), and p_3 is the pure water permeance after cleaning (L·h^{-1}·m^{-2}·bar^{-1}).

Three cycles of filtration and cleaning were performed using the same membrane to investigate their reusability in long-term applications. The number of filtration steps within each cycle was two. The emulsion was prepared as described above as well as the filtration and self-cleaning experiments.

4.3 RESULTS AND DISCUSSION

4.3.1 ET2 immobilization

The lyophilized ET2 was immobilized by PDA coating using the two-step and one-step methods and by simple adsorption in the membrane for comparison. Table 9 shows the results of enzyme loading, membrane hydrolytic activity, specific hydrolytic activity, and residual activity. The residual activities were calculated based on the specific activity of free lyophilized ET2: 1.39 ± 0.01 mmol·min^{-1}·g^{-1}.

Immobilization by simple adsorption (using the membrane with no functionalization) resulted in a very low enzyme loading on the membrane (0.9 ± 0.2 g·m^{-2}) and, consequently, a low membrane hydrolytic activity (0.69 ± 0.08 mmol·min^{-1}·m^{-2}). The use of PDA greatly increased the enzyme loading on the membrane for both the two-step (3.1 ± 0.2 g·m^{-2}) and the one-step (3.1 ± 0.1 g·m^{-2}) approaches, which resulted in higher membrane hydrolytic activities. Similar results were obtained by Ren et al. (2011) when comparing adsorption with a two-step PDA method for immobilization of *Candida rugosa* lipase type VII on iron oxide nanoparticles: the use of PDA tripled the enzyme loading. However, the formation of covalent bonds between ET2 and PDA decreased the specific activity of the immobilized ET2 compared to the adsorption method, as evident in the lower residual enzyme activity resulting from the two PDA immobilization methods. This is attributed to structural changes or denaturing of the enzyme as well as blockage of active sites by PDA. Adsorption, on the other hand, involves weaker, non-specific interactions, causing fewer or no changes in the enzyme structure (FACIN et al., 2019; MOHAMAD et al., 2015). Nevertheless, all immobilization methods caused a large drop in enzyme activity compared to the free enzyme, as indicated by the low residual activity.

Table 9 – Enzyme loadings (EL) and hydrolytic activities of the ET2 immobilized on the α-alumina membranes by different protocols

Immobilization strategy	**EL (g·m^{-2})**	**MHA (mmol·min^{-1}·m^{-2})**	**MHA$_S$ (mmol·min^{-1}·g^{-1})**	**Residual activity (%)**
Adsorption	0.91 ± 0.16^a	0.69 ± 0.08^a	0.76 ± 0.05^a	54.3 ± 3.4^a
Two-step PDA	3.12 ± 0.23^b	1.82 ± 0.08^b	0.59 ± 0.06^b	42.3 ± 4.3^b
One-step PDA	3.10 ± 0.10^b	1.99 ± 0.04^b	0.64 ± 0.02^b	46.1 ± 1.3^b

All values are averages of triplicate tests and their respective standard deviations. Values in the same column with different superscripts indicate statistically significant differences according to Tukey's test ($p < 0.05$).
Source: Author

When using the one-step strategy, there was a concern that the PDA might cover the enzyme and make the active site less accessible to the reactant. However, our results show that the two methods resulted in similar protein loading and hydrolytic activity; the Tukey test did not show a statistically significant difference between the two approaches.

4.3.2 Free and immobilized ET2 optimum operating pH and temperature

The stability of enzymes as a function of temperature, pH, and operating time is an important factor in determining their suitability for applications that may encounter fluctuation of temperature and solution pH, and require a long lifetime of the enzyme. Figure 21 shows the activity of free and immobilized ET2 as a function of temperature, pH, and time. Regardless of the method used, immobilization did not alter the enzyme's optimal operating temperature (around 40 °C), but it increased ET2 activity at other temperatures, especially at temperatures higher than the optimal one (Figure 21a). In the temperature range of 40 to 60 ºC, the one-step immobilization method yielded significantly higher enzyme activity than the two-step approach. This improved thermostability can be attributed to a larger number of attachment points between the enzyme and PDA (as schematized on Figure 25b). As the enzyme moieties involved in the immobilization reaction are fixed in location, they increase the enzyme rigidity and hinder conformational changes when temperature increases (BARBOSA et al., 2013; CHENG et al., 2019).

Figure 21b shows that ET2 immobilization using PDA coating increased the enzyme's optimum operating pH from pH 6 for the free enzyme to pH 7 and 9 for the one-step and two-step PDA-immobilized enzymes, respectively. The immobilization resulted in lower enzyme activity at pH < 7 as well as pH 10 but increased its activity in the pH range of 7 to 9. Touqeer et al. (2019) observed a similar change after immobilizing *Aspergillus terreus* lipase on PDA-coated iron oxide nanoparticles: the maximum enzyme activities were obtained at more alkaline pH values after immobilization.

The lipase immobilized by the one-step method showed higher activities than the one immobilized by the two-step method for all the pH values tested except pH 9. It is hard to determine exactly why this happened. It is an agreement in the literature that immobilization can help to improve stability in the microenvironment near the immobilized enzyme (KLIBANOV, 1979). So, in this case, although both methods used PDA as a bonding agent, they resulted in slightly different coatings, as demonstrated by the XPS analysis (Figure 24), which can indicate some variances in the microenvironment near the enzyme and, therefore, different behaviors at the same pH values.

Figure 21c shows the enzyme stability over time for the free and immobilized ET2. Both immobilization methods increased the operational stability of the enzyme, showing superior relative activity over 4 hours of the hydrolysis reaction. The free and immobilized ET2 had similar relative activities in the first two hours, consistent with the *MHA* results reported in Table 9 for 30 min of reaction. After 2 h, the relative activity of free ET2 dropped much faster than those immobilized by either method. The enzyme immobilized by the one-step strategy showed the highest stability, which is consistent with the larger number of attachment points and, therefore, higher rigidity of the enzyme.

Figure 21 – Relative activity as a function of (a) temperature, (b) pH, and (c) operational time of the free and immobilized ET2 by the two-step and one-step approaches using PDA

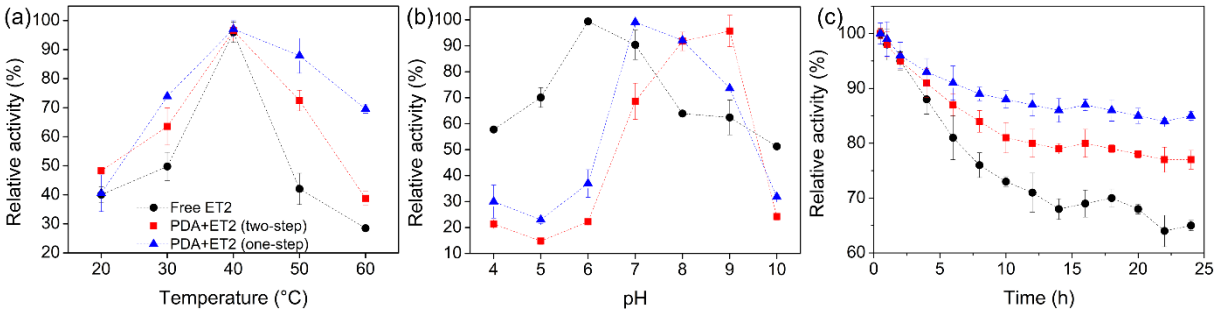

Source: Author

4.3.3 Membrane Characterization

Figure 22 shows the SEM images of the pristine membrane as well as membranes after different coating steps. Analyzing the SEM images, the membrane modified by the one-step strategy (Figure 22g) showed a more uniform coating than the one modified by the two-step method (Figure 22e), which can be a result of different PDA polymerization times (6 h of polymerization for the two-step modified membrane and 12 h of simultaneous polymerization and immobilization for the one-step modified membrane). EDX analysis (Table 10) showed an increase in the carbon content of the membrane surface after enzyme immobilization: from 20% for the PDA-coated membrane to 24% and 28% for the membranes with ET2 immobilized by the two-step and one-step method, respectively. The EDX mapping for each membrane (Figure 22b, 22d, 22f and 22h) shows a homogeneous distribution of carbon and oxygen on the membrane surface, suggesting that the coating was uniform.

Figure 22 – SEM images and EDX mapping (aluminum in blue, carbon in red, and oxygen in green) of the surface of the (a,b) pristine membrane, (c,d) PDA-coated membrane, (e,f) membrane with ET2 immobilized by the two-step method, and (g,h) membrane with ET2 immobilized by the one-step method

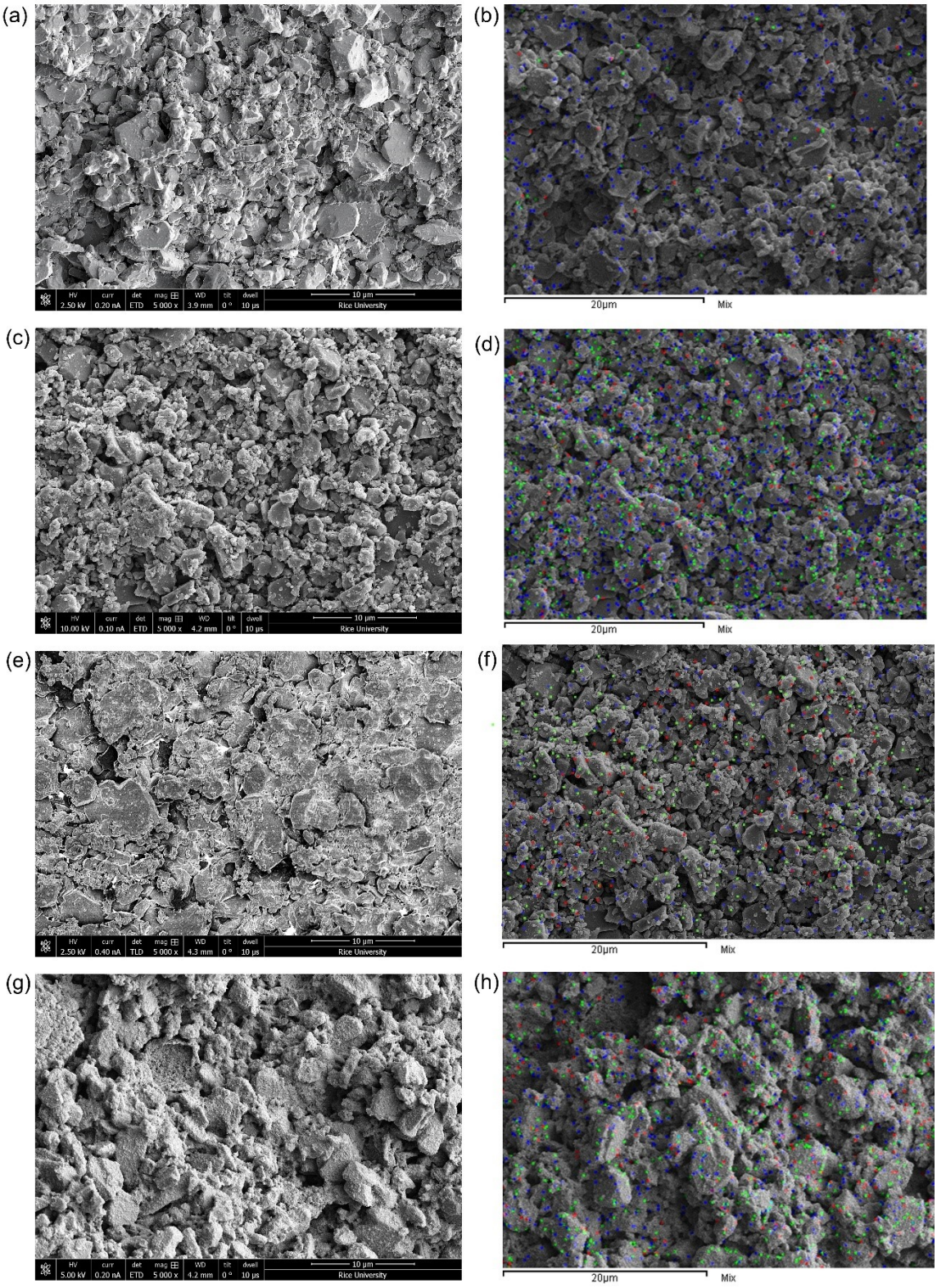

Source: Author

Table 10 – Elemental analyses of the membranes' surfaces by EDX

Element	Atomic composition (%)			
	Pristine	PDA	PDA+ET2 (two-step)	PDA+ET2 (one-step)
C	0.1 ± 0.7	20.4 ± 0.7	23.6 ± 1.0	27.7 ± 0.9
O	68.7 ± 1.2	55.5 ± 1.1	50.2 ± 1.3	48.3 ± 1.2
Al	31.3 ± 0.9	24.1 ± 0.8	26.2 ± 0.8	23.9 ± 0.7

Source: Author

ATR-FTIR analyses (Figure 23) show no significant difference in surface chemistry of the ET2 immobilized membranes obtained using the two-step and one-step methods, which corroborates the similar hydrolytic activities obtained using these membranes. The membranes with immobilized ET2 also presented similar functional groups found in the free lipase sample: O-H stretching (3280 cm^{-1}), a combination of N-H stretching from amine groups, and C-H stretching from alkenes (2920 cm^{-1}), C=O stretching of primary amides from the α-helix secondary assignment, common in the secondary structure of proteins (1650 cm^{-1}), and N-H bending of secondary amides (1540 cm^{-1}) (BRESOLIN et al., 2020; KONG; YU, 2007). It also showed a signal at 1050 cm^{-1}, corresponding to C-N stretching from amines, present at both enzyme and PDA coating (CAO et al., 2018; DONG et al., 2018). The intensity of C=O and C-N peaks were higher for the membrane modified by the two-step method compared to the one-step method, suggesting that part of the enzymes can be covered by the PDA coating when the one-step strategy was applied.

Figure 23 – ATR-FTIR of the pristine membrane, PDA-coated membrane, membranes with immobilized ET2 by the two-step and one-step methods, and lyophilized ET2

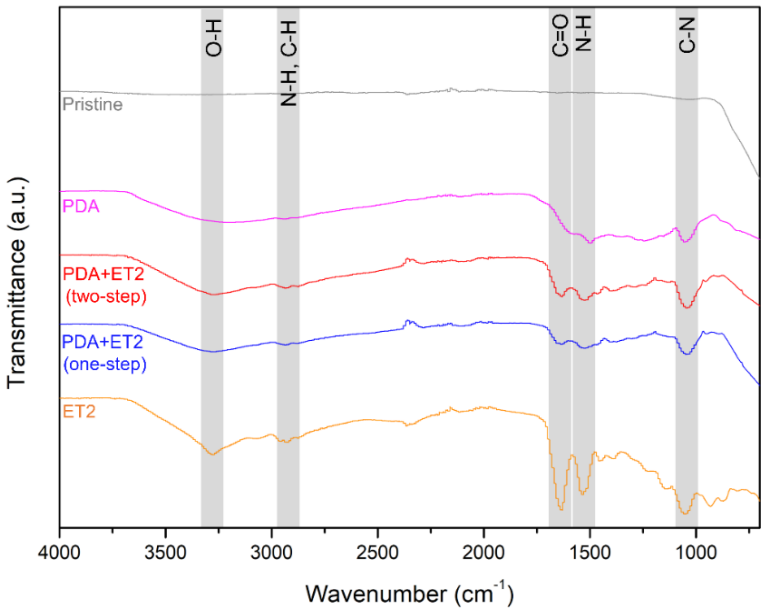

Source: Author

Figure 24 and Table 11 show the surface chemical composition of the membranes and the free ET2 characterized by XPS analysis. Almost no aluminum was detected after the membrane modification while the carbon content increased, indicating a successful modification of the membrane surface. Moreover, nitrogen peaks appeared after PDA coating and increased after ET2 immobilization. Table 11 shows the relative amounts of the elements detected by the XPS analysis. After ET2 immobilization, the N/C atomic ratio increased from 0.12 ± 0.01 (PDA-coated membrane) to 0.20 ± 0.01 for the two-step method and 0.19 ± 0.03 for the one-step approach, which corroborates the similar results for enzyme loading in both membranes.

Figure 24b shows the fitted carbon spectra of the modified membranes. The ET2-immobilized membranes exhibit an increase in the content of C=O or C=N and a decrease in C-H and C-C contents, suggesting a Schiff base reaction between the quinone groups of PDA and the amino groups of ET2, as schematized on Figure 25a. It may also be attributed to the oxidation of the remaining PDA catechol groups to quinone groups in the alkali environment (pH 8.5) as describe by Lu and Yu (2018) and the condensation reaction of the carboxyl groups in the enzyme with the amino groups of the PDA (Figure 25a). Wang et al. (2021b) also noticed an increase in C=O

after immobilizing perhydrolase on the PDA coating and attributed it to the formation of protein-PDA complexes.

The N 1s spectrum (Figure 24c) shows a considerable increase in the intensity of R_2NH binding energy when ET2 was immobilized on the membrane, suggesting that the amino groups of the enzyme could have bonded to the quinone groups of the polydopamine not only by Schiff base reaction but also by Michael addition (Figure 25a). The N 1s spectra for the membrane modified by both two-step and one-step methods show a decrease in RNH_2 intensity, which can be due to the condensation reaction between PDA's amino groups and enzymes' carboxylic groups (Figure 25a). Also, for the membrane modified by the two-step method, there is a shift in the RNH_2 binding energy, suggesting a change in the environment near the nitrogen. For the membrane modified by the one-step method, no shift was detected, indicating that PDA can cover part of the enzyme structure (Figure 25b).

Figure 24 – (a) XPS spectra of the pristine membrane, modified membranes, and free ET2, (b) fitted carbon (C 1s), and (c) nitrogen (N 1s) spectra for the membranes with PDA coating and with immobilized ET2 by the two-step and one-step methods

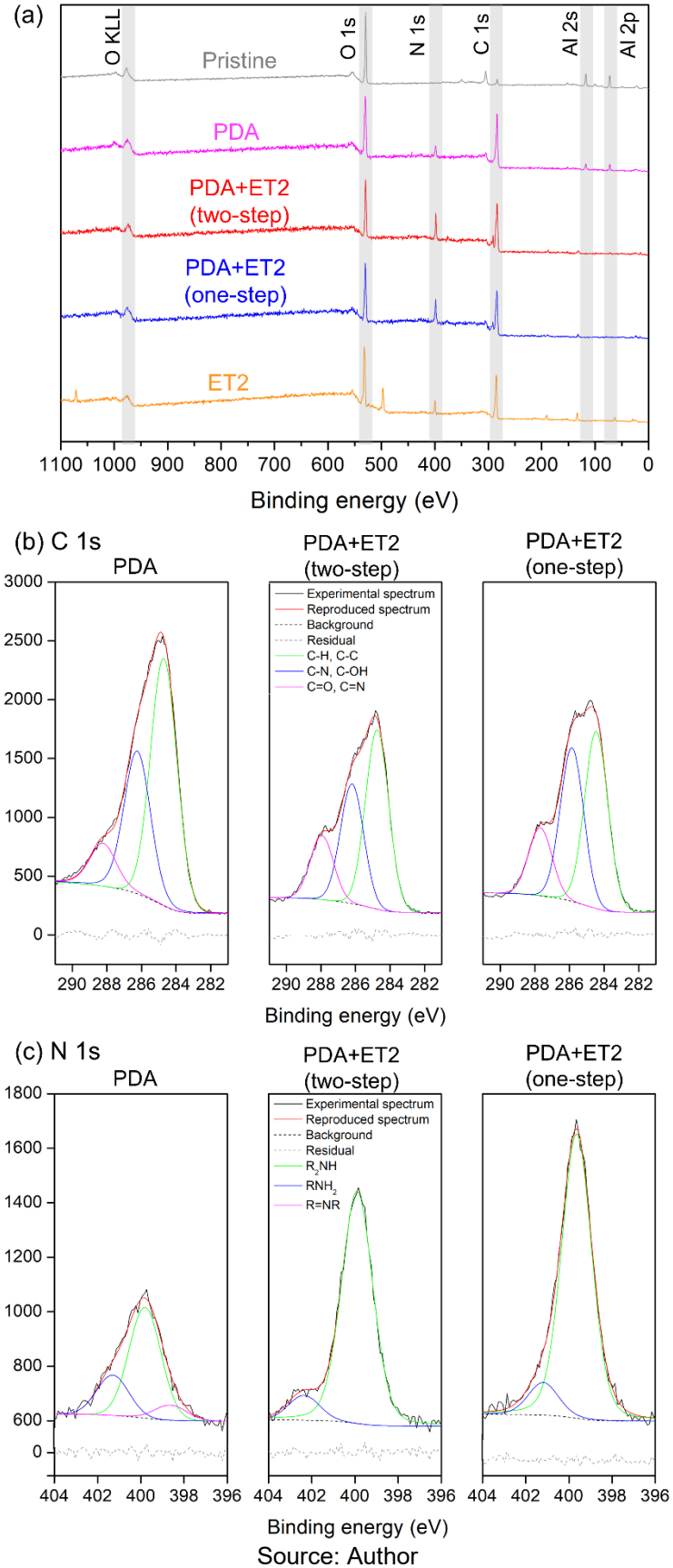

Source: Author

Table 11 – Elemental composition of free ET2 and pristine, PDA modified, and ET2-immobilized membranes analyzed by XPS

Sample	Atomic composition (%)			
	C	N	O	Al
Pristine	17.78 ± 3.27	-	62.83 ± 3.24	19.39 ± 0.03
PDA	64.05 ± 3.60	7.56 ± 0.13	26.41 ± 2.60	1.99 ± 1.13
PDA+ET2 (two-step)	60.45 ± 0.46	11.86 ± 0.41	25.12 ± 0.48	0.96 ± 0.29
PDA+ET2 (one-step)	58.71 ± 1.54	12.68 ± 1.94	27.15 ± 0.25	-
ET2	57.10 ± 0.91	6.80 ± 0.73	32.25 ± 1.84	-

Source: Author

Figure 25 – (a) Proposed immobilization mechanism for both two-step and one-step methods: Schiff base reaction, Michael addition and condensation reaction; (b) multipoint attachment occurring during the one-step modification and partial covering of PDA on the enzyme surface

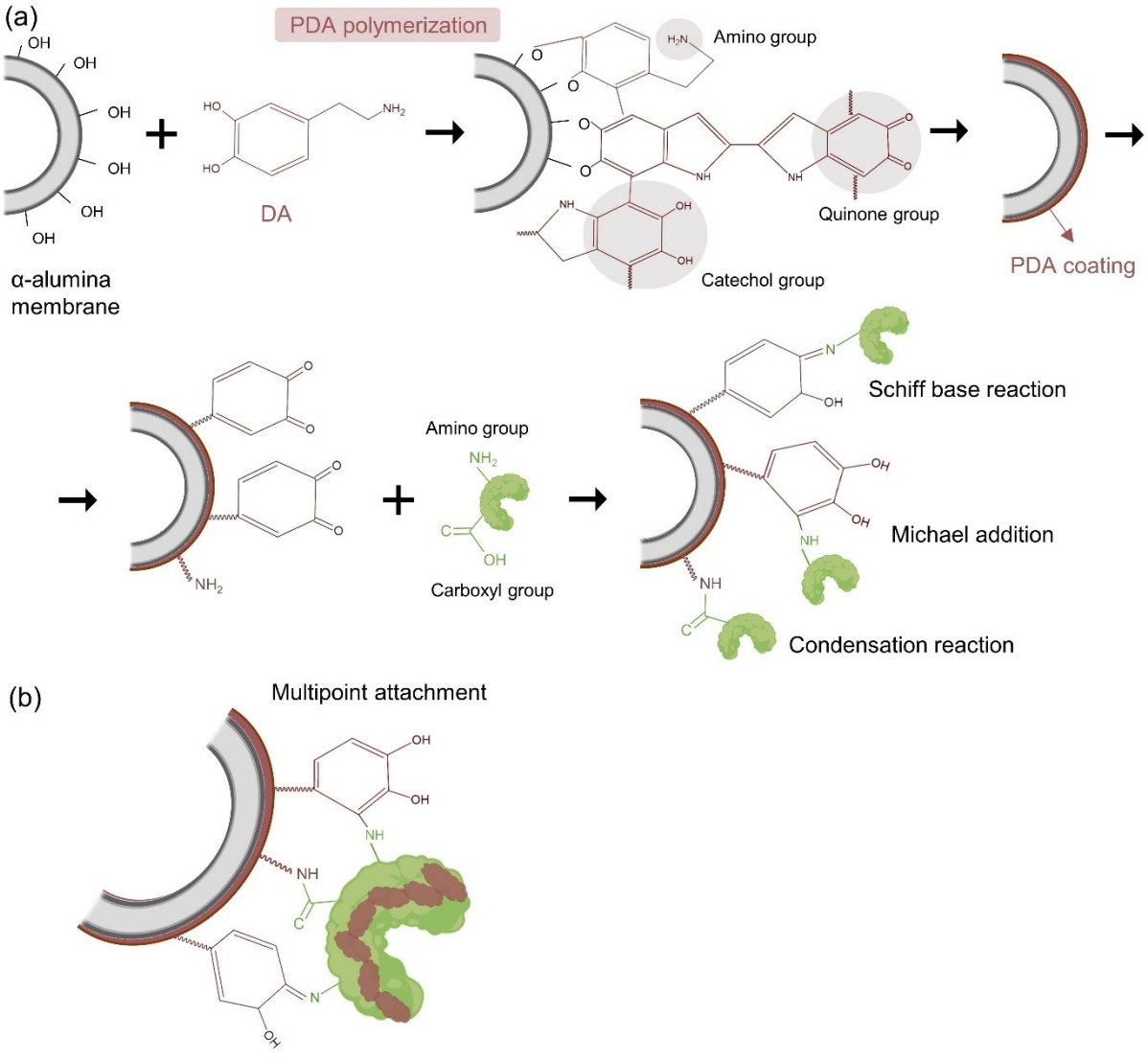

Source: Author.

Figure 26 compares the hydrophilicity/hydrophobicity of the membranes. As expected, water vapor adsorption by all the membranes was much greater than n-heptane vapor adsorption due to the hydrophilic nature of alumina. Consistent with our previous observation, PDA coating reduced both water and n-heptane vapor adsorption, which can be a result of pore blockage. Due to the hydrophilic character of PDA, the decline of n-heptane vapor uptake by the PDA-coated membrane was more intense than that of water, resulting in a higher water/n-heptane ratio. On the contrary, the addition of ET2 to the membrane surface greatly increased the adsorption of both vapors, which can be attributed to the enzyme's amphiphilic nature (KAPOOR; GUPTA, 2012). The results also show that the water vapor adsorption is consistent with the enzyme loading on the membrane since the membranes with ET2 immobilized through PDA coating showed higher values. The slightly higher water vapor uptake presented by the membrane modified by the one-step method can be a consequence of a higher quantity of polar covalent bonds on the membrane surface, such as C-OH, C-N, and R_2-NH, as shown in the XPS analysis (Figure 24).

Figure 26 – Water and n-heptane vapor adsorption at 23 °C (left axis) and the ratio of water and n-heptane adsorption (right axis) for the pristine membrane, PDA-coated membrane, and membranes with immobilized ET2 by simple adsorption, two-step, and one-step PDA coating

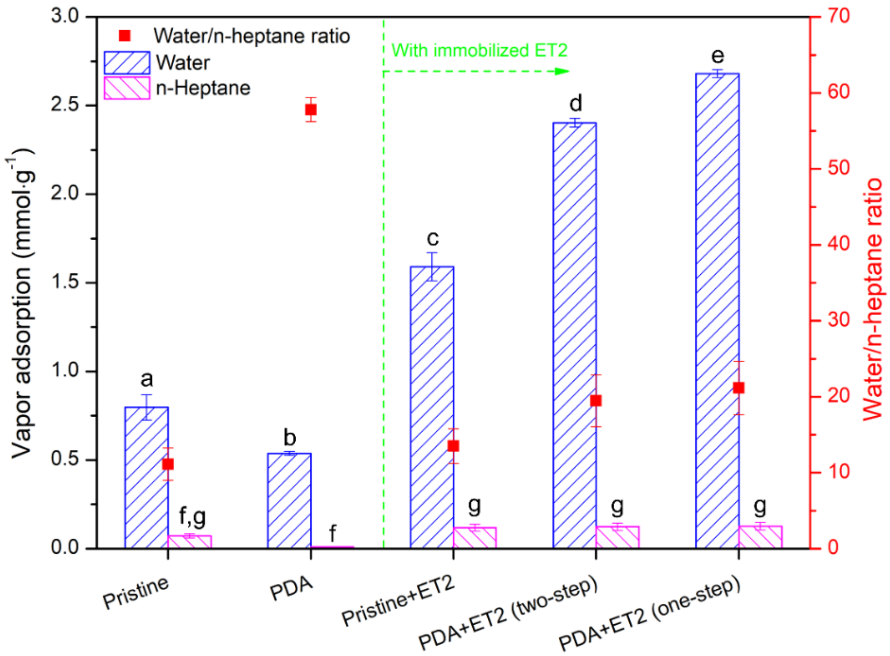

The values are means of triplicates and their respective standard deviations. Bars with different letters are significantly different according to Tukey's test ($p < 0.05$).
Source: Author

4.3.4 Fouling-reducing and self-cleaning capacities of the membranes

Oil-water emulsion filtration experiments were performed to determine the potential of the immobilized lipase ET2 for fouling reduction and membrane cleaning by degrading the oil attached to the membrane surface. Membrane permeate flux was monitored during the filtration experiments (Figure 27b), and pure water permeance was evaluated by pure water filtration before and after emulsion filtration, and after cleaning in 100 mM SPB at pH 7 and 40 ºC (optimal conditions for ET2 activity) (Figure 27a).

Pure water filtration experiments showed that the PDA coating reduced membrane permeance for water slightly (6%), presumably due to the penetration of PDA into membrane pores, which also decreased the water vapor adsorption as shown in Figure 26 and so, the water affinity of the membrane. Immobilization of ET2 on the PDA coating (i.e., the two-step method), on the other hand, slightly increased membrane permeance, which can be attributed to the increase in membrane surface hydrophilicity due to the presence of hydrophilic groups in the immobilized enzyme structure. Although the membrane modified by the one-step ET2 coating strategy was the most hydrophilic (Figure 26), it showed initial water permeance similar to the PDA-coated membrane. This may be the result of the longer polymerization time used (12 h) compared with that in the two-step method (6 h) and, hence, higher PDA loading.

During filtration of the oil-water emulsion, the oil content caused severe fouling of the uncoated membrane, resulting in a 62 ± 2 % reduction in membrane pure water permeance. The pristine membrane also showed lower permeate flux during the oil-water emulsion filtration (Figure 27b). The PDA coating did not have a measurable impact on the pure water permeance loss of the membrane after the two filtration cycles (Figure 27a and Table 12); however, it resulted in increased permeate flux during most of the oil-water emulsion filtration experiment, as it can be seen on Figure 27b. The immobilization of ET2 on the membrane surface, however, significantly reduced membrane fouling by the oil: pure water permeance reduction was limited to 40.2 ± 0.8 % and 35 ± 2 % for membranes modified by the two-step and one-step method, respectively. This may be attributed to the reduced adsorption of oil molecules on the ET2-immobilized membranes due to their higher hydrophilicity (Figure 26) as well as the hydrolysis of adsorbed oil molecules. The membrane with immobilized ET2 by the one-step approach also presented higher permeate fluxes throughout the

experiment than the other membranes (Figure 27b). The better performance of the one-step modified membrane can be attributed to the increased hydrophilicity (Figure 26) and the enhanced stability over reaction time (Figure 21).

The results show that two-step and one-step immobilization led to similar pure water permeances (Figure 27a) after the emulsion filtration, demonstrating that the one-step or one-pot ET2 immobilization with PDA can be used as an alternative to the conventional two-step procedure. Therefore, simultaneous dopamine polymerization and ET2 immobilization can be used to develop fouling-reducing enzymatic membranes using fewer chemicals in a shorter time.

Interestingly, the one-step ET2-immobilization method resulted in superior self-cleaning performance than the two-step method. As shown in Figure 27a and Table 12, the pristine membrane recovered 48.0 ± 0.8 % of its pure water permeance after the cleaning procedure, while the permeance of the PDA-coated, two-step, and one-step ET2-immobilized membranes resumed to 53.8 ± 1.4, 73.5 ± 0.7, and 89.7 ± 2.7 % of their initial permeance, respectively. Therefore, besides decreasing membrane fouling during emulsion filtration in a similar way as the two-step approach, the enzyme immobilization by the one-step procedure had a superior performance in terms of permeance recovery after cleaning, which can be a result of both increased water affinity (Figure 26) and increased stability over reaction time as described in Figure 21c.

Figure 27 – Performance of pristine and enzyme-active α-alumina membranes in the filtration of soybean oil in water emulsion (1 g·L^{-1}): (a) water permeance before the emulsion filtration (initial), after the final backwash (after filtration), and after the cleaning procedure; and (b) normalized permeate flux during the oil-water emulsion filtration

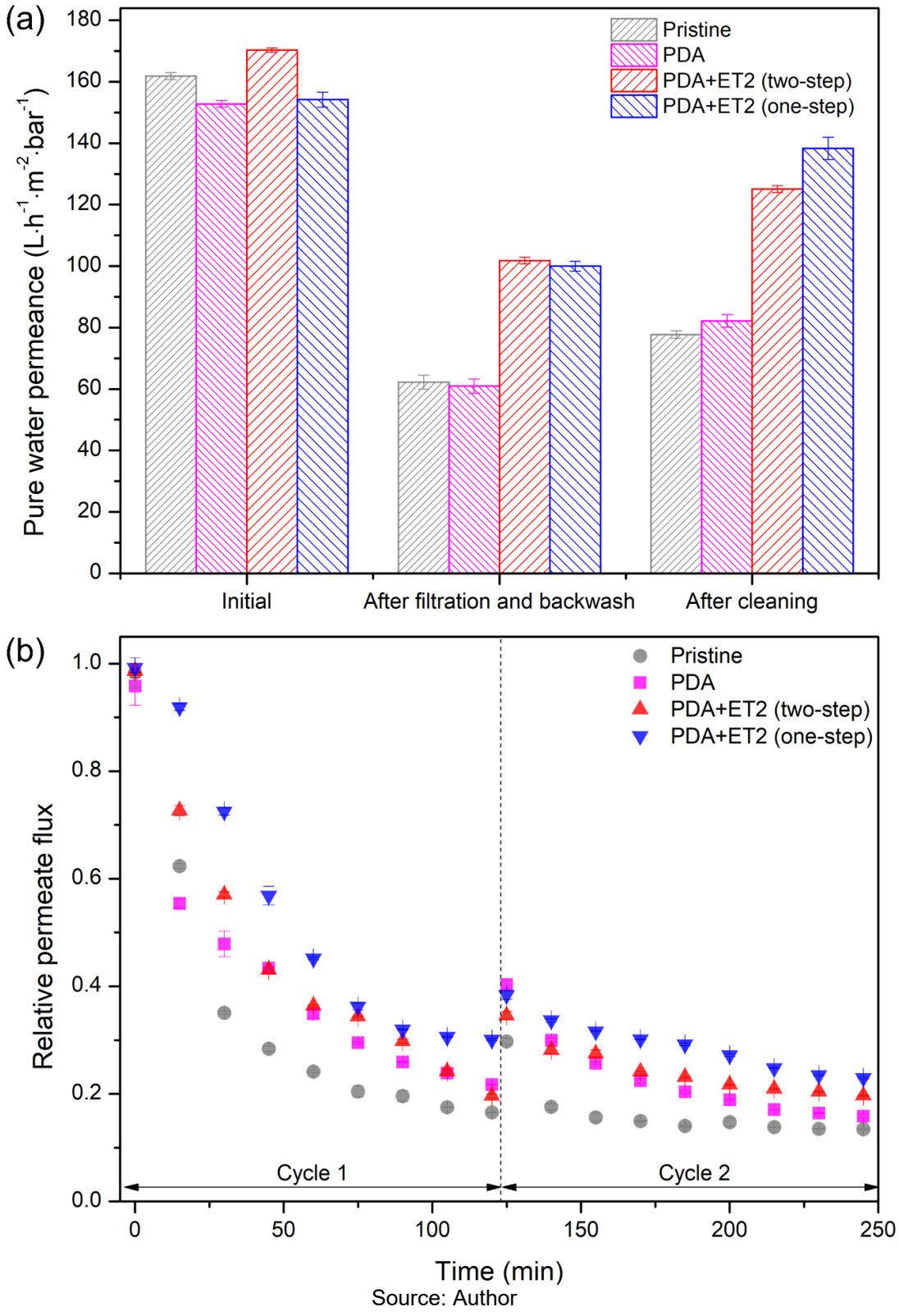

Source: Author

Table 12 – Summary of pure water permeance changes for the emulsion filtration test as shown in Figure 27 for the pristine and enzymatically active membranes

Membrane	Change in water permeance (%)	
	Reduction after emulsion filtration	Permeance recovery after cleaning
Pristine	61.5 ± 1.6	48.0 ± 0.8
PDA	60.1 ± 1.7	53.8 ± 1.4
PDA+ET2 (two-step)	40.2 ± 0.8	73.5 ± 0.7
PDA+ET2 (one-step)	35.1 ± 2.0	89.7 ± 2.7

Source: Author

The oil fouling control capacity (evaluated by pure water permeance reduction after filtration and backwash) of the membrane developed in this study was superior to those found in the literature for membranes with immobilized lipases (Table 13). This can be attributed to several factors, including the higher membrane hydrolytic activity, the crossflow filtration mode (which contributes to decreasing the fouling) instead of dead-end filtration, fewer filtration cycles, and also higher hydrophilicity since a ceramic membrane was used instead of a polymeric membrane. The self-cleaning capacity (evaluated by permeance recovery after cleaning) was also superior to most of the studies, which can also be a consequence of the higher membrane hydrolytic activity.

The membrane retention did not change considerably throughout the experiments. The pristine membrane had an oil retention of 90.6 ± 1.7 %, the PDA coated membrane 87.8 ± 3.0 %, the two-step modified membrane 93.1 ± 2.8 %, and the one-step modified membrane 96.1 ± 2.6 %. The same tendency of the water vapor adsorption (Figure 26) can be noticed here, showing that the increased hydrophilicity of the modified membranes can also help to increase the membrane oil retention.

Table 13 – Comparison of pure water permeance changes between this study and literature using lipase-immobilized membranes

Membrane configuration and material	Lipase	Immobilization agent	MHA[1]	Feed	Filtration conditions	Cleaning conditions	Changes in water permeance (%)		Ref.
							Reduction after filtration	Recovery after cleaning	
Tubular α-alumina	ET2	PDA	1986	1 g·L^{-1} soybean oil in aqueous SDS solution	Cross-flow, 1 bar, 1 L·min^{-1} of retentate flow rate, 2 cycles of 2 h each	SPB 100 mM pH 7, 12 h, 40 °C	35	90	This work
Flat sheet polyethersulphone (PES)	Pancreatin[2]	EDC[3] + NHS[4]	Not informed	0.5 g·L^{-1} linseed oil in aqueous SDS solution	Dead-end, 6 cycles filtrating 400 mL	PBS[5] pH 8, 12 h, 37 °C	40	75	Shulze et al. (2017)
Flat sheet polyvinylidene fluoride (PVDF)	PPL[6] II and *Candida rugosa* lipase	EDC + NHS	828	1 g·L^{-1} linseed oil in aqueous SDS solution	Dead-end, 7-8 cycles filtrating 200 mL	PBS pH 8, 12 h, 37 °C	58	72	Schmidt et al. (2018)
Flat sheet PVDF	*Thermomyces lanuginosus* lipase	Electron beam irradiation	823	1 g·L^{-1} olive oil in aqueous SDS solution	Dead-end, 4 cycles filtrating 500 mL	PBS pH 8, 3 h, 37 °C	68	100	Schmidt et al. (2022)

[1]μmol·min^{-1}·m^{-2}; [2]Mixture of lipase, protease and amylase; [3]1-ethyl-3-(3-dimethylaminopropyl) carbodiimide; [4]*N*-hydroxysuccinimid; [5]phosphate buffered saline; [6]porcine pancreatin lipase.

As presented in Figure 28, after three filtration and cleaning cycles, the pristine membrane had a reduction in pure water permeance of 91%. In contrast, the membrane with ET2 immobilized by the two-step method had a reduction of 69% and the membrane modified by the one-step strategy had a reduction of only 38%. After the first cycle, the pristine, two-step and one-step modified membranes recovered 48%, 73% and 90% of their initial pure water permeance, which decreased to 43%, 68%, and 86% after the second cycle, and 415, 61%, and 81% after the third cycle, respectively. Even though decreasing over the filtration and cleaning cycles, the permeance recovery showed by the membranes with immobilized ET2 was still significantly higher than the one shown by the pristine membrane. The improved stability of the enzymes immobilized by the one-step method (Figure 21) results in increased reusability over multiple filtration and cleaning cycles compared to the two-step immobilized lipase. These results can also be a consequence of increased rigidity of the ET2 immobilized by the one-step approach since more enzyme moieties were possibly used for the immobilization.

Figure 28 – Results of repeated filtration and cleaning experiments for the pristine, two-step and one-step modified membrane with PDA and ET2

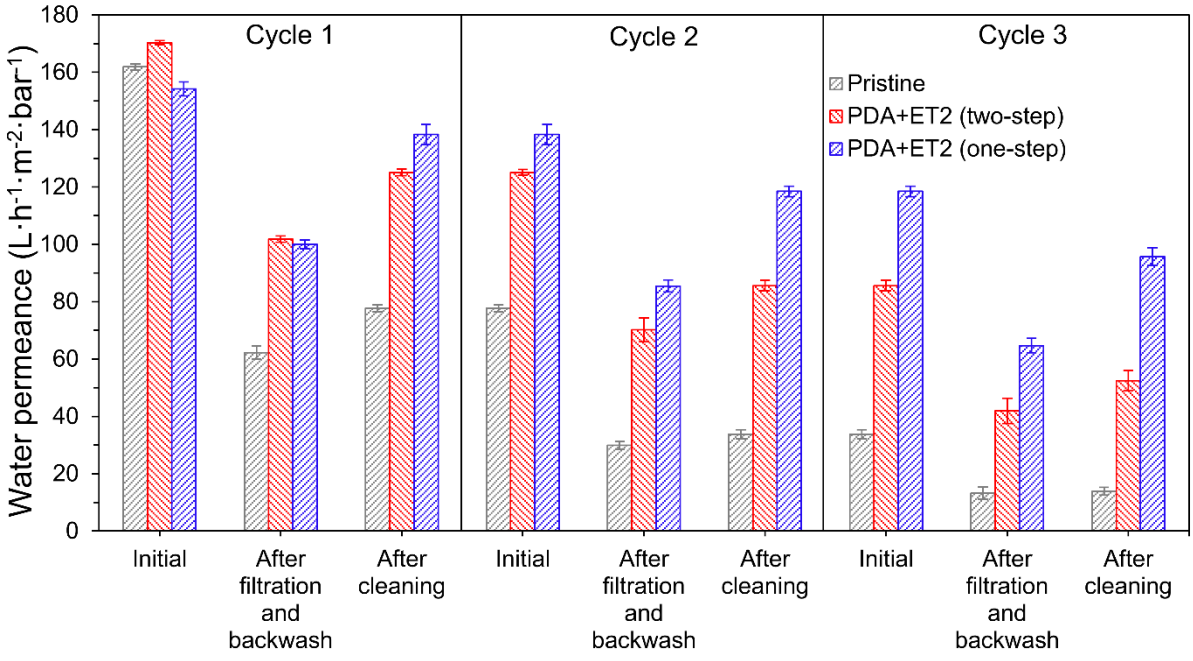

Source: Author

4.4 CONCLUSION

In this study, we demonstrated that one-step lipase ET2 immobilization using polydopamine as the bonding agent was an excellent alternative to the two-step approach. Not only did it achieve an enzyme loading and a membrane hydrolytic activity similar to the conventional two-step method, but it also enhanced the stability of the immobilized enzyme. ET2 immobilization using both the one-step and two-step methods rendered the membrane strong fouling resistance (reduction in pure water permeance of 35% and 40% after oil fouling, respectively) and self-cleaning capability, with the one-step immobilization method outperforming the two-step method (90% and 74% of permeance recovery, respectively). Furthermore, the one-step enzyme immobilization method using PDA is faster, uses fewer chemicals, consumes less water, and produces less wastewater, making it a lower-cost and more environmentally friendly approach. For being a simpler method, the one-step immobilization can be easier to scale up, which, combined to the advantages described above, make it more attractive to industry and research institutions.

5 IN-SITU ONE-STEP IMMOBILIZATION

Enzyme immobilization on membranes, mainly inorganic ones, is a challenging task that generally is multi-step, time-consuming, uses toxic chemicals, and is done ex-situ (outside the membrane filtration system). Developing an in-situ immobilization method is essential to facilitate the scale-up of the process. Therefore, the goal of this chapter was to develop a one-step in-situ method to immobilize the lipase Eversa Transform 2.0 (ET2) on the α-alumina membrane using polydopamine (PDA) as the bonding agent. The in-situ immobilization proved to be feasible, and by optimizing the dopamine hydrochloride (DA) and ET2 concentration in the immobilization solution to 0.3 $mg \cdot mL^{-1}$ and 4 $mg \cdot mL^{-1}$, respectively, the modified membrane reached an enzyme loading of 10 $g \cdot m^{-2}$ which resulted in an improved water affinity and membrane hydrolytic activity (38 $mmol \cdot min^{-1} \cdot m^{-2}$). Thereafter, the modified membrane showed a strong fouling resistance (pure water permeance reduction limited to 43% after oil-water emulsion filtration) and self-cleaning capacity (pure water permeance recovery of 97% after cleaning with deionized water at 40 °C for 6 h). The membrane regeneration by calcination and in-situ chemical cleaning was also tested to evaluate the reusability of the membrane after it was no longer active. The results showed that, after 5 cycles of modification-regeneration, no morphological or chemical changes were observed at the membrane surface. The in-situ enzyme immobilization and chemical regeneration are huge advantages that can facilitate the scale-up of the process. The reuse of the membrane coupled with the one-step modification using PDA can reduce costs and make the process more environmentally friendly.

5.1 INTRODUCTION

The development of biocatalytic membranes through the immobilization of enzymes can aim at producing target products (CHEN et al., 2019b; RANIERI et al., 2016; ZARE et al., 2019) or forming a fouling control and self-cleaning coating (KOLESNYK et al., 2019; SCHMIDT et al., 2018; SCHULZE et al., 2017). Most of the enzyme immobilization in membranes is done ex-situ, which means the membrane is modified outside the filtration module, generally by immersing it in the enzymatic solution (AGHABABAIE et al., 2016; BRISOLA et al., 2022; VASCONCELOS et al., 2020). Few studies have done the modification in situ (membrane inside the filtration

module), which can facilitate the scale-up of the process and the reuse of the membrane (CHEN et al., 2019b; GUO et al., 2018; MARPANI et al., 2015).

After some time, the enzymes lose their activity and must be replaced. In an in-situ immobilization, to reuse the membrane, both cleaning and modification steps could be performed directly in the filtration setup, so the membrane would not have to be removed and replaced in the system. This way, in situ immobilization, can save time and decrease operational costs.

For the filtration of oily wastewater, the immobilization of the enzyme lipase (triacylglycerol hydrolases, EC 3.1.1.3) in the membrane could be an alternative to improve the antifouling and self-cleaning capacity of the membrane. The immobilized lipase can degrade the triacylglycerols of the oil into fatty acids and glycerol, which can increase permeate flux during the filtration and avoid the use of chemicals during the cleaning (MULINARI et al., 2022; SCHMIDT et al., 2018; SCHULZE et al., 2017).

In this work, the enzyme lipase Eversa Transform 2.0 was immobilized on the surface of an α-alumina membrane using polydopamine as a bonding agent. The immobilization was performed in one step (dopamine polymerization and enzyme immobilization simultaneously) as described in the previous chapter by an in-situ method. The immobilization conditions, such as lipase concentration and dopamine concentration in the initial solution, were evaluated. Oil-water emulsion was filtered through the membrane to assess its fouling resistance and cleaning properties.

5.2 MATERIAL AND METHODS

5.2.1 Material and chemicals

Purified and concentrated lipase Eversa Transform 2.0 (ET2) produced by a genetically modified strain of *Aspergillus oryzae* was used (Novozymes, Denmark). The commercial enzymatic solution was dialyzed for 120 h using a cellulose membrane (12-14 KDa) and sodium phosphate buffer at 50 mmol·L^{-1} and pH 6.0. The buffer was replaced every 12 h. The purified enzyme solution was frozen at -50 °C and lyophilized for 48 h (Liotop model L101n). The resulting powder was stored at 4 °C until use.

Tubular α-alumina membranes were custom-made (Tecnicer, Brazil). They are 25 cm in length, 1.2 cm in outer diameter, and 0.8 cm in inner diameter. The total porosity of the membranes is 30 ± 2 %, and it was calculated using the apparent density

(2.8 ± 0.1 g·cm^{-3}) determined by the Archimedes' principle using distilled water (ASTM C20, 2000) and the absolute density (4.0 ± 0.1 g·cm^{-3}) determined by helium pycnometry.

Analytical grade dopamine hydrochloride (DA, 98%, $C_8H_{11}NO_2$.HCl, Sigma-Aldrich, USA), sodium dodecyl sulfate (SDS, ≥99%, $C_{12}H_{25}SO_4Na$, Sigma-Aldrich, USA), sodium hydroxide (95%, NaOH, Spectrum, USA), and ethanol (99,5%, C_2H_6O, Fisher Scientific, USA) were used as purchased. Tris(hydroxymethyl)aminomethane hydrochloride buffer 1 M at pH 8.5 (Tris-HCl, Teknova, USA) was used to prepare the 50 mM Tris-HCl buffer at pH 8.5. The 100 mM sodium phosphate buffer at pH 7 was prepared using sodium phosphate monobasic (99%, NaH_2PO_4, Thermo Scientific, USA) and sodium phosphate dibasic (≥99%, Na_2HPO_4, Sigma-Aldrich, USA). Refined soybean oil (Happy Belly®) was used to prepare the oil-water emulsion.

5.2.2 ET2 hydrolytic activity

The ET2 hydrolytic activity was determined using soybean oil as the substrate. Soybean oil emulsion (25% g·g^{-1}) was prepared immediately before each experiment by emulsifying soybean oil in a 2 mM aqueous solution of SDS using a magnetic stirrer at 1000 rpm for 10 min. Then, 1 mL of a 10 mg/mL ET2 solution in sodium phosphate buffer 100 mM pH 7 (stirred at 300 rpm for 1 h before the test to break enzyme aggregates) was added to 9 mL of the soybean emulsion, resulting in a soybean oil concentration of 225 g/L. After incubation for 30 min at 40 °C and agitation at 300 rpm, the reaction was interrupted by adding 15 mL of ethanol. The amount of fatty acids liberated during the reaction was determined by titration using NaOH 0.05 mol·L^{-1} until pH 11. Control assays were carried out by adding ethanol right before the addition of the enzyme. The specific hydrolytic activity (HA_S) was calculated using Eq. 15. All tests were performed in triplicate. It is important to noticed that the hydrolytic activity measurement method used in this chapter (with SDS as emulsifier) is different from the method used in the previous chapters (with PVA as emulsifier).

$$HA_S\ (mmol/min.g) = \frac{(V_s - V_c) \times M}{t \times V \times PC} \quad (15)$$

where V_s is the NaOH volume used to titrate the sample (mL), V_c is the NaOH volume used to titrate the control assay (mL), M is NaOH molarity (mol·L^{-1}), t is the reaction time (min), V is the volume of enzymatic solution added to the reaction media (mL), and PC is the protein content of the enzymatic solution (g·mL^{-1}) determined by the Bradford method using bovine serum albumin as a standard (Bradford, 1976).

5.2.3 ET2 immobilization

The in-situ enzyme immobilization was performed using the setup described in Figure 29 with no applied pressure and a 1.5 GPH (0.09 L·min^{-1}) flow rate. Differently from the previous studies, the inner side of the membrane was modified during the in-situ modification. A solution containing ET2 and dopamine was prepared by mixing the desired concentration of ET2 in the Tris-HCl buffer at 50 mM pH 8.5 for 1 h and then adding dopamine. A central composite rotatable design 2^2 was performed by varying the ET2 concentration (0.6-3.6 mg·mL^{-1}) and dopamine concentration (0.6-3.6 mg·mL^{-1}) in the solution. Further tests were performed using higher concentrations of ET2 (4.0-5.0 mg·mL^{-1}) and lower concentrations of dopamine (0.1-0.3 mg·mL^{-1}). Moreover, since our previous studies showed an increase in membrane hydrophilicity after ET2 immobilization (MULINARI et al., 2022), a control test was performed to check the contributions of the increased hydrophilicity and the oil hydrolysis during oil-water emulsion filtration and membrane cleaning. For that, active (with hydrolytic activity) and denatured (without hydrolytic activity) ET2 were immobilized and the performance of each membrane in the oil-water emulsion filtration and cleaning was performed. The lipase ET2 was denatured by boiling it for 10 min and its hydrolytic activity was determined to check if it was indeed denatured.

The enzymatic dopamine solution recirculated in the inner part of the membrane for 12 h at room temperature with stirring at 300 rpm. After the immobilization, sodium phosphate buffer 100 mmol·L^{-1} at pH 7 was passed through the membrane to remove loosely bounded enzymes until no protein was detected by the Bradford method. The tests were performed in triplicate.

Figure 29 – In-situ immobilization setup (0.09 L·min^{-1}, no applied pressure, total recirculation, module at vertical position)

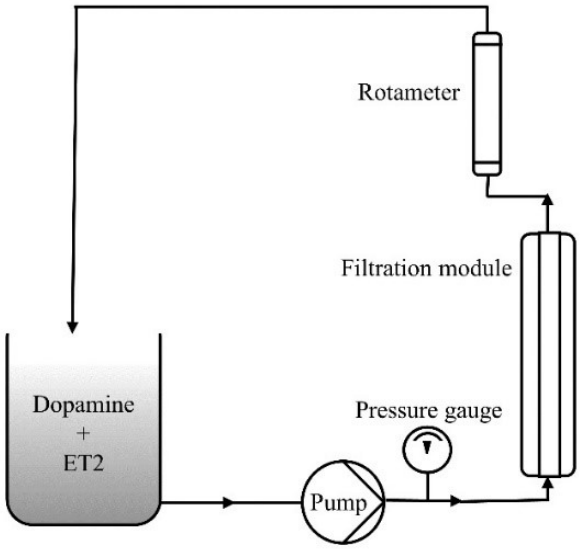

Source: Author

The amount of enzyme immobilized on the membrane was determined by the change in ET2 concentration in the solution before and after the immobilization, as measured by the Bradford method, also accounting for the enzyme removed during the rinsing step. Enzyme loading (*EL*) was calculated according to Eq. 16.

$$EL\ (g \cdot m^{-2}) = \frac{(C_o - C_f) \times V - M_r}{A} \quad (16)$$

where C_0 is the initial enzyme concentration in the solution (before the immobilization) (g·mL^{-1}), C_f is the final protein content (after the immobilization) (g·mL^{-1}), V is the volume of enzyme solution used in the test (mL), M_r is the amount of loosely bound enzyme removed by the rinsing step (g), and A is the membrane projected internal area (m^2).

The hydrolytic activity of the immobilized ET2 was evaluated using the same soybean oil emulsion used to determine the free ET2 activity. The soybean oil emulsion (225 g·L^{-1}) was kept at 40 °C and 300 rpm and was recirculated at 1.5 GPH (0.09 L·min^{-1}) in the inner part of the membrane for 1 h with no applied pressure as described in Figure 29. Then, a sample of 10 mL was withdrawn from the solution and titrated with 0.05 mol·L^{-1} NaOH until pH 11 to determine the amount of free fatty acids formed from the hydrolysis reactions. Control assays were performed under the same

conditions using membranes subjected to the same immobilization protocols but without the ET2 enzyme. The membrane hydrolytic activity (*MHA*) and the specific hydrolytic activity of the immobilized ET2 (MHA_S) were determined according to Eq. 17 and 18, respectively.

$$MHA\ (mmol \cdot min^{-1}.m^{-2}) = \frac{(V_s - V_c) \times M \times (V_t/V)}{t \times A} \quad (17)$$

$$MHA_S\ (mmol \cdot min^{-1}.g^{-1}) = \frac{(V_s - V_c) \times M \times (V_t/V)}{t \times A \times EL} \quad (18)$$

where V_s is the NaOH volume used to titrate the sample (mL), V_c is the NaOH volume used to titrate the control assay (mL), M is NaOH molarity ($mol \cdot L^{-1}$), V_t is the total volume of emulsion used in the test (mL), V is the volume of the emulsion sample titrated (mL), t is the reaction time (min), A is the membrane projected internal area (m^2), and EL is the enzyme loading in the membrane ($g \cdot m^{-2}$).

Relative activity, as defined by E. 19, was used to estimate the effect of immobilization on enzyme activity.

$$Relative\ activity\ (\%) = 100 \times \frac{MHA_S}{HA_S} \quad (19)$$

Analysis of variance (ANOVA) and Tukey's test ($p < 0.05$) were performed on enzyme loading, membrane hydrolytic activity, and specific hydrolytic activity.

5.2.4 Membrane characterization

The surface morphology and elemental composition of the pristine and the membrane modified by the best condition were characterized by Scanning Electron Microscopy (SEM, FEI Helios NanoLab 660 Dual) coupled with Electron Dispersion X-ray (EDX). Membrane hydrophilicity/hydrophobicity was determined using water and n-heptane vapor adsorption measurements as described by Mulinari (2022) and adapted from Nishihora et al. (2018) and Prenzel et al. (2014). Membrane surface chemistry was characterized by X-ray Photoelectron Spectroscopy (XPS, PHI Quantera, MN, USA) using monochromatic Al Kα X-rays. Since alumina is an insulating material, the spectra of all samples were charged correctly by shifting all peaks to the

adventitious C 1s spectral component (C-C, C-H) at 284.8 eV. The membranes and the lyophilized ET2 were also analyzed by attenuated total reflectance Fourier transform infrared spectroscopy (ATR-FTIR, Cary 660, Agilent Technologies, CA, USA).

5.2.5 Oil-water emulsion filtration and membrane cleaning tests

The ET2-immobilized membranes were tested for their fouling resistance and self-cleaning function in a soybean oil in water emulsion filtration according to previously reported protocols (Mulinari et al., 2022; Schmidt et al., 2018; Proner et al., 2020). Since the immobilization was carried out on the membrane's inner surface, filtration was performed inside-out. To prepare the test solution, soybean oil (1 g·L^{-1}) was emulsified in a 2 mmol·L^{-1} SDS aqueous solution by magnetic stirring at 1500 rpm for 10 min, generating an emulsion of oil droplets with an average diameter of 320 ± 21 µm. In the filtration experiment, deionized water was first filtered at 0.7 bar and 0.44 L·min^{-1} of retentate flow rate to determine the initial pure water permeance of the membrane (p_1). Then, two filtration steps of 2 h each were performed using the soybean oil emulsion in crossflow mode with complete recirculation of the retentate and permeate back to the feed reservoir. At the end of each filtration step, a backwash was carried out for 5 min at 0.7 bar and 0.44 L·min^{-1} of retentate flow rate using distilled water. After the final backwash, pure water permeance (p_2) was measured again to evaluate the degree of fouling expressed as the reduction in pure water permeance (*PWP*) calculated by E. 20. Sealing rings were fixed at 1 cm from each end of the membrane, resulting in an effective membrane length of 23 cm with an effective area of 57.8 cm^2.

$$PWP\ reduction\ after\ filtration\ (\%) = 100 \times \frac{(p_1 - p_2)}{p_1} \quad (20)$$

After the filtration experiments, the membranes were cleaned by recirculating the cleaning solution as schematized in Figure 29 using 1.5 GPH (0.09 L·min^{-1}). The cleaning solution, temperature, and time were evaluated. Sodium phosphate buffer 100 mmol·L^{-1} at pH 7 and deionized water were tested for 12 h at both 40 °C and room temperature (24 °C). The pH 7 and 40 °C were chosen since they resulted in the

highest hydrolytic activity for the immobilized ET2, as reported in our previous study. With the best solution and temperature, the cleaning time was evaluated from 3 to 12 h. After the cleaning procedure, the membranes' pure water permeance (p_3) was measured again at 0.7 bar and 0.44 L·min^{-1}. The performance of the cleaning procedures was evaluated by calculating the pure water permeance increase after cleaning (E. 21) and the overall permeance recovery (Eq. 22). SEM images were obtained to compare the membrane before and after oil fouling, and after the cleaning procedure.

$$PWP\ increase\ after\ cleaning\ (\%) = 100 \times \frac{(p_3 - p_2)}{p_1} \quad (21)$$

$$Overall\ PWP\ recovery\ (\%) = 100 \times \frac{p_3}{p_1} \quad (22)$$

Samples of the initial feed, final feed, permeate, and initial and final cleaning solution were compared qualitatively through liquid chromatography coupled with mass spectroscopy (LC-MS). LC-MS analyses were conducted using an Agilent 1290 Infinity II HPLC system operated at a flow rate of 0.4 mL·min^{-1}. Mobile phase A was water with 0.1% formic acid, and mobile phase B was acetonitrile with 0.1% formic acid. The analytical gradient ran from 55%B to 95%B over 12 min, followed by a column flush at 95%B for 3 min and re-equilibration at initial conditions for 3 min. Separations were carried out using an Agilent Zorbax Eclipse Plus C18 column (2.1 mm ID x 50 mm; 1.8 µm) operated at 25 °C. The LC was interfaced with an Agilent MSD-XT Single Quadrupole Mass Spectrometer through a standard electrospray ionization (ESI) source operated in the negative mode.

Three cycles of filtration and cleaning were performed using the same membrane to investigate their reusability in long-term applications. The number of filtration steps within each cycle was two. The emulsion was prepared as described above as well as the filtration and self-cleaning experiments.

5.2.6 Membrane regeneration

Two regeneration protocols were performed to evaluate if the same membrane could be modified several times after the immobilized ET2 was no longer active:

membrane calcination and chemical cleaning. The calcination was done at 700 ºC for 3 h to remove the organic coating. The chemical cleaning was performed using an aqueous solution of 15 $g \cdot L^{-1}$ of NaOH, which was recirculated through the membrane with a flow rate of 1.5 GPH (0.09 $L \cdot min^{-1}$) and no applied pressure, as shown in Figure 29. Three consecutive chemical cleanings of 15 min each were carried out using new alkali solutions. After that, deionized water was passed through the membrane until no pH changes could be observed. After the regeneration, the ET2 was immobilized again on the membrane surface, and the pure water permeance and membrane hydrolytic activity were evaluated after each regeneration-modification step. The two regeneration protocols were tested five times using the same membrane.

5.3 RESULTS AND DISCUSSION

5.3.1 ET2 immobilization

The lyophilized ET2 was immobilized by PDA coating using the one-step method under different concentrations of dopamine hydrochloride and ET2 in the solution. Table 14 shows the CCRD 2^2 results of enzyme loading, membrane hydrolytic activity, specific hydrolytic activity, and residual activity for each condition tested. The relative activities were calculated based on the specific activity of the free lyophilized ET2: 13.0 ± 0.6 $mmol \cdot min^{-1} \cdot g^{-1}$.

According to the results, when comparing fixed concentrations of DA (for example, tests 1 and 3 for 1 $mg \cdot mL^{-1}$ of DA, and tests 2 and 4 for 3 $mg \cdot mL^{-1}$ of DA), an increase in the ET2 concentration results in an increase in the enzyme loading (*EL*) on the membrane. No significant differences can be noticed when the DA concentration changes (for example, tests 1 and 2 for 1 $mg \cdot mL^{-1}$ of ET2, and tests 3 and 4 for 3 $mg \cdot mL^{-1}$ of ET2). This behavior indicates that even the lowest concentrations of DA used in the experiments are enough to immobilize the enzyme on the membrane; moreover, the increase in enzyme loading when increasing the ET2 concentration indicates that more enzymes can be immobilized by the used amount of DA.

Table 14 – Enzyme loadings (EL) and hydrolytic activities of the ET2 immobilized on the α-alumina membranes by different protocols

Test	ET2 ($mg \cdot mL^{-2}$)	DA ($mg \cdot mL^{-1}$)	EL ($g \cdot m^{-2}$)	MHA ($mmol \cdot min^{-1} \cdot m^{-2}$)	MHA_S ($mmol \cdot min^{-1} \cdot g^{-1}$)	Relative activity (%)
1	-1 (1.0)	-1 (1.0)	2.1 ± 0.3	6.3 ± 0.3	3.0 ± 0.4	22.7 ± 3.2
2	-1 (1.0)	1 (3.0)	3.1 ± 0.7	4.6 ± 0.2	1.5 ± 0.4	11.3 ± 2.8
3	1 (3.0)	-1 (1.0)	4.6 ± 0.7	13.2 ± 0.4	2.9 ± 0.4	22.3 ± 3.5
4	1 (3.0)	1 (3.0)	4.9 ± 0.8	6.3 ± 0.1	1.3 ± 0.2	9.8 ± 1.7
5	-1.41 (0.6)	0 (2.0)	3.1 ± 0.4	5.0 ± 0.4	1.6 ± 0.3	12.5 ± 2.2
6	1.41 (3.6)	0 (2.0)	3.7 ± 0.2	10.3 ± 0.4	2.8 ± 0.2	21.5 ± 1.8
7	0 (2.0)	-1.41 (0.6)	2.9 ± 0.3	8.6 ± 0.1	3.0 ± 0.3	22.7 ± 2.4
8	0 (2.0)	1.41 (3.6)	2.8 ± 0.2	4.3 ± 0.1	1.5 ± 0.1	11.8 ± 0.9
9	0 (2.0)	0 (2.0)	2.5 ± 0.2	7.2 ± 0.3	2.9 ± 0.3	22.1 ± 2.6
10	0 (2.0)	0 (2.0)	2.3 ± 0.3	6.8 ± 0.3	3.0 ± 0.5	23.0 ± 3.6
11	0 (2.0)	0 (2.0)	2.5 ± 0.4	7.4 ± 0.2	3.0 ± 0.5	23.3 ± 3.7

All values are averages of triplicate tests and their respective standard deviations.
Source: Author

The results of the experimental design for the membrane hydrolytic activity were subjected to the analysis of variance (ANOVA) (Table 15) and a refined empirical mathematical model (Eq. 23) of the membrane hydrolytic activity as a function of dopamine hydrochloride and ET2 concentrations in the solution was obtained. The determination coefficient ($R^2 = 0.95$) and the F-test validated the model ($p < 0.05$), so it was possible to generate the response surface of Figure 30.

Table 15 – The ANOVA for the membrane hydrolytic activity (MHA) as a function of the lipase ET2 and the dopamine hydrochloride concentrations in the immobilization solution

Source of variation	Sum of squares	Degrees of freedom	Mean squares	F_{calc}	F_{tab}
Regression	66.1	3	22.0	49.4	4.3
Residual	3.1	7	0.4		
Total	69.2	10			

Source: Author

$$MHA = 7.3 + 1.9 \times ET2 - 1.8 \times DA - 1.3 \times ET2 \times DA \quad (23)$$

where *MHA* is the membrane hydrolytic activity (mmol·min^{-1}·m^{-2}), *ET2* is the lipase concentration (mg·mL^{-1}) and *DA* is the dopamine hydrochloride concentration (mg·mL^{-1}) in the immobilization solution.

Figure 30 – (a) Surface response and (b) surface profile for the membrane hydrolytic activity (MHA) as a function of the lipase ET2 and the dopamine hydrochloride concentrations in the immobilization solution

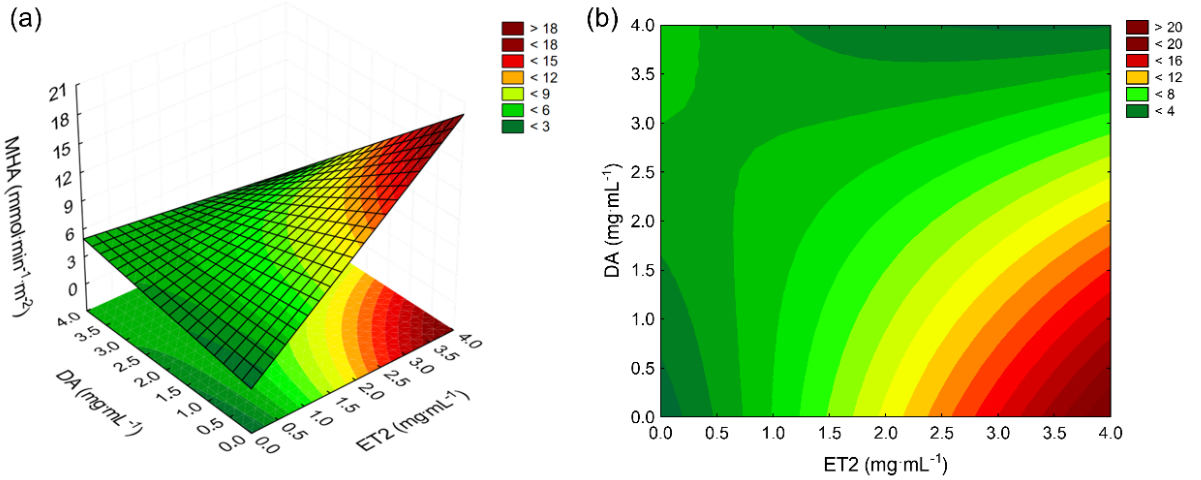

Source: Author

The experimental design suggested that higher concentrations of ET2 and lower concentrations of DA in the immobilization solution resulted in higher membrane hydrolytic activities. The concentration intervals tested in the experimental design (0.6-3.6 mg·mL^{-1} of ET2 and DA) were not enough to reach the optimized immobilization condition, which is why lower concentrations of DA and higher concentrations of ET2 were tested. First, lower DA concentrations were tested using a fixed concentration of 2 mg·mL^{-1} of ET2 (Figures 31a, 31c, and 31e), and then, with the best DA concentration (0.3 mg·mL^{-1}), the ET2 concentration was evaluated (Figures 31b, 31d, and 31f).

The additional tests showed that the membrane hydrolytic activity (*MHA*) increased with the decrease of the DA concentration (Figure 31c) until it reached 0.3 mg·mL^{-1}. When using less DA (0.1 mg·mL^{-1}), the enzyme loading decreased significantly (Figure 31a), resulting in a lower *MHA*. Even though *EL* was the same, the lower *MHA* in higher DA concentrations (0.6 – 3.6 mg·mL^{-1}) can be a consequence of polydopamine covering the enzyme and blocking the active site. This fact is

corroborated by the immobilized enzyme specific activity (MHA_s) that decreases as the DA concentration increases (Figure 31e).

Figure 31 – Additional tests to evaluate the (a,b) enzyme loading (EL), (c,d) membrane hydrolytic activity (MHA), and (e,f) specific activity (MHAs) of (a,c,e) lower dopamine hydrochloride (DA) concentrations and (b,d,f) higher ET2 concentrations in the immobilization solution

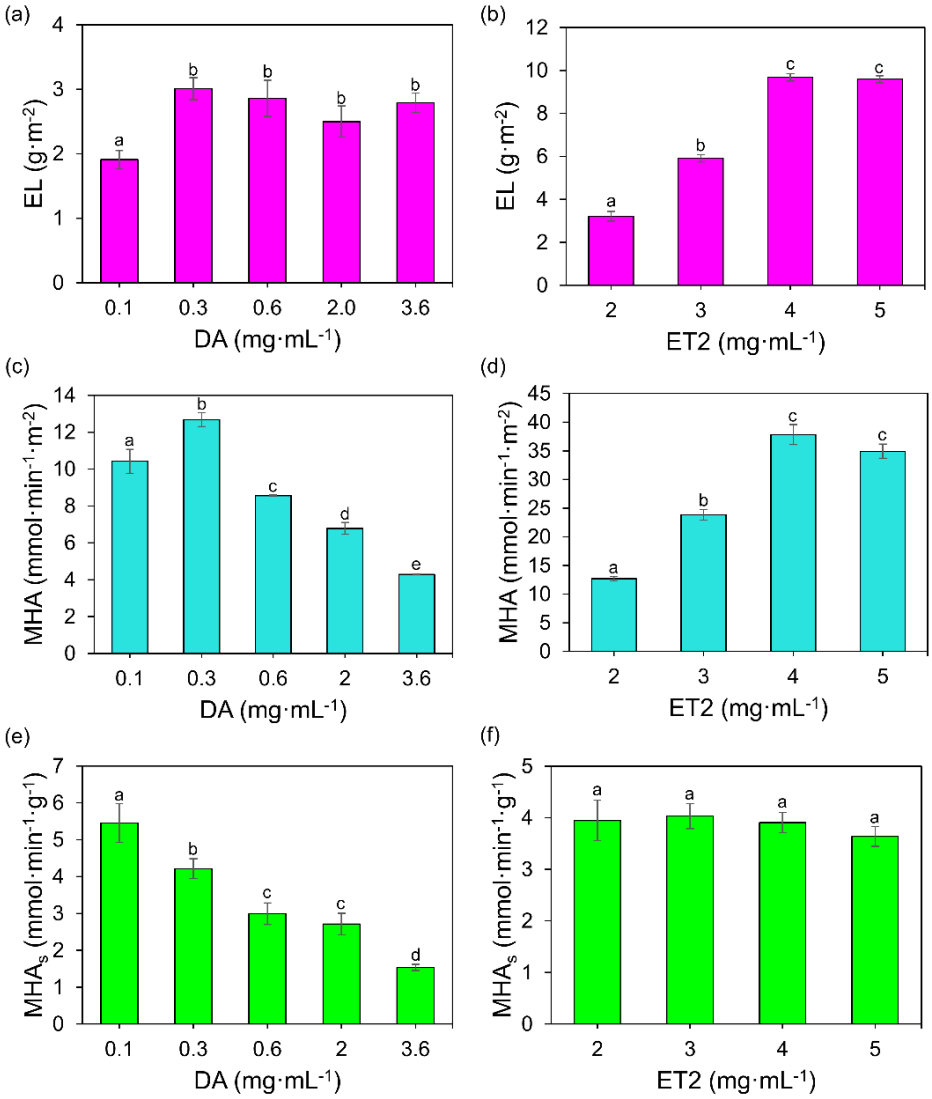

The values are means of triplicates and their respective standard deviations. Bars with different letters are significantly different according to Tukey's test ($p < 0.05$).
Source: Author

By fixing DA concentration at 0.3 mg·mL^{-1} and increasing ET2 concentration, the enzyme loading on the membrane only increased until 4 mg·mL^{-1} of ET2 (Figure 31b), suggesting that the available bonding sites of the polydopamine had been filled and adding more enzyme to the solution would not increase the amount of lipase immobilized. The *MHA* increased proportionally to the enzyme loading and reached

the highest value at 4 mg·mL^{-1} of ET2 as well (Figure 31d). The immobilized enzyme specific activity (MHA_s) did not change significantly with the different ET2 concentrations (Figure 31f), suggesting that even though more enzyme was immobilized, they did not block access to each other's active site. Therefore, the DA concentration of 0.3 mg·mL^{-1} and the ET2 concentration of 4 mg·mL^{-1} were used in the next steps.

5.3.2 Membrane Characterization

Figure 32 shows the SEM images of the pristine membrane, the PDA-coated membrane, and the membrane with immobilized ET2. The enzymatically active membrane (Figure 32e) showed a uniform coating, and the EDX analysis showed an increase in the carbon content of the membrane surface from 11% for the PDA-coated membrane to 30%, as well as the nitrogen content from 1% to 4%.

Figure 33 shows the hydrophilicity/hydrophobicity of the membranes. As shown in our previous work, water vapor adsorption was much more considerable than n-heptane vapor adsorption for all the membranes due to the hydrophilic nature of alumina. Our previous study showed a decrease in the adsorption of both vapors after PDA modification by 2 mg·mL^{-1} of DA (MULINARI et al., 2022). In this study, however, a lower concentration of DA was used (0.3 mg·mL^{-1}), and the coating did not affect the adsorption of the vapors, suggesting that a thinner coating was formed. Similar to the results of previous studies (KUJAWA et al., 2021; MULINARI et al., 2022), the addition of ET2 significantly increased the adsorption of both vapors by the membrane, possibly due to the enzyme's amphiphilic nature (KAPOOR; GUPTA, 2012).

The ATR-FTIR analysis (Figure 34) shows that the membranes with immobilized ET2 presented similar functional groups found in the free lipase sample: C=O stretching of primary amides from the α-helix secondary assignment, common in the secondary structure of proteins (1650 cm^{-1}), N-H bending of secondary amides (1540 cm^{-1}), and C-N stretching from amines (1050 cm^{-1}) (BRESOLIN et al., 2020; KONG; YU, 2007). The signals of the PDA coating did not appear at the membrane with immobilized ET2, probably due to the low concentration of DA and high concentration of ET2 used for the immobilization.

Figure 32 – SEM images and EDX mapping of the active surface of: (a,b) pristine membrane; (c,d) PDA-coated membrane; (e,f) membrane with ET2 immobilized by the optimized method (0.3 mg·mL^{-1} of DA and 4 mg·mL^{-1} of ET2); (g) elemental analysis of the membranes by EDX

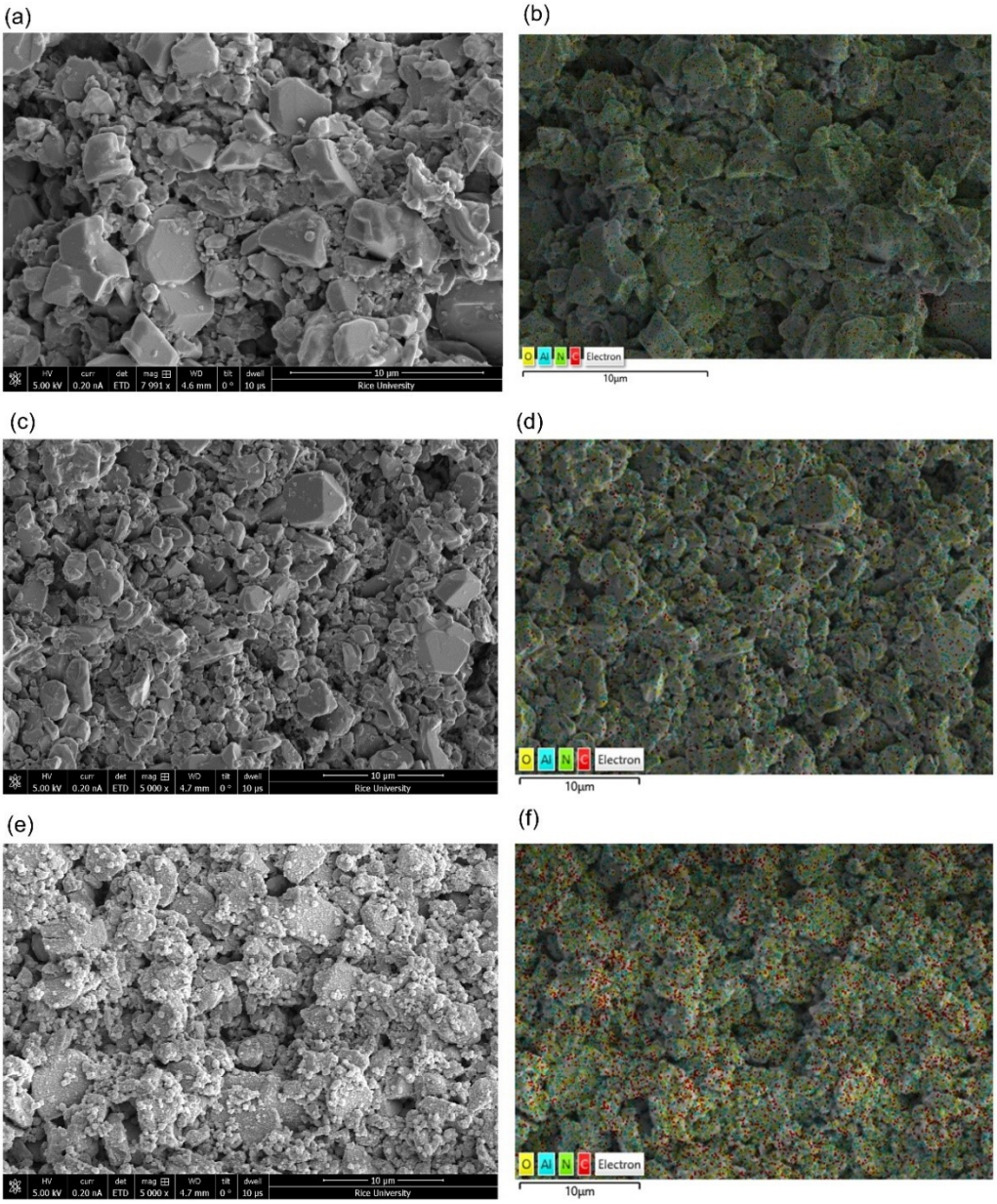

(g)

Element	Atomic%		
	Pristine	PDA	PDA+ET2
C	0.1 ± 0.7	10.8 ± 0.5	29.8 ± 1.5
O	68.7 ± 1.2	39.6 ± 1.7	30.9 ± 0.8
N	-	0.9 ± 0.2	3.7 ± 0.6
Al	31.3 ± 0.9	48.6 ± 2.1	35.7 ± 1.5

Source: Author

Figure 33 – Water and n-heptane vapor adsorption at 23 °C (left axis) and the ratio of water and n-heptane adsorption (right axis) for the pristine membrane, PDA-coated membrane, and membrane with immobilized ET2 by the optimized method (0.3 mg·mL^{-1} of DA and 4 mg·mL^{-1} of ET2)

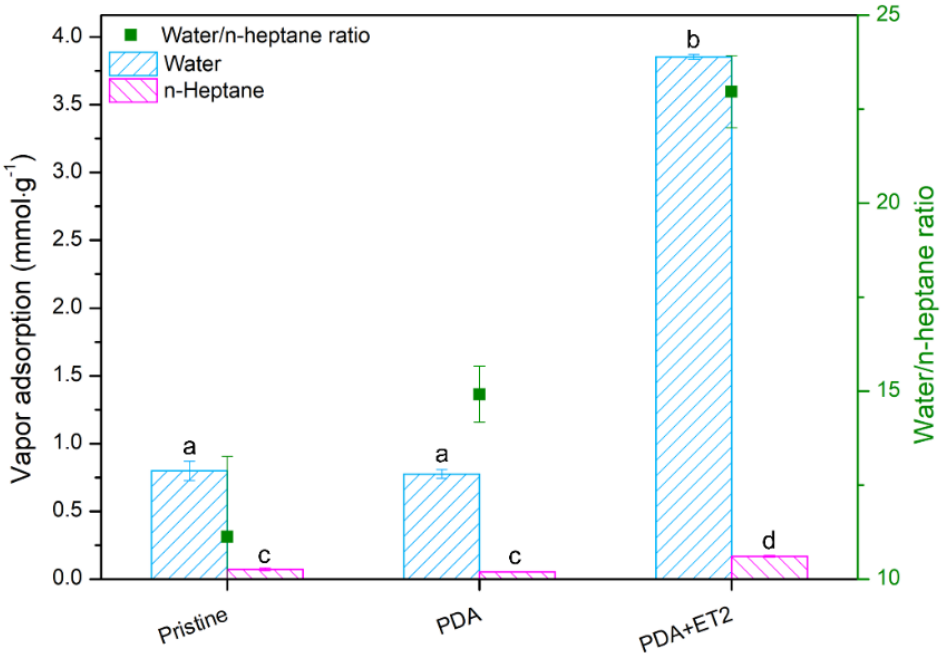

The values are means of triplicates and their respective standard deviations. Bars with different letters are significantly different according to Tukey's test ($p < 0.05$).
Source: Author

Figure 34 – ATR-FTIR of the pristine membrane, PDA-coated membrane, membrane with immobilized ET2 by the optimized method (0.3 mg·mL^{-1} of DA and 4 mg·mL^{-1} of ET2), and free lyophilized ET2

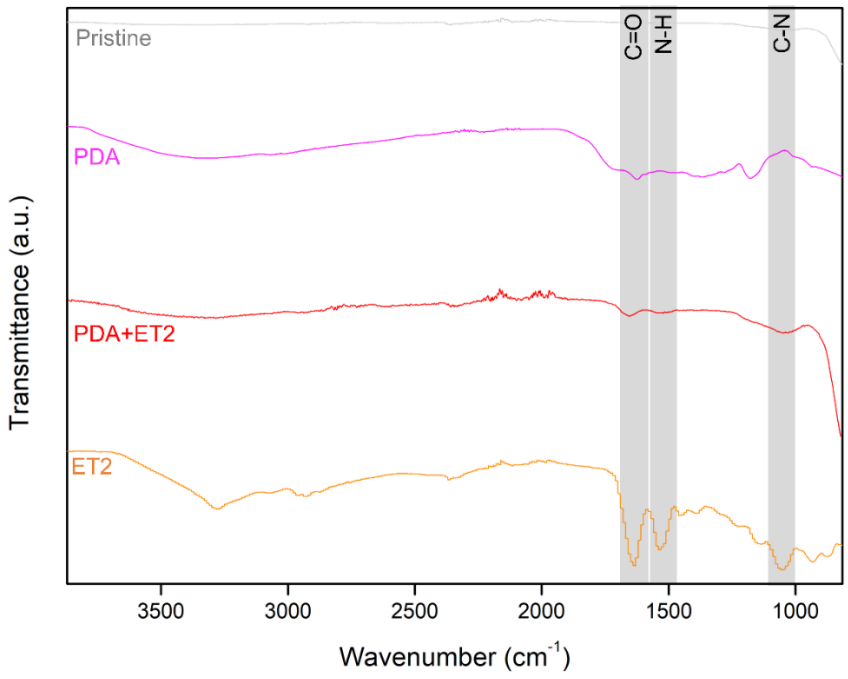

Source: Author

Figure 35 and Table 16 show the surface chemical composition of the membranes and the free ET2 characterized by XPS analysis. No aluminum was detected in the modified membranes, and the carbon content increased, demonstrating a successful modification of the membrane surface. Furthermore, nitrogen peaks appeared after PDA coating and increased after ET2 immobilization. Table 16 shows the relative amounts of the elements detected by the XPS analysis. The N/C atomic ratio increased from 0.15 ± 0.01 for the PDA-coated membrane to 0.21 ± 0.01 for the membrane with immobilized ET2.

Figure 35b shows the fitted carbon spectra of the modified membranes. The ET2-immobilized membrane had a significant increase in the content of C=O or C=N and C-N or C-OH and a decrease in C-H and C-C contents, suggesting that the amino groups of the ET2 could have reacted with the quinone groups of the PDA by both Schiff base reaction and Michael addition (MULINARI et al., 2022; TOUQEER et al., 2019). The increase in C=O can also be attributed to the carboxyl groups in the enzyme and was reported by other studies as a result of the formation of PDA-protein complexes (WANG et al., 2021). Moreover, a condensation reaction may have occurred between the carboxyl groups of the ET2 and the amino groups of the PDA.

The N 1s spectrum (Figure 35c) shows that the intensity of R_2NH binding energy considerably increases after ET2 immobilization on the membrane, which is another indication that Michael addition is occurring between the amino groups of the enzyme and the quinone groups of the PDA. The RNH_2 peak intensity of the membrane with ET2 decreased and the R=NR peak disappeared. Also, there is a shift in the R_2NH and the RNH_2 binding energy, suggesting a modification in the environment near the nitrogen. This shift was not detected in our previous study for the one-step immobilization using PDA, probably because the higher DA concentration used during the immobilization could have covered part of the enzymes.

Figure 35 – XPS spectra of: (a) pristine membrane, modified membranes, and free ET2; (b) fitted carbon (C 1s) and (c) nitrogen (N 1s) spectra for the membranes with PDA coating and with immobilized ET2 by the optimized immobilization method (0.3 mg·mL^{-1} of DA and 4 mg·mL^{-1} of ET2)

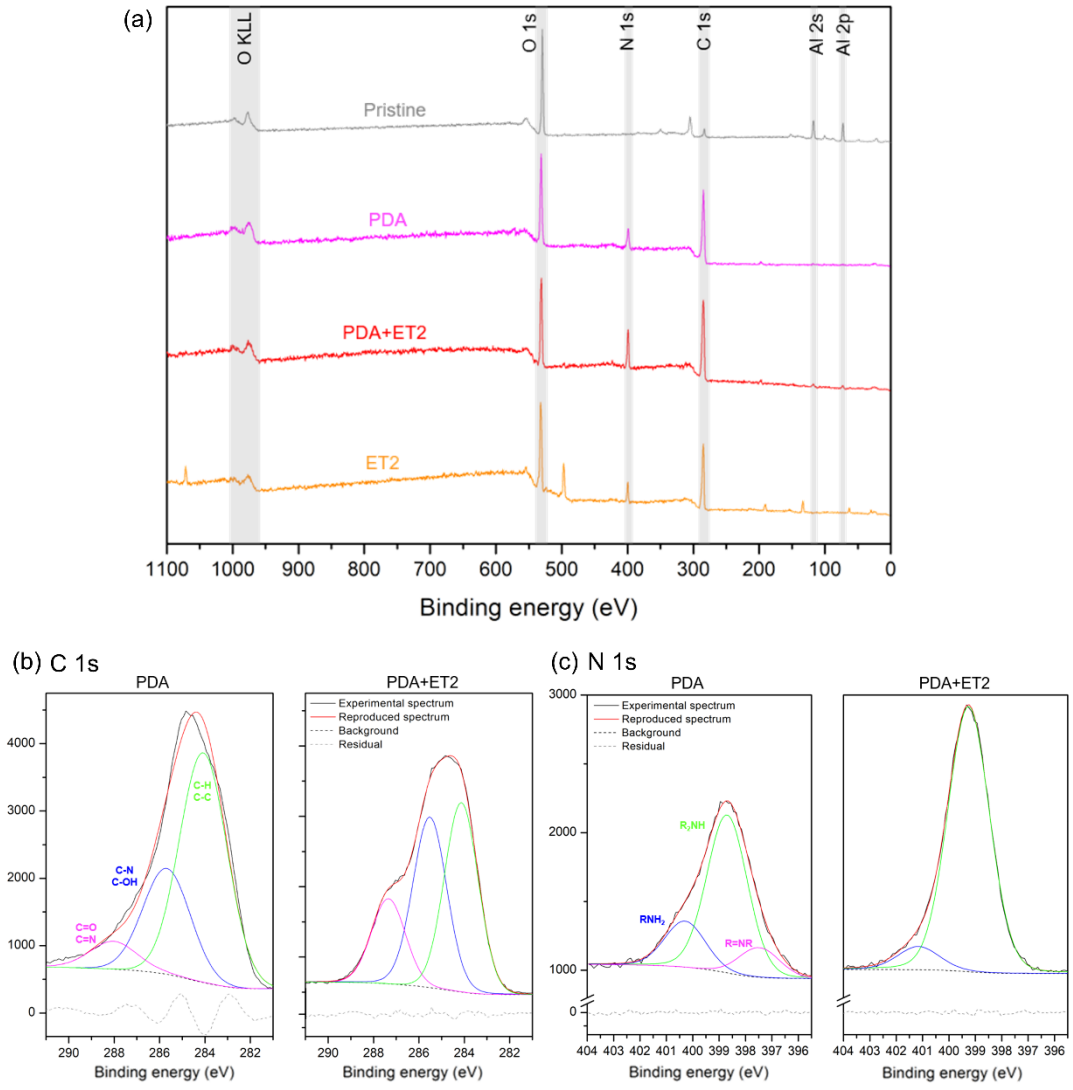

Source: Author

Table 16 – XPS elemental composition of the pristine, PDA-coated, PDA+ET2-immobilized membranes, and free ET2

Sample	Atomic composition (%)			
	C	N	O	Al
Pristine	17.8 ± 3.3	-	62.8 ± 3.2	19.4 ± 0.1
PDA	62.4 ± 0.4	9.5 ± 0.4	28.1 ± 0.2	-
PDA+ET2	62.0 ± 0.4	13.6 ± 0.4	24.4 ± 0.4	-
ET2	57.1 ± 0.9	6.8 ± 0.7	32.3 ± 1.8	-

Source: Author

5.3.3 Fouling-reducing and self-cleaning capacities of the membranes

Our previous studies showed that the membranes with immobilized ET2 can have fouling-reducing and self-cleaning properties towards oil fouling (MULINARI et al., 2022). Therefore, oil-water emulsion filtration experiments were performed to test the performance of the membrane modified by the optimized in-situ immobilization method. To evaluate the intensity of the oil fouling, pure water permeance was determined by pure water filtration before and after oil-water emulsion filtration followed by backwash, and after cleaning the membrane in 100 mM sodium phosphate buffer at pH 7 and 40 ºC (optimal conditions for ET2 activity) (Figure 36a). The membrane modified by the one-step in-situ optimized immobilization method (0.3 $mg \cdot mL^{-1}$ of DA and 4 $mg \cdot mL^{-1}$ of ET2) was compared to the membrane modified by the one-step method used to compare it to the two-step method in the previous chapter, in which 2 $mg \cdot mL^{-1}$ of DA and 2 $mg \cdot mL^{-1}$ of ET2 were used in the immobilization solution. Also, to check if the improved performance shown by the modified membranes was a result of enzymatic hydrolysis or increased water affinity (Figure 33), a membrane with denatured ET2 was tested.

Pure water filtration experiments showed that the membranes with immobilized ET2 had slightly higher initial pure water permeances (Figure 36a), which is expected due to the increase in membrane surface hydrophilicity (Figure 33). The oil-water emulsion filtration caused severe fouling of the pristine and PDA-coated membranes, resulting in an 83 ± 3 % and 76 ± 4 % reduction in pure water permeance, respectively (Figure 36b). However, the immobilization of ET2 (both denatured and active) on the membrane surface significantly reduced the fouling by the oil-water emulsion. The membranes modified by both denatured and active ET2 using 2 $mg \cdot mL^{-1}$ of DA and 2 $mg \cdot mL^{-1}$ of ET2, as described in our previous study, had statistically similar pure water permeance reductions: 62 ± 7 % and 57 ± 4 %, respectively. This fact demonstrates that, during emulsion filtration, the improved performance of the membrane with immobilized ET2 is due to the higher hydrophilicity provided by the modification rather than the enzymatic hydrolysis. However, the increase in water permeance after the cleaning procedure was significantly higher for the membrane with the active enzyme (28 ± 4 %) in comparison to the membrane with the denatured ET2 (6 ± 2 %), which, in turn, was similar to the pure water permeance increases of the membranes without ET2 (5 ± 2 % for the pristine membrane and 5 ± 1 % for the PDA-

coated membrane). The higher increase in pure water permeance of the active membrane after cleaning demonstrates that, during the cleaning procedure, enzymatic hydrolysis plays the key role and not the higher hydrophilicity.

The membrane modified by the in-situ one-step optimized method using 0.3 $mg \cdot mL^{-1}$ of DA and 4 $mg \cdot mL^{-1}$ of ET2 showed a better fouling-reducing and self-cleaning performance than the membrane modified by the previous one-step method using 2 $mg \cdot mL^{-1}$ of DA and 2 $mg \cdot mL^{-1}$ of ET2. The optimized membrane showed a higher membrane hydrolytic activity (37.8 ± 1.8 $mmol \cdot min^{-1} \cdot m^{-2}$ as shown in Figure 31d) than the membrane modified using 2 $mg \cdot mL^{-1}$ of DA and 2 $mg \cdot mL^{-1}$ of ET2 (7.2 ± 0.3 $mmol \cdot min^{-1} \cdot m^{-2}$ as shown in Table 14) and a higher water vapor uptake (3.9 ± 0.1 $mmol \cdot g^{-1}$ as shown in Figure 33) compared to the previous membrane (2.7 ± 0.1 $mmol \cdot g^{-1}$ as shown in Figure 26).

Figure 36 – Performance of pristine, PDA-coated, and ET2-immobilized α-alumina membranes in the filtration of soybean oil in water emulsion (1 g/L): (a) water permeance before the emulsion filtration (initial), after the emulsion filtration and final backwash, and after the cleaning procedure; and (b) summary of the pure water permeance changes

(a)

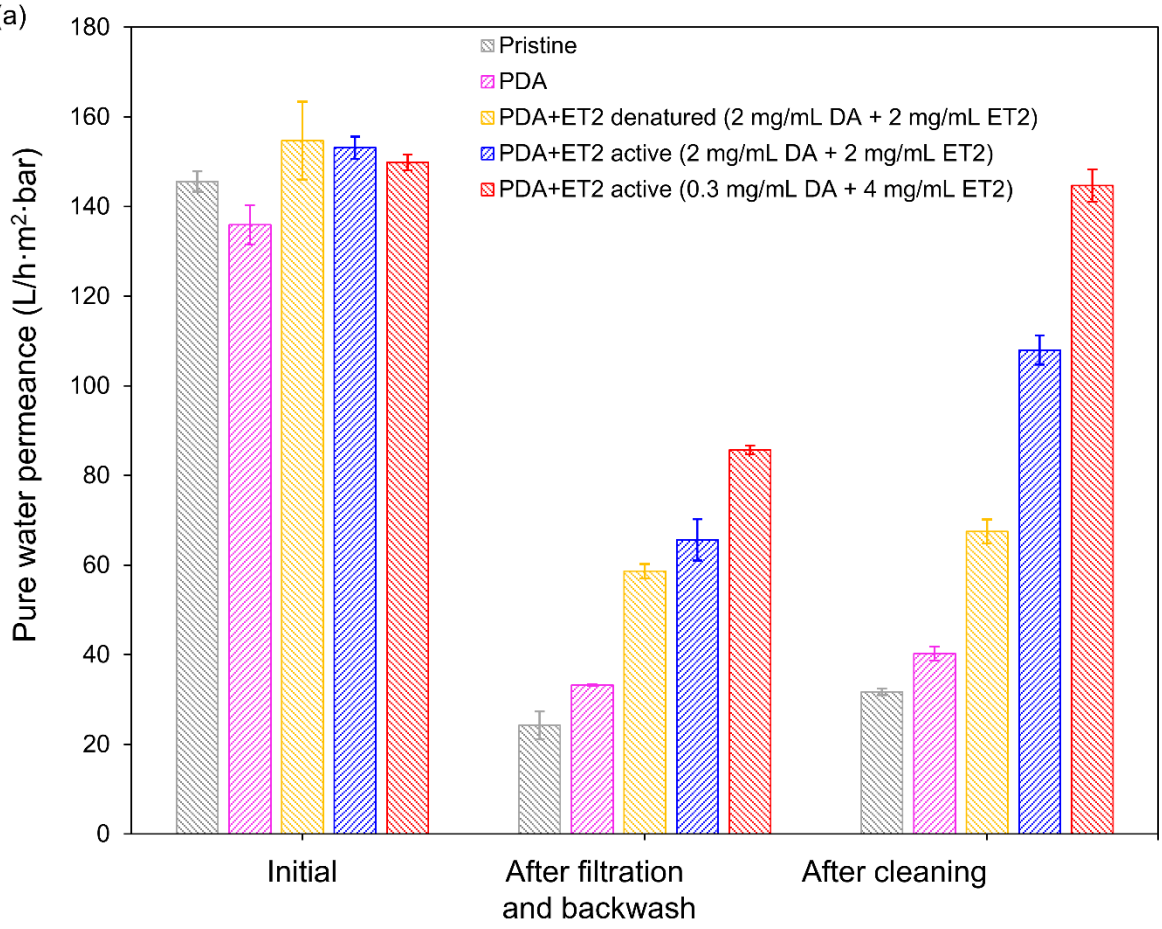

(b)

Membrane	Change in water permeance (%)		
	Reduction after emulsion filtration and backwash	Increase after cleaning	Overall permeance recovery (%)
Pristine	83.4 ± 3.0^{a}	5.1 ± 2.2^{a}	21.8 ± 3.7^{a}
PDA	75.5 ± 4.0^{a}	5.2 ± 1.2^{a}	26.6 ± 4.2^{a}
PDA+ET2 denatured (2 mg·mL^{-1} DA + 2 mg·mL^{-1} ET2)	62.1 ± 6.7^{b}	5.7 ± 2.0^{a}	43.6 ± 7.0^{b}
PDA+ET2 active (2 mg·mL^{-1} DA + 2 mg·mL^{-1} ET2)	57.1 ± 4.0^{b}	27.7 ± 3.7^{b}	70.5 ± 5.2^{c}
PDA+ET2 active (0.3 mg·mL^{-1} DA + 4 mg·mL^{-1} ET2)	42.8 ± 1.4^{c}	39.4 ± 2.5^{c}	96.6 ± 2.9^{d}

Numbers with different letters are significantly different according to Tukey's test ($p < 0.05$).
Source: Author

Since only the cleaning step was affected by the hydrolytic activity of the immobilized enzyme, the cleaning solution, temperature, and time were further evaluated for the membrane modified by the in-situ one-step immobilization method (Figure 37). Figure 37a shows that both sodium phosphate buffer 100 mM at pH 7 and deionized water at 40 °C resulted in similar pure water permeance recoveries: 97 ± 3 % and 95 ± 2 %, respectively. The fact that pure water can clean the membrane at the same level as the buffer is a huge advantage for industrial applications since it is cheaper and does not require any chemicals. Figure 37b shows the kinetics for the membrane cleaning using deionized water and 40 °C. After 6 h, the pure water permeance of the membrane did not significantly increase, suggesting that 6 h is enough to reach more than 97% of permeance recovery.

Figure 37 – Cleaning evaluation of the membrane modified by the optimized in-situ one-step method (0.3 mg·mL-1 of DA and 4 mg·mL-1 of ET2): (a) evaluation of different cleaning solutions (sodium phosphate buffer 100 mM at pH 7 and deionized water) and temperatures (40 °C and room temperature of 24 °C); (b) cleaning kinetics using water at 40 °C

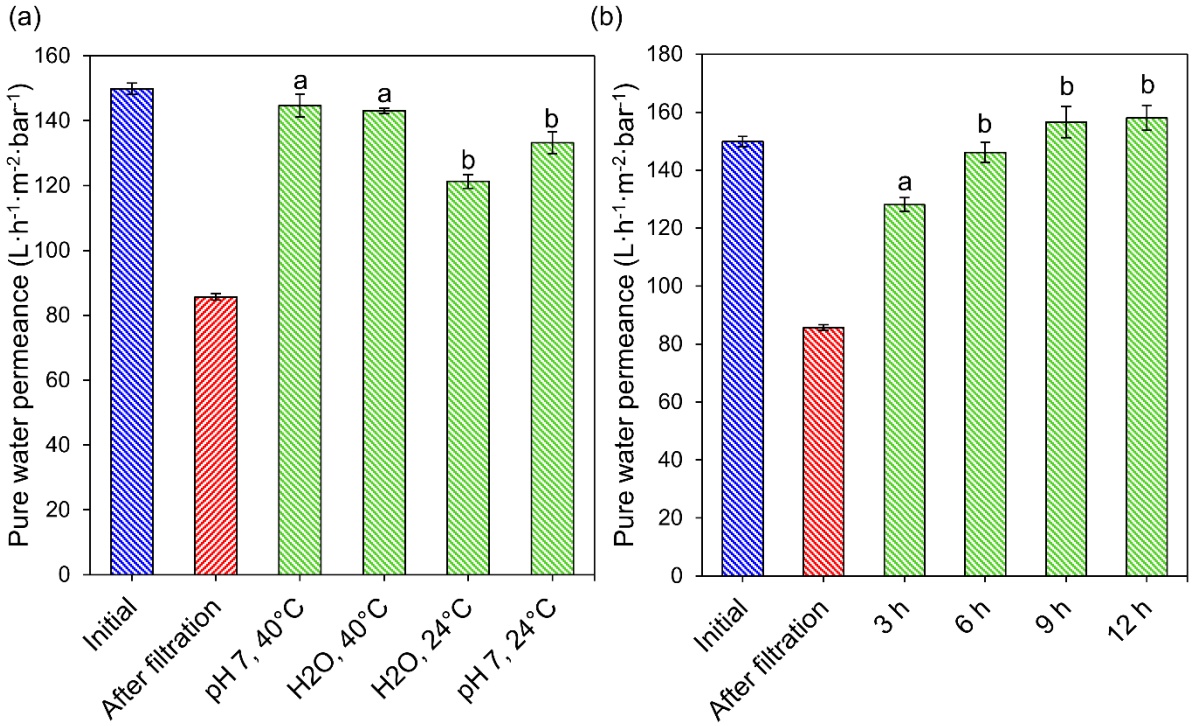

The values are means of triplicates and their respective standard deviations. Bars with different letters are significantly different according to Tukey's test ($p < 0.05$).
Source: Author

The SEM images of the membranes after emulsion filtration and after cleaning (Figure 38) also shows the efficacy of the immobilized enzymes in reducing the fouling.

The difference after cleaning is clear in the modified membrane (Figure 38e) when compared to the pristine membrane (Figure 38c).

Figure 38 – SEM images of the (a) pristine membrane before emulsion filtration, (b) after emulsion filtration, and (c) after cleaning with water at 40 °C for 6 h, and (d) modified membrane (0.3 mg·mL^{-1} DA and 4 mg·mL^{-1} ET2) after emulsion filtration and (e) after cleaning

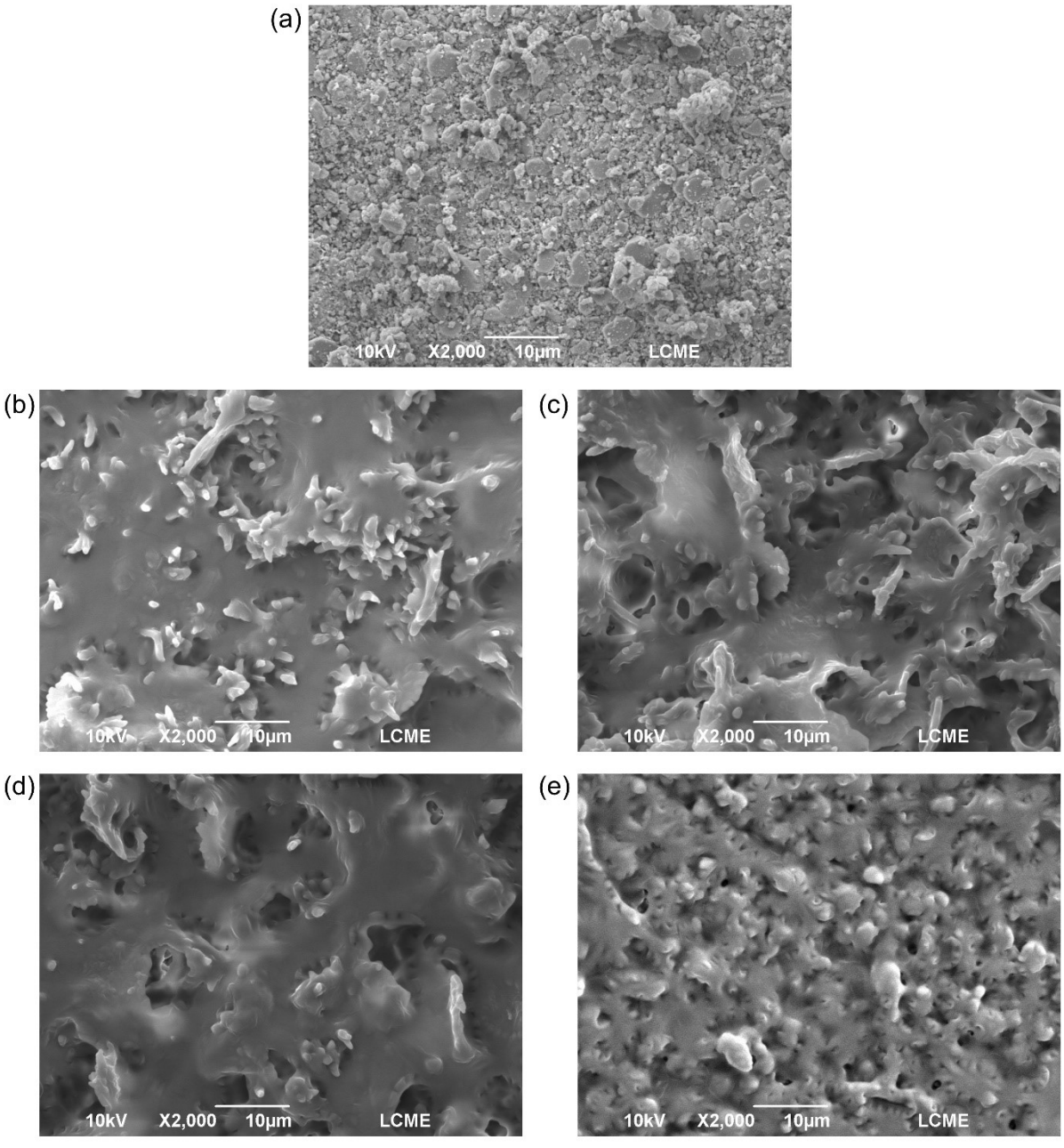

Source: Author

Figure 39 shows that, after three filtration and cleaning cycles, the pure water permeance of the pristine membrane was reduced by 91%. In contrast, the pure water permeance of the membrane with ET2 immobilized by the optimized in-situ one-step

method was reduced by only 17%. After the first cycle, the ET2-modified membrane recovered 98% of its initial pure water permeance, which decreased to 94% after the second cycle, and 91% after the third cycle. Compared to the membrane modified by the ex-situ one-step method described in our previous study, the membrane modified by the optimized in-situ method showed improved performance over the filtration and cleaning cycles.

Figure 39 – Results of repeated filtration and cleaning experiments for the pristine and modified membrane after the optimized in-situ one-step immobilization method (0.3 mg·mL^{-1} of DA and 4 mg·mL^{-1} of ET2)

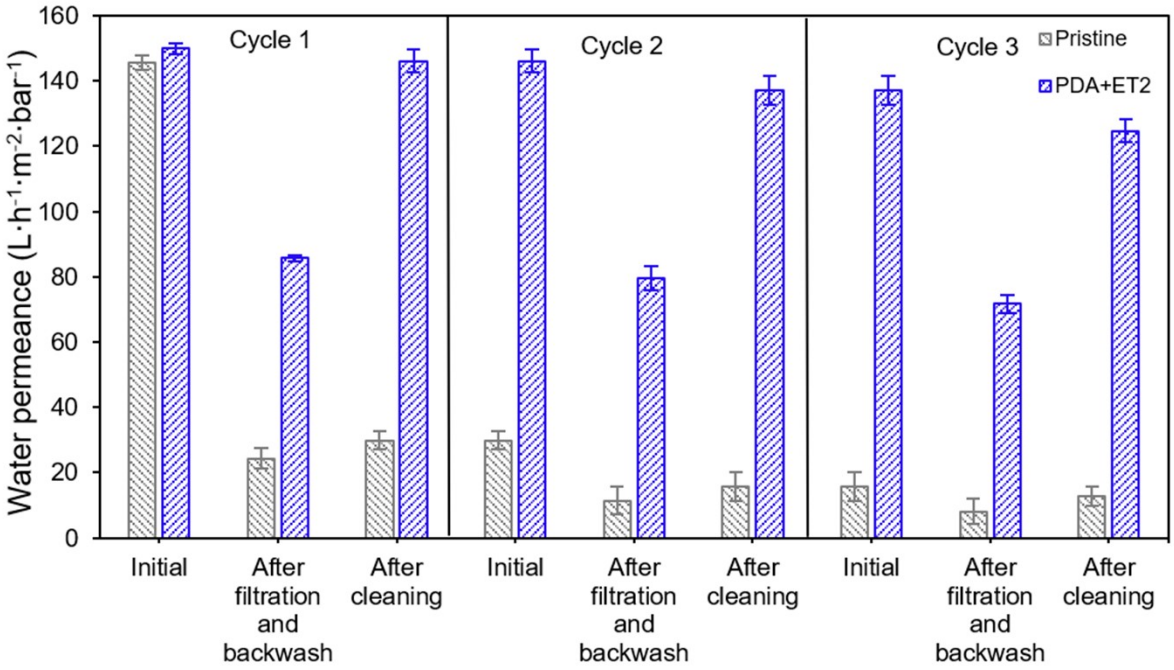

Source: Author

5.3.4 Membrane regeneration

Since one of the main advantages of using ceramic membranes is the possibility of reusing them after simple regenerations, both calcination and chemical cleaning were tested to check if the membranes could be reused after the immobilized enzymes were no longer active. Figure 40 shows the pure water permeance and membrane hydrolytic activity (*MHA*) after five cycles of membrane modification using 0.3 mg·mL^{-1} of DA and 4 mg·mL^{-1} of ET2 followed by calcination (Figure 40a) and chemical cleaning (Figure 40b). No significant differences in pure water permeance and *MHA* can be noticed after five cycles for both regeneration methods. SEM images and EDX

elemental analysis also did not show any differences in surface morphology and chemistry between the pristine membrane (Figure 40c) and the membranes after calcination (Figure 40d) and chemical cleaning (Figure 40e). Calcination is a simple procedure on a lab scale; however, it is not feasible on larger scales. Therefore, in-situ chemical cleaning is a better alternative to scaling up the process.

These results, coupled with the in-situ immobilization method, suggest that a new PDA and ET2 coating could be applied to the same membrane after the enzymes lose their activity. Regeneration by chemical cleaning and enzyme immobilization could be done in situ, which is a massive advantage in large-scale processes: the membrane would not have to be removed from the filtration system, saving labor hours and maintenance time.

Figure 40 – Membrane regeneration evaluation: pure water permeance and membrane hydrolytic activity (MHA) after: (a) 5 cycles of calcination at 700 °C for 3 h; (b) 5 cycles of chemical cleaning with 15 g·L^{-1} of NaOH. SEM images and EDX elemental analysis for: (c) pristine membrane; (d) membrane after the 5th calcination at 700 °C; (e) membrane after the 5th chemical cleaning with 15 g·L^{-1} of NaOH

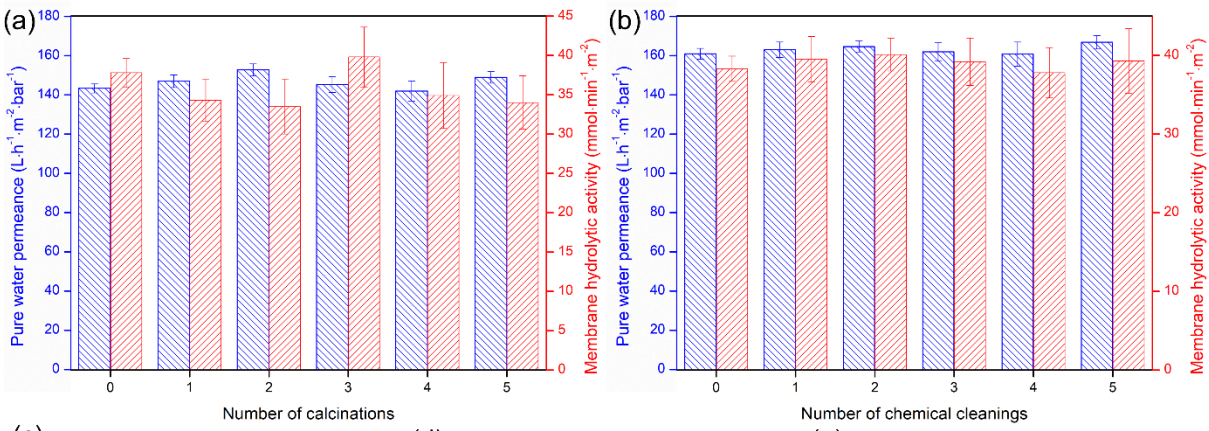

(c)

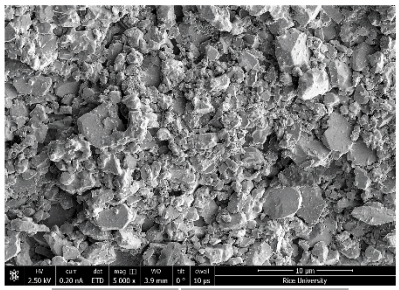

Element	Atomic%
C	0.1 ± 0.7
O	68.7 ± 1.2
Al	31.3 ± 0.9

(d)

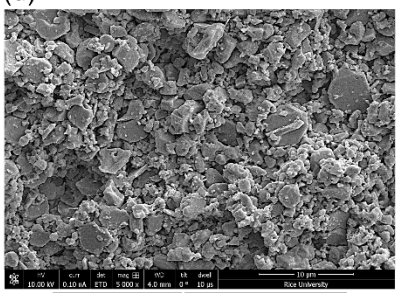

Element	Atomic%
C	0.1 ± 0.4
O	64.9 ± 1.7
Al	35.1 ± 1.6

(e)

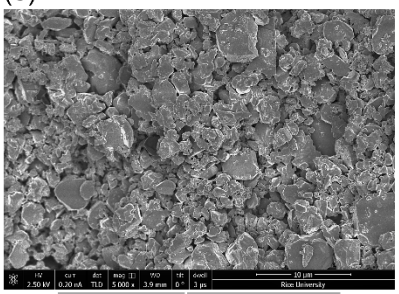

Element	Atomic%
C	0.1 ± 0.6
O	66.1 ± 0.9
Al	33.9 ± 0.7

Source: Author

5.4 CONCLUSION

In this study, we demonstrated that in-situ one-step immobilization of lipase ET2 on a ceramic membrane using PDA as the bonding agent is feasible. By optimizing the concentrations of ET2 and dopamine hydrochloride (DA) in the immobilization solution, the active membrane reached enzyme loadings up to 10 $g \cdot m^{-2}$ when using 0.3 $mg \cdot mL^{-1}$ of DA and 4 $mg \cdot mL^{-1}$ of ET2. The higher enzyme loading resulted in a higher hydrolytic activity (38 $mmol \cdot min^{-1} \cdot m^{-2}$) and higher water affinity when compared to the membrane modified by the ex-situ one-step method proposed in our previous study. The modification of the membrane by the optimized method provided a strong oil fouling resistance (pure water permeance reduction limited to 43% after oil-water emulsion filtration) due to the increased water affinity and better self-cleaning capacity (pure water permeance recovery of 97% after cleaning with deionized water at 40 °C for 6 h) due to the higher hydrolytic activity. Moreover, regeneration tests showed that the same ceramic membrane could be reused by applying a new coating after the immobilized enzymes are no longer active. The in-situ enzyme immobilization and the in-situ chemical regeneration are huge advantages that can facilitate the scale-up of the process by saving maintenance time and labor force. The reuse of the membrane coupled with the one-step modification using PDA can reduce the costs of the process and make it more environmentally friendly.

6 FINAL CONCLUSION

This work presents a simpler and more sustainable method for the immobilization of enzymes in inorganic membranes. The use of PDA proved to be a competitive technique compared to traditional immobilization methods, such as the use of APTES and glutaraldehyde. It resulted in a greater enzymatic load and greater hydrolytic activity of the membrane, in addition to being simpler and more environmentally friendly. The immobilization strategy in just one step proved to be an excellent alternative to the two-step method, since, besides increasing the stability of the immobilized enzyme at higher temperatures, it is a faster and less pollutant (lower consumption of chemicals and lower generation of effluents) approach. The enzyme immobilized ex situ by PDA proved to be a good fouling-reducing modification with self-cleaning ability in the filtration of oil-water emulsion. However, an ex-situ modification would not be industrially attractive. Therefore, the in-situ immobilization by PDA using the same one-step method was tested and proved to be viable. The immobilization parameters (DA and ET2 concentrations) were evaluated using the in-situ method and optimized concentrations (0.3 $mg \cdot mL^{-1}$ of DA and 4 $mg \cdot mL^{-1}$ of ET2) led to a higher enzyme loading (10 $g \cdot m^{-2}$) and membrane hydrolytic activity (38 $mmol \cdot min^{-1} \cdot m^{-2}$). The membrane modified by the optimized method showed strong fouling resistance, presenting a reduction of only 43% in the pure water permeance compared to 76% of the pristine membrane after the oil-water emulsion filtration. It also showed a strong self-cleaning capacity (using just water at 40 °C) due to enzymatic hydrolysis of the fouled oil, recovering 97% of its initial pure water permeance after the cleaning procedure. In addition to the in situ enzymatic immobilization, in situ chemical regeneration was also viable and demonstrated that membrane reuse is possible, which is a great advantage that can facilitate the scale-up of the process, make it cheaper and more sustainable.

REFERENCES

ABBASI, M.; SALAHI, A.; MIRFENDERESKI, M.; MOHAMMADI, T.; REKABDAR, F.; HEMMATI, M. Oily wastewater treatment using mullite ceramic membrane. **Desalination and Water Treatment**, v. 37, n. 1–3, p. 21–30, 2012.

ADLERCREUTZ, P. Immobilisation and application of lipases in organic media. **Chemical Society Reviews**, v. 42, n. 15, p. 6406–6436, 2013.

AGHABABAIE, M.; BEHESHTI, M.; RAZMJOU, A.; BORDBAR, A-KI. Covalent immobilization of *Candida rugosa* lipase on a novel functionalized Fe_3O_4@SiO_2 dip-coated nanocomposite membrane. **Food and Bioproducts Processing**, v. 100, p. 351–360, 2016.

AGUILLÓN, A. R.; AVELAR, M. N.; GOTARDO, L. E.; SOUZA, S. P.; LEÃO, R. A. C.; ITABAIANA JR., I.; MIRANDA, L. S. M.; SOUZA, R. O. M. A. Immobilized lipase screening towards continuous-flow kinetic resolution of (±)-1,2-propanediol. **Molecular Catalysis**, v. 467, p. 128–134, 2019.

AL-AMOUDI, A.; LOVITT, R. W. Fouling strategies and the cleaning system of NF membranes and factors affecting cleaning efficiency. **Journal of Membrane Science**, v. 303, n. 1, p. 4–28, 2007.

AL-HUSAINI, I. S.; YUSOFF, A. R. M.; LAU, W. J.; ISMAIL, A. F.; AL-ABRI, M. Z.; AL-GHAFRI, B. N.; WIRZAL, M. D. H. Fabrication of polyethersulfone electrospun nanofibrous membranes incorporated with hydrous manganese dioxide for enhanced ultrafiltration of oily solution. **Separation and Purification Technology**, v. 212, p. 205–214, 2019.

ALMASI, A.; MAHMOUDI, M.; MOHAMMADI, M.; DARGAHI, A.; BIGLARI, H. Optimizing biological treatment of petroleum industry wastewater in a facultative stabilization pond for simultaneous removal of carbon and phenol. **Toxin Reviews**, p. 1–9, 2019.

ALMEIDA, J. M.; MARTINI, V. P.; IULEK, J.; ALNOCH, R. C.; MOURE, V. R.; MÜLLER-SANTOS, M.; SOUZA, E. M.; MITCHELL, D. A.; KRIEGER, N. Biochemical characterization and application of a new lipase and its cognate foldase obtained from a metagenomic library derived from fat-contaminated soil. **International Journal of Biological Macromolecules**, v. 137, p. 442–454, 2019.

AMEUR, S. B.; GIJIU, C. L.; BELLEVILLE, M. P.; SANCHEZ, J.; PAOLUCCI-JEANJEAN, D. Development of a multichannel monolith large-scale enzymatic membrane and application in an immobilized enzymatic membrane reactor. **Journal of Membrane Science**, v. 455, p. 330–340, 2014.

AN, N.; ZHOU, C. H.; ZHUANG, X. Y.; TONG, D. S.; YU, W. H Immobilization of enzymes on clay minerals for biocatalysts and biosensors. **Applied Clay Science**, v. 114, p. 283–296, 2015.

AN, Z.; CAO, W.; WANG, H.; RUAN, G. Rapid deposition on polydopamine coated PVDF membranes with enhanced anti-protein and antiantibacterial performance for

wastewater treatment. *In:* International Conference on Electron Device and Mechanical Engineering (ICEDME), 3., 2020, Suzhou, China. **Anais...** Suzhou: IEEE, 2020. p. 433-436.

ANTINK, M. M. H.; SEWCZYK, T.; KROLL, S.; ÁRKI, P.; BEUTEL, S.; REZWAN, K.; MAAS, M. Proteolytic ceramic capillary membranes for the production of peptides under flow. **Biochemical Engineering Journal**, v. 147, p. 89–99, 2019.

ARANA-PEÑA, S.; LOKHA, Y.; FERNÁNDEZ-LAFUENTE, R. Immobilization of Eversa Lipase on Octyl Agarose Beads and Preliminary Characterization of Stability and Activity Features. **Catalysts**, v. 8, n. 11, p. 511, 2018.

ASMAT, S.; ANWER, A. H.; HUSAIN, Q. Immobilization of lipase onto novel constructed polydopamine grafted multiwalled carbon nanotube impregnated with magnetic cobalt and its application in synthesis of fruit flavours. **International Journal of Biological Macromolecules**, v. 140, p. 484–495, 2019.

ASTM. **C20 - Test Methods for Apparent Porosity, Water Absorption, Apparent Specific Gravity, and Bulk Density of Burned Refractory Brick and Shapes by Boiling Water**. [s.l.] ASTM International, 2000. Disponível em: <http://www.astm.org/cgi-bin/resolver.cgi?C20-00R10>. Acesso em: 20 out. 2020.

BAHARFAR, R.; MOHAJER, S. Synthesis and Characterization of Immobilized Lipase on Fe3O4 Nanoparticles as Nano biocatalyst for the Synthesis of Benzothiazepine and Spirobenzothiazine Chroman Derivatives. **Catalysis Letters**, v. 146, n. 9, p. 1729–1742, 2016.

BAKER, R. W. **Membrane technology and applications**. 3. ed. Chichester, UK: John Wiley & Sons Ltd., 2012.

BARBOSA, O.; TORRES, R.; ORTIZ, C.; BERENGUER-MURCIA, A.; RODRIGUES, R. C.; FERNANDEZ-LAFUENTE, R. Heterofunctional supports in enzyme immobilization: from traditional immobilization protocols to opportunities in tuning enzyme properties. **Biomacromolecules**, v. 14, n. 8, p. 2433–2462, 2013.

BARBOSA, O.; ORTIZ, C.; BERENGUER-MURCIA, Á.; TORRES, R.; RODRIGUES, R. C.; FERNANDEZ-LAFUENTE, R. Strategies for the one-step immobilization–purification of enzymes as industrial biocatalysts. **Biotechnology Advances**, v. 33, n. 5, p. 435–456, 2015.

BEAUCHAMP, R. O.; CLAIR, M. B. G. S.; FENNELL, T. R.; CLARKE, D. O.; MORGAN, K. T.; KARL, F. W. A Critical review of the toxicology of glutaraldehyde. **Critical Reviews in Toxicology**, v. 22, n. 3–4, p. 143–174, 1992.

BERNAL, C.; RODRÍGUEZ, K.; MARTÍNEZ, R. Integrating enzyme immobilization and protein engineering: An alternative path for the development of novel and improved industrial biocatalysts. **Biotechnology Advances**, v. 36, n. 5, p. 1470–1480, 2018.

BI, Y.; ZHOU, H.; JIA, H.; WEI, P. Polydopamine-mediated preparation of an enzyme-immobilized microreactor for the rapid production of wax ester. **RSC Advances**, v. 7, n. 20, p. 12283–12291, 2017.

BILAL, M.; RASHEED, T.; ZHAO, Y.; IQBAL, H. M. N.; CUI, J. “Smart” chemistry and its application in peroxidase immobilization using different support materials. **International Journal of Biological Macromolecules**, v. 119, p. 278–290, 2018.

BOROWIECKI, P.; DRANKA, M. A facile lipase-catalyzed KR approach toward enantiomerically enriched homopropargyl alcohols. **Bioorganic Chemistry**, v. 93, p. 102754, 2019.

BOURKAIB, M. C.; GAUDIN, P.; VIBERT, F.; GUIAVARC’H, Y.; DELAUNAY, S.; FRAMBOISIER, X.; HUMEAU, C.; CHEVALOT, I.; BLIN, J.-K. APTES modified SBA15 and meso-macro silica materials for the immobilization of aminoacylases from *Streptomyces ambofaciens*. **Microporous and Mesoporous Materials**, v. 323, p. 111226, 2021.

BRADFORD, M. M. A rapid and sensitive method for the quantitation of microgram quantities of protein utilizing the principle of protein-dye binding. **Analytical Biochemistry**, v. 72, p. 248–254, 1976.

BRESOLIN, D.; HAWERROTH, B.; ROMERA, C. O.; SAYER, C.; ARAÚJO, P. H. H.; OLIVEIRA, D. Immobilization of lipase Eversa Transform 2.0 on poly(urea–urethane) nanoparticles obtained using a biopolyol from enzymatic glycerolysis. **Bioprocess and Biosystems Engineering**, v. 43, n. 7, p. 1279–1286, 2020.

BRISOLA, J.; ANDRADE, G. J. S.; OLIVERIA, S. A.; VIANA, R. M. R.; TISCHER, P. C. S. F.; TISCHER, C. A. Covalent immobilization of lipase on bacterial cellulose membrane and nanocellulose. **Materials Research**, v. 25, p. e20210350, 2022.

BURZIO, L. A.; WAITE, J. H. Cross-linking in adhesive quinoproteins: studies with model decapeptides. **Biochemistry**, v. 39, p. 11147–11153, 2000.

CAI, Y.; CHEN, D.; LI, N.; XU, Q.; LI, H.; HE, J.; LU, J. Nanofibrous metal–organic framework composite membrane for selective efficient oil/water emulsion separation. **Journal of Membrane Science**, v. 543, p. 10–17, 2017.

CAO, X.; LUO, J.; WOODLEY, J. M.; WAN, Y. Mussel-inspired co-deposition to enhance bisphenol A removal in a bifacial enzymatic membrane reactor. **Chemical Engineering Journal**, v. 336, p. 315–324, 2018.

CHAKRABORTY, S.; RUSLI, H.; NATH, A.; SIKDER, J.; BHATTACHARJEE, C.; CURCIO, S.; DRIOLI, E. Immobilized biocatalytic process development and potential application in membrane separation: a review. **Critical Reviews in Biotechnology**, v. 36, n. 1, p. 43–58, 2016.

CHAO, C.; LIU, J.; WANG, J.; ZHANG, Y.; ZHANG, B.; ZHANG, Y.; XIANG, X.; CHEN, R. Surface modification of halloysite nanotubes with dopamine for enzyme immobilization. **ACS Applied Materials & Interfaces**, v. 5, n. 21, p. 10559–10564, 2013.

CHAPMAN, J.; ISMAIL, A. E.; DINU, C. Z. Industrial applications of enzymes: recent advances, techniques, and outlooks. **Catalysts**, v. 8, n. 6, p. 238, 2018.

CHARCOSSET, C. Principles on membrane and membrane processes. *In*: CHARCOSSET, C. **Membrane processes in biotechnology and pharmaceutics**. Amsterdam: Elsevier, 2012. p. 1–41.

CHEN, J.; WANG, L.; ZHU, Z. Preparation of enzyme immobilized membranes and their self-cleaning and anti-fouling abilities in protein separations. **Desalination**, v. 86, n. 3, p. 301–315, 1992.

CHEN, N.; ZHANG, C.; LIU, Y.; DONG, X.; SUN, Y. Cysteine-modified poly(glycidyl methacrylate) grafted onto silica nanoparticles: new supports for significantly enhanced performance of immobilized lipase. **Biochemical Engineering Journal**, v. 145, p. 137–144, 2019a.

CHEN, P.-C.; MA, Z.; ZHU, X-Y.; CHEN, D-J.; HUANG, X-J. Fabrication and optimization of a lipase immobilized enzymatic membrane bioreactor based on polysulfone gradient-pore hollow fiber membrane. **Catalysts**, v. 9, p. 11, 2019b.

CHEN, X.; HUANG, G.; AN, C.; FENG, R.; YAO, Y.; ZHAO, S.; HUANG, C.; WU, Y. Plasma-induced poly(acrylic acid)-TiO_2 coated polyvinylidene fluoride membrane for produced water treatment: synchrotron X-Ray, optimization, and insight studies. **Journal of Cleaner Production**, v. 227, p. 772–783, 2019c.

CHEN, F.; SHI, X.; CHEN, X.; CHEN, W. An iron (II) phthalocyanine/poly(vinylidene fluoride) composite membrane with antifouling property and catalytic self-cleaning function for high-efficiency oil/water separation. **Journal of Membrane Science**, v. 552, p. 295-304, 2018.

CHEN, Y.; ZHAO, S.; CHEN, M.; ZHANG, W.; MAO, J.; ZHAO, Y.; MAITZ, M. F.; HUANG, N.; WAN, G. Sandwiched polydopamine (PDA) layer for titanium dioxide (TiO_2) coating on magnesium to enhance corrosion protection. **Corrosion Science**, v. 96, p. 67–73, 2015.

CHEN, Z.; SUN, Z.; MING, S.; LI, S.; ZHU, Z.; ZHANG, W. Bioinspired proteolytic membrane (BPM) with bilayer pepsin structure for protein hydrolysis. **Separation and Purification Technology**, v. 259, p. 118214, 2021.

CHENG, H.; HU, M.; ZHAI, Q.; LI, S.; JIANG, Y. Polydopamine tethered CPO/HRP-TiO_2 nano-composites with high bio-catalytic activity, stability and reusability: enzyme-photo bifunctional synergistic catalysis in water treatment. **Chemical Engineering Journal**, v. 347, p. 703–710, 2018.

CHENG, W.; LI, Y.; LI, X.; BAI, W.; LIANG, Y. Preparation and characterization of PDA/SiO_2 nanofilm constructed macroporous monolith and its application in lipase immobilization. **Journal of the Taiwan Institute of Chemical Engineers**, v. 104, p. 351–359, 2019.

CHERYAN, M.; RAJAGOPALAN, N. Membrane processing of oily streams: wastewater treatment and waste reduction. **Journal of Membrane Science**, v. 151, n. 1, p. 13–28, 1998.

CUI, J.; ZHOU, Z.; XIE, A.; MENG, M.; CUI, Y.; LIU, S.; LU, J.; ZHOU, S.; YAN, Y.; DONG, H. Bio-inspired fabrication of superhydrophilic nanocomposite membrane

based on surface modification of SiO_2 anchored by polydopamine towards effective oil-water emulsions separation. **Separation and Purification Technology**, v. 209, p. 434–442, 2019.

CUI, J. D.; JIA, S. R. Optimization protocols and improved strategies of cross-linked enzyme aggregates technology: current development and future challenges. **Critical Reviews in Biotechnology**, v. 35, n. 1, p. 15–28, 2015.

DALSIN, J. L.; HU, B-H.; LEE, B. P.; MESSERSMITH, P. B. Mussel adhesive protein mimetic polymers for the preparation of nonfouling surfaces. **Journal of the American Chemical Society**, v. 125, n. 14, p. 4253–4258, 2003.

DATTA, S.; CHRISTENA, L. R.; RAJARAM, Y. R. S. Enzyme immobilization: an overview on techniques and support materials. **3 Biotech**, v. 3, n. 1, p. 1–9, 2013.

DE MENESES, A. C.; LERIN, L. A.; ARAÚJO, P. H. H.; SAYER, C.; DE OLIVEIRA, D. Benzyl propionate synthesis by fed-batch esterification using commercial immobilized and lyophilized Cal B lipase. **Bioprocess and Biosystems Engineering**, v. 42, n. 10, p. 1625–1634, 2019.

DIAO, Z.; WANG, L.; YU, P.; FENG, H.; ZHAO, W.; ZHOU, W.; FU, H. Super-stable non-woven fabric-based membrane as a high-efficiency oil/water separator in full pH range. **RSC Advances**, v. 7, n. 32, p. 19764–19770, 2017.

DING, Y.; WENG, L.-T.; YANG, M.; YANG, Z.; LU, X.; HUANG, N.; LENG, Y. Insights into the aggregation/deposition and structure of a polydopamine film. **Langmuir**, v. 30, n. 41, p. 12258–12269, 2014.

DONG, L.; LIU, X.; XIONG, Z.; SHENG, D.; LIN, C.; ZHOU, Y.; YANG, Y. Fabrication of highly efficient ultraviolet absorbing PVDF membranes via surface polydopamine deposition. **Journal of Applied Polymer Science**, v. 135, n. 4, p. 45746, 2018.

DOS SANTOS, L. K.; BOTTI, R. F.; INNOCENTINI, M. D. M.; MARQUES, R. F. C.; COLOMBO, P.; DE PAULA, A. V.; FLUMIGNAN, D. L. 3D printed geopolymer: an efficient support for immobilization of *Candida rugosa* lipase. **Chemical Engineering Journal**, v. 414, p. 128843, 2021.

DU PLESSIS, D. M.; BOTES, M.; DICKS, L. M. T.; CLOETE, T. E. Immobilization of commercial hydrolytic enzymes on poly (acrylonitrile) nanofibers for anti-biofilm activity. **Journal of Chemical Technology & Biotechnology**, v. 88, n. 4, p. 585–593, 2013.

EDWARDS, W.; LEUKES, W. D.; BEZUIDENHOUT, J. J. Ultrafiltration of petrochemical industrial wastewater using immobilised manganese peroxidase and laccase: application in the defouling of polysulphone membranes. **Desalination**, v. 149, n. 1, p. 275–278, 2002.

ELDIN, M. S. M.; SEUROR, E. I.; NASR, M. A.; TIEAMA, H. A. Affinity covalent immobilization of glucoamylase onto ρ-benzoquinone-activated alginate beads: II. Enzyme immobilization and characterization. **Applied Biochemistry and Biotechnology**, v. 164, n. 1, p. 45–57, 2011.

EOM, J.-H.; YEOM, H-J.; KIM, Y-W.; SONG, I-H. Ceramic membranes prepared from a silicate and clay-mineral mixture for treatment of oily wastewater. **Clays and Clay Minerals**, v. 63, n. 3, p. 222–234, 2015.

FACIN, B. R.; MELCHIORS, M. S.; VALÉRIO, A.; OLIVEIRA, J. V.; OLIVEIRA, D. Driving immobilized lipases as biocatalysts: 10 years state of the art and future prospects. **Industrial & Engineering Chemistry Research**, v. 58, n. 14, p. 5358–5378, 2019.

FARD, A. K.; BUKENHOUDT, A.; JACOBS, M.; MCKAY, G.; ATIEH, M. A. Novel hybrid ceramic/carbon membrane for oil removal. **Journal of Membrane Science**, v. 559, p. 42–53, 2018.

FATHI, Z.; DOUSTKHAH, E.; ROSTAMNIA, S.; DARVISHI, D.; GHODSI, A.; IDE, Y. Interaction of *Yarrowia lipolytica* lipase with dithiocarbamate modified magnetic carbon Fe_3O_4@C-$NHCS_2H$ core-shell nanoparticles. **International Journal of Biological Macromolecules**, v. 117, p. 218–224, 2018.

FRAAS, R.; FRANZREB, M. Reversible covalent enzyme immobilization methods for reuse of carriers. **Biocatalysis and Biotransformation**, v. 35, n. 5, p. 337–348, 2017.

FRAGA, M. C.; SANCHES, S.; PEREIRA, V. J.; CRESPO, J. G.; YUAN, L.; MARCHER, J.; YUSO, M. V. M.; RODRÍGUEZ-CASTELLÓN, E.; BENAVENTE, J. Morphological, chemical surface and filtration characterization of a new silicon carbide membrane. **Journal of the European Ceramic Society**, v. 37, n. 3, p. 899–905, 2017.

FRANK, M.; BARGEMAN, G.; ZWIJNENBURG, A.; WESSLING, M. Capillary hollow fiber nanofiltration membranes. **Separation and Purification Technology**, v. 22–23, p. 499–506, 2001.

FU, X.; ZHU, X.; GAO, K.; DUAN, J. Oil and fat hydrolysis with lipase from *Aspergillus* sp. **Journal of the American Oil Chemists' Society**, v. 72, n. 5, p. 527–531, 1995.

GAMA, R. S.; BOLINA, I. C. A.; CREN, É. C.; MENDES, A. A. A novel functionalized SiO_2-based support prepared from biomass waste for lipase adsorption. **Materials Chemistry and Physics**, v. 234, p. 146–150, 2019.

GAO, N.; FAN, W.; XU, Z.-K. Ceramic membrane with protein-resistant surface via dopamine/diglycolamine co-deposition. **Separation and Purification Technology**, v. 234, p. 116135, 2020.

GAO, N.; XU, Z.-K. Ceramic membranes with mussel-inspired and nanostructured coatings for water-in-oil emulsions separation. **Separation and Purification Technology**, v. 212, p. 737–746, 2019.

GAO, Z.; CHU, J.; JIANG, T.; XU, T.; WU, B.; HE, B. Lipase immobilization on functionalized mesoporous TiO_2: specific adsorption, hyperactivation and application in cinnamyl acetate synthesis. **Process Biochemistry**, v. 64, p. 152–159, 2018.

GEBREYOHANNES, A. Y.; MAZZEI, R.; CURCIO, E.; POERIO, T.; DRIOLI, E.; GIORNO, L. Study on the in situ enzymatic self-cleansing of microfiltration membrane for valorization of olive mill wastewater. **Industrial & Engineering Chemistry Research**, v. 52, n. 31, p. 10396–10405, 2013.

GEBREYOHANNES, A. Y.; BILAD, M. R.; VERBIEST, T.; COURTIN, C. M.; DORNEZ, E.; GIORNO, L.; CURCIO, E.; VANKELECOM, I. F. J. Nanoscale tuning of enzyme localization for enhanced reactor performance in a novel magnetic-responsive biocatalytic membrane reactor. **Journal of Membrane Science**, v. 487, p. 209–220, 2015.

GEBREYOHANNES, A. Y.; MAZZEI, R.; POERIO, T.; AIMAR, P.; VANKELECOM, I. F. J.; GIORNO, L. Pectinases immobilization on magnetic nanoparticles and their anti-fouling performance in a biocatalytic membrane reactor. **RSC Advances**, v. 6, n. 101, p. 98737–98747, 2016.

GEBREYOHANNES, A. Y.; GIORNO, L.; VANKELECOM, I. F. J.; VERBIEST, T.; AIMAR, P. Effect of operational parameters on the performance of a magnetic responsive biocatalytic membrane reactor. **Chemical Engineering Journal**, v. 308, p. 853–862, 2017.

GEBREYOHANNES, A. Y.; DHARMJEET, M.; SWUSTEN, T.; MERTENS, M.; VERSPREET, J.; VERBIEST, T.; COURTIN, C. M.; VANKELECOM, I. F. J. Simultaneous glucose production from cellulose and fouling reduction using a magnetic responsive membrane reactor with superparamagnetic nanoparticles carrying cellulolytic enzymes. **Bioresource Technology**, v. 263, p. 532–540, 2018.

GIORNO, L.; DONATO, L.; TODISCO, S.; DRIOLI, E. Study of fouling phenomena in apple juice clarification by enzyme membrane reactor. **Separation Science and Technology**, v. 33, n. 5, p. 739–756, 1998.

GOLDSTEIN, L.; MANECKE, G. The Chemistry of enzyme immobilization. *In*: WINGARD, L. B.; KATCHALSKI-KATZIR, E.; GOLDSTEIN, L. **Applied biochemistry and bioengineering**: immobilized enzyme principles. Elsevier, 1976. v. 1. p. 23–126.

GOLUNSKI, S. M.; MULINARI, J.; CAMARGO, A. F.; VENTURIN, B.; BALDISSARELLI, D. P.; MARQUES, C. T.; VARGAS, G. D. L. P.; COLLA, L. M.; MOSSI, A.; TREICHEL, H. Ultrasound effects on the activity of *Aspergillus niger* lipases in their application in dairy wastewater treatment. **Environmental Quality Management**, v. 27, n. 1, p. 95–101, 2017.

GUO, X.; LI, C.; FAN, S.; GAO, Z.; TONG, L.; GAO, H.; ZHOU, Q.; SHAO, H.; LIAO, Y.; LI, Q.; HU, W. Engineering polydopamine-glued sandwich-like nanocomposites with antifouling and antibacterial properties for the development of advanced mixed matrix membranes. **Separation and Purification Technology**, v. 237, p. 116326, 2020.

GUO, Y.; ZHU, X.; FANG, F.; HONG, X.; WU, H.; CHEN, D.; HUANG, X. Immobilization of enzymes on a phospholipid bionically modified polysulfone gradient-pore membrane for the enhanced performance of enzymatic membrane

bioreactors. **Molecules : A Journal of Synthetic Chemistry and Natural Product Chemistry**, v. 23, n. 1, p. 144, 2018.

GUPTA, S.; BHATTACHARYA, A.; MURTHY, C. N. Tune to immobilize lipases on polymer membranes: techniques, factors and prospects. **Biocatalysis and Agricultural Biotechnology**, v. 2, n. 3, p. 171–190, 2013.

GUSTAFSSON, H.; JOHANSSON, E.M.; BARRABINO, A.; ODÉN, M.; HOLMBERG, K. Immobilization of lipase from *Mucor miehei* and *Rhizopus oryzae* into mesoporous silica: the effect of varied particle size and morphology. **Colloids and Surfaces B: Biointerfaces**, v. 100, p. 22–30, 2012.

HAN, X.; CHEN, X.; YAN, M.; LIU, H. Synergetic effect of polydopamine particles and in-situ fabricated gold nanoparticles on charge-dependent catalytic behaviors. **Particuology**, v. 44, p. 63–70, 2019.

HE, S.; ZHAN, Y.; BAI, Y.; HU, J.; LI, Y.; ZHANG, G.; ZHAO, S. Gravity-driven and high flux super-hydrophobic/super-oleophilic poly(arylene ether nitrile) nanofibrous composite membranes for efficient water-in-oil emulsions separation in harsh environments. **Composites Part B: Engineering**, v. 177, p. 107439, 2019.

HE, Y.; XU, L.; FENG, X.; ZHAO, Y.; CHEN, L. Dopamine-induced nonionic polymer coatings for significantly enhancing separation and antifouling properties of polymer membranes: codeposition versus sequential deposition. **Journal of Membrane Science**, v. 539, p. 421–431, 2017.

HOLLERMANN, G.; DHEKANE, R.; KROLL, S.; REZWAN, K. Functionalized porous ceramic microbeads as carriers in enzymatic tandem systems. **Biochemical Engineering Journal**, v. 126, p. 30–39, 2017.

HOLZ, J. C. P.; PEREIRA, G. N.; OLIVEIRA, J. V.; LERIN, L. A.; OLIVEIRA, D. Enzyme-catalyzed production of emollient cetostearyl stearate using different immobilized commercial lipases under vacuum system. **Biocatalysis and Agricultural Biotechnology**, v. 15, p. 229–234, 2018.

HOWELL, J. A.; VELICANGIL, Ö. Protein ultrafiltration: theory of membrane fouling and its treatment with immobilized proteases. *In*: COOPER, A. R. **Ultrafiltration membranes and applications**: polymer science and technology. Boston, MA: Springer US, 1980. p. 217–229.

HOWELL, J. A.; VELICANGIL, O. Theoretical considerations of membrane fouling and its treatment with immobilized enzymes for protein ultrafiltration. **Journal of Applied Polymer Science**, v. 27, n. 1, p. 21–32, 1982.

HU, B.; PAN, J.; YU, H.-L.; LIU, J.-W.; XU, J.-H. Immobilization of *Serratia marcescens* lipase onto amino-functionalized magnetic nanoparticles for repeated use in enzymatic synthesis of diltiazem intermediate. **Process Biochemistry**, v. 44, n. 9, p. 1019–1024, 2009.

HU, X.; YU, Y.; ZHOU, J.; WANG, Y.; LIANG, J.; ZHANG, X.; CHANG, Q.; SONG, L. The improved oil/water separation performance of graphene oxide modified Al_2O_3 microfiltration membrane. **Journal of Membrane Science**, v. 476, p. 200–204, 2015.

HUANG, N.; ZHANG, S.; YANG, L.; LIU, M.; LI, H.; ZHANG, Y.; YAO, S. Multifunctional electrochemical platforms based on the Michael addition/Schiff base reaction of polydopamine modified reduced graphene oxide: construction and application. **ACS Applied Materials & Interfaces**, v. 7, n. 32, p. 17935–17946, 2015.

HUANG, S.; RAS, R. H. A.; TIAN, X. Antifouling membranes for oily wastewater treatment: Interplay between wetting and membrane fouling. **Current Opinion in Colloid & Interface Science**, Wetting and Spreading. v. 36, p. 90–109, 2018.

IKHSAN, S. N. W.; YUSOF, N.; AZIZ, F.; MISDAN, N.; ISMAIL, A. F.; LAU, W.-J.; JAAFAR, J.; WAN SALLEH, W. N.; HAIROM, N. H. H. Efficient separation of oily wastewater using polyethersulfone mixed matrix membrane incorporated with halloysite nanotube-hydrous ferric oxide nanoparticle. **Separation and Purification Technology**, v. 199, p. 161–169, 2018.

ILYAS, H.; SHAWUTI, S.; SIDDIQ, M.; NIAZI, J. H.; QURESHI, A. PEG functionalized graphene oxide-silver nano-additive for enhanced hydrophilicity, permeability and fouling resistance properties of PVDF-co-HFP membranes. **Colloids and Surfaces A: Physicochemical and Engineering Aspects**, v. 579, p. 123646, 2019.

INDELICATO, S.; BONGIORNO, D.; CERAULO, L.; EMMANUELLO, C.; MAZZOTTI, F.; SICILIANO, C.; PIAZZESE, D. One-pot analysis: a new integrated methodology for determination of TAG and FA determination through LC/MS and in-silico saponification. **Food Analytical Methods**, v. 11, n. 3, p. 873–882, 2018.

ISMAIL, N. H.; SALLEH, W. N. W.; ISMAIL, A. F.; HASBULLAH, H.; YUSOF, N.; AZIZ, F.; JAAFAR, J. Hydrophilic polymer-based membrane for oily wastewater treatment: a review. **Separation and Purification Technology**, v. 233, p. 116007, 2020.

ISSAOUI, M.; LIMOUSY, L. Low-cost ceramic membranes: synthesis, classifications, and applications. **Comptes Rendus Chimie**, v. 22, n. 2–3, p. 175–187, 2019.

ITTRAT, P.. CHACHO, T.; PHOLPRAYOON, J.; SUTTIWARAYANON, N.; CHAROENPANICH, J. Application of agriculture waste as a support for lipase immobilization. **Biocatalysis and Agricultural Biotechnology**, v. 3, n. 3, p. 77–82, 2014.

JENQ, C. Y.; WANG, S. S.; DAVIDSON, B. Ultrafiltration of raw sewage using an immobilized enzyme membrane. **Enzyme and Microbial Technology**, v. 2, n. 2, p. 145–149, 1980.

JEONG, Y.; KIM, Y.; JIN, Y.; HONG, S.; PARK, C. Comparison of filtration and treatment performance between polymeric and ceramic membranes in anaerobic membrane bioreactor treatment of domestic wastewater. **Separation and Purification Technology**, v. 199, p. 182–188, 2018.

JEONG, Y.-H.; IHM, S.-K.; WON, Y.-S. Experimental investigation of the oil/water/oil liquid-membrane separation of toluene and n-heptane: II. Continuous test of a

countercurrent permeator. **Journal of Membrane Science**, v. 32, n. 1, p. 47–57, 1987.

JESIONOWSKI, T.; ZDARTA, J.; KRAJEWSKA, B. Enzyme immobilization by adsorption: a review. **Adsorption**, v. 20, n. 5, p. 801–821, 2014.

JIANG, C.; CHENG, C.; HAO, M.; WANG, H.; WANG, Z.; SHEN, C.; CHEONG, L-Z. Enhanced catalytic stability of lipase immobilized on oxidized and disulfide-rich eggshell membrane for esters hydrolysis and transesterification. **International Journal of Biological Macromolecules**, v. 105, p. 1328–1336, 2017.

JIN, Q.; LI, X.; DENG, C.; ZHANG, Q.; YI, D.; WANG, X.; TANG, Y.; WANG, Y. Silica nanowires with tunable hydrophobicity for lipase immobilization and biocatalytic membrane assembly. **Journal of Colloid and Interface Science**, v. 531, p. 555–563, 2018.

JOSHI, R.; SHARMA, R.; KUILA, A. Lipase production from *Fusarium incarnatum* KU377454 and its immobilization using Fe_3O_4 NPs for application in waste cooking oil degradation. **Bioresource Technology Reports**, v. 5, p. 134–140, 2019.

KAPOOR, M.; GUPTA, M. N. Lipase promiscuity and its biochemical applications. **Process Biochemistry**, v. 47, n. 4, p. 555–569, 2012.

KASEMSET, S.; HE, Z.; MILLER, D. J.; FREEMAN, B. D.; SHARMA, M. M. Effect of polydopamine deposition conditions on polysulfone ultrafiltration membrane properties and threshold flux during oil/water emulsion filtration. **Polymer**, v. 97, p. 247–257, 2016.

KEHAIL, A. A.; BRIGHAM, C. J. Anti-biofilm activity of solvent-cast and electrospun Ppolyhydroxyalkanoate membranes treated with lysozyme. **Journal of Polymers and the Environment**, v. 26, n. 1, p. 66–72, 2018.

KHAN, A.; TOUFIQ, A. M.; TARIQ, F.; KHAN, Y.; HUSSAIN, R.; AKHTAR, N.; UR RAHMAN, S. Influence of Fe doping on the structural, optical and thermal properties of α-MnO_2 nanowires. **Materials Research Express**, v. 6, n. 6, p. 065043, 2019a.

KHAN, M. F.; KUNDU, D.; HAZRA, C.; PATRA, S. A strategic approach of enzyme engineering by attribute ranking and enzyme immobilization on zinc oxide nanoparticles to attain thermostability in mesophilic *Bacillus subtilis* lipase for detergent formulation. **International Journal of Biological Macromolecules**, v. 136, p. 66–82, 2019b.

KHOOBI, M.; MOTEVALIZADEH, S. F.; ASADGOL, Z.; FOROOTANFAR, H.; SHAFIEE, A.; FARAMARZI, M. A. Synthesis of functionalized polyethylenimine-grafted mesoporous silica spheres and the effect of side arms on lipase immobilization and application. **Biochemical Engineering Journal**, v. 88, p. 131–141, 2014.

KHOOBI, M.; MOTEVALIZADEH, S. F.; ASADGOL, Z.; FOROOTANFAR, H.; SHAFIEE, A.; FARAMARZI, M. A. Polyethyleneimine-modified superparamagnetic Fe_3O_4 nanoparticles for lipase immobilization: characterization and application. **Materials Chemistry and Physics**, v. 149–150, p. 77–86, 2015.

KHOUNI, I.; LOUHICHI, G.; GHRABI, A.; MOULIN, .P Efficiency of a coagulation/flocculation–membrane filtration hybrid process for the treatment of vegetable oil refinery wastewater for safe reuse and recovery. **Process Safety and Environmental Protection**, v. 135, p. 323–341, 2020.

KIM, H.-M.; LEE, J.; SEO, J.; SEO, J-H. Methylsilicone-functionalized superhydrophobic polyurethane porous membranes as antifouling oil absorbents. **Colloids and Surfaces A: Physicochemical and Engineering Aspects**, v. 572, p. 47–57, 2019.

KIM, J.-H.; CHOI, D.-C.; YEON, K.-M.; KIM, S.-R.; LEE, C.-H. Enzyme-immobilized nanofiltration membrane to mitigate biofouling based on quorum quenching. **Environmental Science & Technology**, v. 45, n. 4, p. 1601–1607, 2011.

KIM, T. H.; LEE, I.; YEON, K.-M.; KIM, J. Biocatalytic membrane with acylase stabilized on intact carbon nanotubes for effective antifouling via quorum quenching. **Journal of Membrane Science**, v. 554, p. 357–365, 2018.

KIM, T. S.; NAM, J.; KIM, D. W.; JUNG, H.-T.; YEON, K.-M.; KIM, J. Antifouling membranes employing a 2D planar nanobiocatalyst of crosslinked glucose oxidase aggregates wrapping extra-large graphene oxide. **Chemical Engineering Journal**, v. 424, p. 130343, 2021.

KISO TO RINSHO. **Clinical report**. Tokyo, Japan: Kindai Igakusha, v. 8, p. 2311, 1974.

KLIBANOV, A. M. Enzyme stabilization by immobilization. **Analytical Biochemistry**, v. 94, p. 1-25, 1979.

KOLESNYK, I.; KONOVALOVA, V.; KHARCHENKO, K.; BURBAN, A.; KNOZOWSKA, K.; KUJAWSKI, W.; KUJAWA, J. Improved antifouling properties of polyethersulfone membranes modified with α-amylase entrapped in Tetronic® micelles. **Journal of Membrane Science**, v. 570–571, p. 436–444, 2019.

KOLESNYK, I.; KONOVALOVA, V.; KHARCHENKO, K.; BURBAN, A.; KUJAWA, J.; KUJAWSKI, W. Enhanced transport and antifouling properties of polyethersulfone membranes modified with α-amylase incorporated in chitosan-based polymeric micelles. **Journal of Membrane Science**, v. 595, p. 117605, 2020.

KONG, J.; YU, S. Fourier transform infrared spectroscopic analysis of protein secondary structures. **Acta Biochimica Et Biophysica Sinica**, v. 39, n. 8, p. 549–559, 2007.

KOSEOGLU-IMER, D. Y.; DIZGE, N.; KOYUNCU, I. Enzymatic activation of cellulose acetate membrane for reducing of protein fouling. **Colloids and Surfaces B: Biointerfaces**, v. 92, p. 334–339, 2012.

KUJAWA, J.; GLODEK, M.; KOTER, I.; OSMIALOWSKI, B.; KNOZOWSKA, K.; AL-GHARABLI, S.; DUMÉE, L. F.; KUJAWSKI, W. Molecular decoration of ceramic supports for highly effective enzyme immobilization: material approach. **Materials**, v. 14, n. 1, p. 201, 2021.

KUMAR, A.; PARK, G. D.; PATEL, S. K. S.; KONDAVEETI, S.; OTARI, S.; ANWAR, M. Z.; KALIA, V. C.; SINGH, Y.; KIM, S. C.; CHO, B-K.; SOHN, J-H.; KIM, D. R.; KANG, Y. C.; LEE, J-K. SiO_2 microparticles with carbon nanotube-derived mesopores as an efficient support for enzyme immobilization. **Chemical Engineering Journal**, v. 359, p. 1252–1264, 2019.

KUMAR, R. V.; GHOSHAL, A. K.; PUGAZHENTHI, G. Elaboration of novel tubular ceramic membrane from inexpensive raw materials by extrusion method and its performance in microfiltration of synthetic oily wastewater treatment. **Journal of Membrane Science**, v. 490, p. 92–102, 2015.

LAN, Y.; HIEBNER, D. W.; CASEY, E. Self-assembly and regeneration strategy for mitigation of membrane biofouling by the exploitation of enzymatic nanoparticles. **Chemical Engineering Journal**, v. 412, p. 128666, 2021.

LEE, J.; WON, Y.-J.; CHOI, D.-C.; LEE, S.; PARK, P.-K.; CHOO, K.-H.; OH, H.-S.; LEE, C.-H. Micro-patterned membranes with enzymatic quorum quenching activity to control biofouling in an MBR for wastewater treatment. **Journal of Membrane Science**, v. 592, p. 117365, 2019a.

LEE, W. J.; GOH, P. S.; LAU, W. J.; ONG, C. S.; ISMAIL; A. F. Antifouling zwitterion embedded forward osmosis thin film composite membrane for highly concentrated oily wastewater treatment. **Separation and Purification Technology**, v. 214, p. 40–50, 2019b.

LEWIS, R. J. **Sax's dangerous properties of industrial materials**. 11. ed. Wiley & Sons, 2004.

LI, F.; MENG, J.; YE, J.; YANG, B.; TIAN, Q.; DENG, C. Surface modification of PES ultrafiltration membrane by polydopamine coating and poly(ethylene glycol) grafting: morphology, stability, and anti-fouling. **Desalination**, v. 344, p. 422–430, 2014.

LI, X.; SHAN, H.; CAO, M.; LI, B. Mussel-inspired modification of PTFE membranes in a miscible THF-Tris buffer mixture for oil-in-water emulsions separation. **Journal of Membrane Science**, v. 555, p. 237–249, 2018.

LI, Y.; WANG, H.; LU, J.; CHU, A.; ZHANG, L.; DING, Z.; XU, S.; GU, Z.; SHI, G. Preparation of immobilized lipase by modified polyacrylonitrile hollow membrane using nitrile-click chemistry. **Bioresource Technology**, v. 274, p. 9–17, 2019.

LIN, J. C.-T.; LEE, D.-J.; HUANG, C. Membrane fouling mitigation: membrane cleaning. **Separation Science and Technology**, v. 45, n. 7, p. 858–872, 2010.

LIN, Y.-M.; RUTLEDGE, G. C. Separation of oil-in-water emulsions stabilized by different types of surfactants using electrospun fiber membranes. **Journal of Membrane Science**, v. 563, p. 247–258, 2018.

LIU, D.-M.; CHEN, J.; SHI, Y.-P. Advances on methods and easy separated support materials for enzymes immobilization. **TrAC Trends in Analytical Chemistry**, v. 102, p. 332–342, 2018.

LIU, L.; LUO, X.-B.; DING, L.; LUO, S.-L.; LUO, X.; DENG, F. Application of nanotechnology in the removal of heavy metal from water. *In*: LUO, X.; DENG, F. **Nanomaterials for the Removal of Pollutants and Resource Reutilization**. Micro and Nano Technologies. Elsevier, 2019. p. 83–147.

LIU, W.; CAI, M.; HE, Y.; WANG, S.; ZHENG, J.; XU, X. Development of antibacterial polyacrylonitrile membrane modified with a covalently immobilized lysozyme. **RSC Advances**, v. 5, n. 103, p. 84432–84438, 2015.

LUO, H.; GU, C.; ZHENG, W.; DAI, F.; WANG, X.; ZHENG, Z. Facile synthesis of novel size-controlled antibacterial hybrid spheres using silver nanoparticles loaded with poly-dopamine spheres. **RSC Advances**, v. 5, n. 18, p. 13470–13477, 2015.

LUO, J.; MEYER, A. S.; MATEIU, R. V.; KALYANI, D.; PINELO, M. Functionalization of a membrane sublayer using reverse filtration of enzymes and dopamine coating. **ACS Applied Materials & Interfaces**, v. 6, n. 24, p. 22894–22904, 2014.

LYU, J.; LI, Z.; MEN, J.; JIANG, R.; TANG, G.; ZHOU, Y.; GAO, R. Covalent immobilization of *Bacillus subtilis* lipase A on Fe_3O_4 nanoparticles by aldehyde tag: an ideal immobilization with minimal chemical modification. **Process Biochemistry**, v. 81, p. 63–69, 2019.

MAARTENS, A.; SWART, P.; JACOBS, E. P. An enzymatic approach to the cleaning of ultrafiltration membranes fouled in abattoir effluent. **Journal of Membrane Science**, v. 119, n. 1, p. 9–16, 1996.

MACHADO, N. B.; MIGUEZ, J. P.; BOLINA, I. C. A.; SALVIANO, A. B.; GOMES, R. A. B.; TAVANO, O. L.; LUIZ, J. H. H.; TARDIOLI, P. W.; CREN, É. C.; MENDES, A. A. Preparation, functionalization and characterization of rice husk silica for lipase immobilization via adsorption. **Enzyme and Microbial Technology**, v. 128, p. 9–21, 2019.

MAHLICLI, F. Y.; ALTINKAYA, S. A. The effects of urease immobilization on the transport characteristics and protein adsorption capacity of cellulose acetate based hemodialysis membranes. **Journal of Materials Science: Materials in Medicine**, v. 20, n. 10, p. 2167–2179, 2009.

MARPANI, F.; LUO, J.; MATEIU, R. V.; MEYER, A. S.; PINELO, M. In situ formation of a biocatalytic alginate membrane by enhanced concentration polarization. **ACS Applied Materials & Interfaces**, v. 7, n. 32, p. 17682–17691, 2015.

MARQUES, I. R.; ZIN, G.; PRANDO, L. T.; BRETANHA, C. C.; PRONER, M. C.; RIGO, E.; REZZADORI, K.; DA COSTA, C.; DI LUCCIO, M. Deposition of dopamine and polyethyleneimine on polymeric membranes: improvement of performance of ultrafiltration process. **Macromolecular Research**, v. 28, n. 12, p. 1091–1097, 2020.

MARTÍNEZ-SANCHEZ, J. A.; ARANA-PEÑA, S.; CARBALLARES, D.; YATES, M.; OTERO, C.; FERNANDEZ-LAFUENTE, R. Immobilized biocatalysts of Eversa® Transform 2.0 and lipase from *Thermomyces lanuginosus*: comparison of some properties and performance in biodiesel production. **Catalysts**, v. 10, n. 7, p. 738, 2020.

MASOUDNIA, K.; RAISI, A.; AROUJALIAN, A.; FATHIZADEH, M. A hybrid microfiltration/ultrafiltration membrane process for treatment of oily wastewater. **Desalination and Water Treatment**, v. 55, n. 4, p. 901–912, 2015.

MAVUKKANDY, M. O.; IBRAHIM, Y.; ALMARZOOQI, F.; NADDEO, V.; KARANIKOLOS, G. N.; ALHSEINAT, E.; BANAT, F.; HASAN, S. W. Synthesis of polydopamine coated tungsten oxide@poly(vinylidene fluoride-co-hexafluoropropylene) electrospun nanofibers as multifunctional membranes for water applications. **Chemical Engineering Journal**, v. 427, p. 131021, 2022.

MEHRABI, Z.; TAHERI-KAFRANI, A.; ASADNIA, M.; RAZMJOU, A. Bienzymatic modification of polymeric membranes to mitigate biofouling. **Separation and Purification Technology**, v. 237, p. 116464, 2020.

MESHRAM, P.; DAVE, R.; JOSHI, H.; DHARANI, G.; KIRUBAGARAN, R.; VENUGOPALAN, V. P. A fence that eats the weed: alginate lyase immobilization on ultrafiltration membrane for fouling mitigation and flux recovery. **Chemosphere**, v. 165, p. 144–151, 2016.

MIAO, C.; YANG, L.; WANG, Z.; LUO, W.; LI, H.; LV, P.; YUAN, Z. Lipase immobilization on amino-silane modified superparamagnetic Fe_3O_4 nanoparticles as biocatalyst for biodiesel production. **Fuel**, v. 224, p. 774–782, 2018.

MOHAMAD, N. R.; MARZUKI, N. H. C.; BUANG, N. A.; HUYOP, F.; WAHAB, R. A. An overview of technologies for immobilization of enzymes and surface analysis techniques for immobilized enzymes. **Biotechnology & Biotechnological Equipment**, v. 29, n. 2, p. 205–220, 2015a.

MORTHENSEN, S. T.; MEYER, A. S.; JORGENSEN, H.; PINELO, M. Significance of membrane bioreactor design on the biocatalytic performance of glucose oxidase and catalase: Free vs. immobilized enzyme systems. **Biochemical Engineering Journal**, v. 117, p. 41–47, 2017.

MULDER, M. **Basic principles of membrane technology**. 2. ed. Netherlands: Kluwer Academic Publishers, 2000.

MULINARI, J.; VENTURIN, B.; SBARDELOTTO, M.; DALL AGNOL, A.; SCAPINI, T.; CAMARGO, A. F.; BALDISSARELLI, D. P.; MODKOVSKI, T. A.; ROSSETTO, V.; DALLA ROSA, C.; REICHERT JR.; F. W.; GOLUNSKI, S. M.; VIEITEZ, I.; VARGAS, G. D. L. P.; DALLA ROSA, C.; MOSSI, A. J.; TREICHEL, H. Ultrasound-assisted hydrolysis of waste cooking oil catalyzed by homemade lipases. **Ultrasonics Sonochemistry**, v. 35, p. 313–318, 2017.

MULINARI, J.; AMBROSI, A.; INNOCENTINI, M. D. M.; FENG, Y.; LI, Q.; DI LUCCIO, M.; HOTZA, D.; OLIVEIRA, J. V. Lipase immobilization on alumina membranes using a traditional and a nature-inspired method for active degradation of oil fouling. **Separation and Purification Technology**, v. 287, p. 120527, 2022.

MUÑOZ-AGUADO, M. J.; WILEY, D. E.; FANE, A. G. Enzymatic and detergent cleaning of a polysulfone ultrafiltration membrane fouled with BSA and whey. **Journal of Membrane Science**, v. 117, n. 1, p. 175–187, 1996.

NADJAFI, M.; REYHANI, A.; AL ARNI, S. Feasibility of treatment of refinery wastewater by a pilot scale MF/UF and UF/RO system for reuse at boilers and cooling towers. **Journal of Water Chemistry and Technology**, v. 40, n. 3, p. 167–176, 2018.

NAKASHIMA, H.; OMAE, K.; TAKEBAYASHI, T.; ISHIZUKA, C.; UEMURA, T. Toxicity of silicon compounds in semiconductor industries. **Journal of Occupational Health**, v. 40, n. 4, p. 270–275, 1998.

NAVARRO-PARDO, F.; MARTÍNEZ-BARRERA, G.; MARTÍNEZ-HERNÁNDEZ, A. L.; CASTANO, V. M.; RIVERA-ARMENTA, J. L.; MEDELLÍN-RODRÍGUEZ, F.; VELASCO-SANTOS, C. Effects on the thermo-mechanical and crystallinity properties of nylon 6,6 electrospun fibres reinforced with one dimensional (1D) and two dimensional (2D) carbon. **Materials**, v. 6, n. 8, p. 3494–3513, 2013.

NG, F. S. W.; WRIGHT, D. M.; SEAH, S. Y. K. Characterization of a phosphotriesterase-like lactonase from *Sulfolobus solfataricus* and its immobilization for disruption of quorum sensing. **Applied and Environmental Microbiology**, v. 77, n. 4, p. 1181–1186, 2011.

NISHIHORA, R. K.; QUADRI, M. G. N.; HOTZA, D.; REZWAN, K.; WILHELM, M. Tape casting of polysiloxane-derived ceramic with controlled porosity and surface properties. **Journal of the European Ceramic Society**, v. 38, n. 15, p. 4899–4905, 2018.

PADAKI, M.; MURALI, R. S.; ABDULLAH, M. S.; MISDAN, N.; MOSLEHYANI, A.; KASSIM, M. A.; HILAL, N.; ISMAIL, A. F. Membrane technology enhancement in oil–water separation: a review. **Desalination**, v. 357, p. 197–207, 2015.

PÄIVIÖ, M.; PERKIÖ, P.; KANERVA, L. T. Solvent-free kinetic resolution of primary amines catalyzed by *Candida antarctica* lipase B: effect of immobilization and recycling stability. **Tetrahedron: Asymmetry**, v. 23, n. 3, p. 230–236, 2012.

PAN, Y.; WANG, W.; WANG, T.; YAO, P. Fabrication of carbon membrane and microfiltration of oil-in-water emulsion: an investigation on fouling mechanisms. **Separation and Purification Technology**, v. 57, n. 2, p. 388–393, 2007.

PENG, Y.; GUO, F.; WEN, Q.; YANG, F.; GUO, Z. A. novel polyacrylonitrile membrane with a high flux for emulsified oil/water separation. **Separation and Purification Technology**, v. 184, p. 72–78, 2017.

PEREIRA, A. S.; FONTES-SANT'ANA, G. C.; AMARAL, P. F. F. Mango agro-industrial wastes for lipase production from *Yarrowia lipolytica* and the potential of the fermented solid as a biocatalyst. **Food and Bioproducts Processing**, v. 115, p. 68–77, 2019.

PERSSON, X.-M. T.; BŁACHNIO-ZABIELSKA, A. U.; JENSEN, M. D. Rapid measurement of plasma free fatty acid concentration and isotopic enrichment using LC/MS. **Journal of Lipid Research**, v. 51, n. 9, p. 2761–2765, 2010.

PINTOR, A. M. A.; VILAR, V. J. P.; BOTELHO, C. M. S.; BOAVENTURA, R. A. R. Oil and grease removal from wastewaters: sorption treatment as an alternative to

state-of-the-art technologies. A critical review. **Chemical Engineering Journal**, v. 297, p. 229–255, 2016.

PORNEA, A. M.; PUGUAN, J. M. C.; DEONIKAR, V. G.; KIM, H. Robust Janus nanocomposite membrane with opposing surface wettability for selective oil-water separation. **Separation and Purification Technology**, v. 236, p. 116297, 2020.

PRENZEL, T.; DOGE, K.; MOTTA, R. P. O.; WILHELM, M.; REZWAN, K. Controlled hierarchical porosity of hybrid ceramics by leaching water soluble templates and pyrolysis. **Journal of the European Ceramic Society**, v. 34, n. 6, p. 1501–1509, 2014.

PRONER, M. C.; MARQUES, I. R.; AMBROSI, A.; REZZADORI, K.; COSTA, C.; ZIN, G.; TRES, M. V.; DI LUCCIO, M. Impact of MWCO and dopamine/polyethyleneimine concentrations on surface properties and filtration performance of modified membranes. **Membranes**, v. 10, n. 9, p. 239, 2020.

QADIR, D.; MUKHTAR, H.; KEONG, L. K. Mixed matrix membranes for water purification applications. **Separation & Purification Reviews**, v. 46, n. 1, p. 62–80, 2017.

RANIERI, G.; MAZZEI, R.; WU, Z.; LI, K.; GIORNO, L. Use of a ceramic membrane to improve the performance of two-separate-phase biocatalytic membrane reactor. **Molecules**, v. 21, n. 3, 2016.

RASOULI, H.; ILIUTA, I.; BOUGIE, F.; GARNIER, A.; ILIUTA, M. C. Enzyme-immobilized flat-sheet membrane contactor for green carbon capture. **Chemical Engineering Journal**, v. 421, p. 129587, 2021.

REN, Y.; RIVERA, J. G.; HE, L.; KULKARNI, H.; LEE, D-K.; MESSERSMITH, P. B. Facile, high efficiency immobilization of lipase enzyme on magnetic iron oxide nanoparticles via a biomimetic coating. **BMC Biotechnology**, v. 11, n. 1, p. 63, 2011.

RODRIGUEZ-ABETXUKO, A.; SÁNCHEZ-DEALCÁZAR, D.; MUNUMER, P.; BELOQUI, A. Tunable polymeric scaffolds for enzyme immobilization. **Frontiers in Bioengineering and Biotechnology**, 2020.

SAEKI, D.; NAGAO, S.; SAWADA, I.; OHMUKAI, Y.; MARUYAMA, T.; MATSUYAMA, H. Development of antibacterial polyamide reverse osmosis membrane modified with a covalently immobilized enzyme. **Journal of Membrane Science**, v. 428, p. 403–409, 2013.

SANTIN, C. M. T.; MICHELIN, S.; SCHERER, R. P.; VALÉRIO, A.; DI LUCCIO, M.; OLIVEIRA, D.; OLIVEIRA, J. V. Comparison of macauba and soybean oils as substrates for the enzymatic biodiesel production in ultrasound-assisted system. **Ultrasonics Sonochemistry**, v. 35, p. 525–528, 2017.

SANTOS, J. J.; MARANHO, L. T. Rhizospheric microorganisms as a solution for the recovery of soils contaminated by petroleum: a review. **Journal of Environmental Management**, v. 210, p. 104–113, 2018.

SATYAWALI, Y.; VANBROEKHOVEN, K.; DEJONGHE, W. Process intensification: the future for enzymatic processes? **Biochemical Engineering Journal**, v. 121, p. 196-223, 2017.
SCHICK, D.; LINK, K.; SCHWACK, W.; GRANVOGL, M.; OELLIG, C. Analysis of mono-, di-, triacylglycerols, and fatty acids in food emulsifiers by high-performance liquid chromatography–mass spectrometry. **European Food Research and Technology**, v. 247, n. 4, p. 1023–1034, 2021.

SCHMIDT, M.; BREITE, D.; THOMAS, I.; WENT, M.; PRAGER, A.; SCHULZE, A. Polymer membranes for active degradation of complex fouling mixtures. **Journal of Membrane Science**, v. 563, p. 481–491, 2018.

SCHMIDT, M.; PRAGER, A.; SCHONHERR, N.; GLASER, R.; SCHULZE, A. Reagent-free immobilization of industrial lipases to develop lipolytic membranes with self-cleaning surfaces. **Membranes**, v. 12, n. 6, p. 599, 2022.

SCHNABEL, R.; VAULONT, W. High-pressure techniques with porous glass membranes. **Desalination**, v. 24, n. 1, p. 249–272, 1977.

SCHULZE, A.; STOELZER, A.; STRIEGLER, K.; STARKE, S.; PRAGER, A. Biocatalytic self-cleaning polymer membranes. **Polymers**, v. 7, n. 9, p. 1837–1849, 2015.

SCHULZE, A.; BREITE, D.; KIM, Y.; SCHMIDT, M.; THOMAS, I.; WENT, M.; FISCHER, K.; PRAGER, A. Bio-inspired polymer membrane surface cleaning. **Polymers**, v. 9, n. 12, p. 97, 2017.

ŠEREŠ, Z.; MARAVIC, N.; TAKACI, A.; NIKOLIC, I.; SORONJA-SIMOVIC, D.; JOKIC, A.; HODUR, C. Treatment of vegetable oil refinery wastewater using alumina ceramic membrane: optimization using response surface methodology. **Journal of Cleaner Production**, v. 112, p. 3132–3137, 2016.

SHAH, P.; SRIDEVI, N.; PRABHUNE, A.; RAMASWAMY, V. Structural features of penicillin acylase adsorption on APTES functionalized SBA-15. **Microporous and Mesoporous Materials**, v. 116, n. 1, p. 157–165, 2008.

SHAHKARAMIPOUR, N.; TRAN, T. N.; RAMANAN, S.; LIN, H. Membranes with surface-enhanced antifouling properties for water purification. **Membranes**, v. 7, n. 1, 2017.

SHELDON, R. A.; VAN PELT, S. Enzyme immobilisation in biocatalysis: why, what and how. **Chemical Society Reviews**, v. 42, n. 15, p. 6223–6235, 2013.

SHI, Q.; SU, Y.; NING, X.; CHEN, W.; PENG, J.; JIANG, Z. Trypsin-enabled construction of anti-fouling and self-cleaning polyethersulfone membrane. **Bioresource Technology**, v. 102, n. 2, p. 647–651, 2011.

SIGURDARDÓTTIR, S. B.; LEHMANN, J.; OVTAR, S.; GRIVEL, J-C.; DELLA NEGRA, M.; KAISER, A.; PINELO, M. Enzyme immobilization on inorganic surfaces for membrane reactor applications: mass transfer challenges, enzyme leakage and reuse of materials. **Advanced Synthesis & Catalysis**, v. 360, p. 2578–2607, 2018.

SMYTH, H. F.; CARPENTER, C. P.; WELL, C. S.; POZZANI, U. C.; STRIEGEL, J. A. Range-finding toxicity data: list VI. **American Industrial Hygiene Association Journal**, v. 23, n. 2, p. 95–107, 1962.

SULAIMAN, S.; MOKHTAR, M. N.; NOR, M. Z. M.; YUNOS, K. D. M.; NAIM, M. N. Mass transfer with reaction kinetics of the biocatalytic membrane reactor using a fouled covalently immobilised enzyme layer (α–CGTase–CNF layer). **Biochemical Engineering Journal**, v. 152, p. 107374, 2019.

SUN, J.; YENDLURI, R.; LIU, K.; GUO, Y.; LVOV, Y.; YAN, X. Enzyme-immobilized clay nanotube–chitosan membranes with sustainable biocatalytic activities. **Physical Chemistry Chemical Physics**, v. 19, n. 1, p. 562–567, 2016.

SZANIAWSKI, A. R.; SPENCER, H. G. Effects of pectin concentration and crossflow velocity on permeability in the microfiltration of dilute pectin solutions by macroporous titania membranes containing immobilized pectinase. **Biotechnology Progress**, v. 12, n. 3, p. 403–405, 1996.

SZANIAWSKI, A. R.; SPENCER, H. G. Effects of immobilized pectinase on the microfiltration of dilute pectin solutions by macroporous titania membranes: resistance model interpretation. **Journal of Membrane Science**, v. 127, n. 1, p. 69–76, 1997.

TAKIGAWA, T.; ENDO, Y. Effects of glutaraldehyde exposure on human health. **Journal of Occupational Health**, v. 48, n. 2, p. 75–87, 2006.

TANUDJAJA, H. J.; HEJASE, C. A.; TARABARA, V. V.; FANE, A. G.; CHEW, J. W. Membrane-based separation for oily wastewater: A practical perspective. **Water Research**, v. 156, p. 347–365, 2019.

TENG, R.; MENG, Y.; ZHAO, X.; LIU, J.; DING, R.; CHENG, Y.; ZHANG, Y.; ZHANG, Y.; PEI, D.; LI, A. Combination of polydopamine coating and plasma pretreatment to improve bond ability between PEEK and primary teeth. **Frontiers in Bioengineering and Biotechnology**, v. 8, p. 1557, 2021.

THANGARAJ, B.; JIA, Z.; DAI, L.; LIU, D.; DU, W. Effect of silica coating on Fe_3O_4 magnetic nanoparticles for lipase immobilization and their application for biodiesel production. **Arabian Journal of Chemistry**, v. 12, n. 8, p. 4694–4706, 2019.

THOMAS, R. L.; MCKAMY, D. L.; SPENCER, H. G. Applications of immobilized enzymes on formed-in-place membranes in food processing. *In*: CHEMICAL CONGRESS OF NORTH AMERICAN CONTINENT AND SYMPOSIUM ADVANCES IN REVERSE OSMOSIS AND ULTRAFILTRATION, 3., 1989, Toronto. **Anais**… Toronto: Advances in reverse osmosis and ultrafiltration: proceedings of the Symposium on Advances in Reverse Osmosis and Ultrafiltration, 1989.

TOUQEER, T.; MUMTAZ, M. W.; MUKHTAR, H.; IRFAN, A.; AKRAM, S.; SHABBIR, A.; RASHID, U.; NEHDI, I. A.; CHOONG, T. S. Y. Fe_3O_4-PDA-lipase as surface functionalized nano biocatalyst for the production of biodiesel using waste cooking oil as feedstock: characterization and process optimization. **Energies**, v. 13, n. 1, p. 177, 2019.

TREICHEL, H.; SBARDELOTTO, M.; VENTURIN, B.; DALL AGNOL, A.; MULINARI, J.; GOLUNSKI, S. M.; BALDONI, D. B.; BEVILACQUA, C. B.; JACQUES, R. J. S.; VARGAS, G. D. L. P.; MOSSI, A. J. Lipase production from a newly isolated *Aspergillus niger* by solid state fermentation using canola cake as substrate. **Current Biotechnology**, v. 5, n. 4, p. 295–300, 2016.

VAN BIRGELEN, A. P. J. M.; CHOU, B. J.; RENNE, R. A.; GRUMBEIN, S. L.; ROYCROFT, J. H.; HAILEY, J. R.; BUCHER, J. R. Effects of glutaraldehyde in a 2-year inhalation study in rats and Mmice. **Toxicological Sciences**, v. 55, n. 1, p. 195–205, 2000.

VANANGAMUDI, A.; SAEKI, D.; DUMÉE, L. F.; DUKE, M.; VASILJEVIC, T.; MATSUYAMA, H.; YANG, X. Surface-engineered biocatalytic composite membranes for reduced protein fouling and self-cleaning. **ACS Applied Materials & Interfaces**, v. 10, n. 32, p. 27477–27487, 2018a.

VANANGAMUDI, A.; DUMÉE, L. F.; DUKE, M. C.; YANG, X. Dual functional ultrafiltration membranes with enzymatic digestion and thermo-responsivity for protein self-cleaning. **Membranes**, v. 8, n. 3, p. 85, 2018b.

VASCONCELOS, N. F.; ANDRADE, F. K.; VIEIRA, L. A. P.; VIEIRA, R. S.; VAZ, J. M.; CHEVALLIER, P.; MANTOVANI, D.; BORGES, M. F.; ROSA, M. F. Oxidized bacterial cellulose membrane as support for enzyme immobilization: properties and morphological features. **Cellulose**, v. 27, n. 6, p. 3055–3083, 2020.

VELICANGIL, O.; HOWELL, J. A. Protease-coupled membranes for ultrafiltration. **Biotechnology and Bioengineering**, v. 19, n. 12, p. 1891–1894, 1977.

VELICANGIL, O.; HOWELL, J. A. Self-cleaning membranes for ultrafiltration. **Biotechnology and Bioengineering**, v. 23, n. 4, p. 843–854, 1981.

VESCOVI, V.; KOPP, W.; GUISÁN, J. M.; GIORDANO, R. L. C.; MENDES, A. A.; TARDIOLI, P. W. Improved catalytic properties of *Candida antarctica* lipase B multi-attached on tailor-made hydrophobic silica containing octyl and multifunctional amino- glutaraldehyde spacer arms. **Process Biochemistry**, v. 51, n. 12, p. 2055–2066, 2016.

VILA-COSTA, M.; GIOIA, R.; ACEÑA, J.; PÉREZ, S.; CASAMAYOR, E. O.; DACHS, J. Degradation of sulfonamides as a microbial resistance mechanism. **Water Research**, v. 115, p. 309–317, 2017.

VILLA, F.; SECUNDO, F.; POLO, A.; CAPPITELLI, F. Immobilized hydrolytic enzymes exhibit antibiofilm activity against *Escherichia coli* at sub-lethal concentrations. **Current Microbiology**, v. 71, n. 1, p. 106–114, 2015.

WALLACE, T.; GIBBONS, D.; O'DWYER, M.; CURRAN, T. P. International evolution of fat, oil and grease (FOG) waste management: a review. **Journal of Environmental Management**, v. 187, p. 424–435, 2017.

WANCURA, J. H. C.; ROSSET, D. V.; MAZUTTI, M. A.; UGALDE, G. A.; OLIVEIRA, J. V.; TRES, M. V.; JAHN, S. L. Improving the soluble lipase–catalyzed biodiesel

production through a two-step hydroesterification reaction system. **Applied Microbiology and Biotechnology**, v. 103, n. 18, p. 7805–7817, 2019.

WANG, C.; LI, Z.; CHEN, J.; YIN, Y.; WU, H. Structurally stable graphene oxide-based nanofiltration membranes with bioadhesive polydopamine coating. **Applied Surface Science**, v. 427, p. 1092–1098, 2018a.

WANG, C.; WANG, Z.; WEI, X.; LI, X. A numerical study and flotation experiments of bicyclone column flotation for treating of produced water from ASP flooding. **Journal of Water Process Engineering**, v. 32, p. 100972, 2019a.

WANG, H. J.; THOMAS, R. L.; SZANIAWSKI, A. R.; SPENCER, H. G. Enzymes immobilized on formed-in-place membranes for food processing: procedures and properties. **Journal of Food Process Engineering**, v. 17, n. 4, p. 365–381, 1994.

WANG, L.-S.; XU, S.; GOPAL, S.; KIM, E.; KIM, D.; BRIER, M.; SOLANKI, K.; DORDICK, J. S. Facile fabrication of antibacterial and antiviral perhydrolase-polydopamine composite coatings. **Scientific Reports**, v. 11, n. 1, p. 12410, 2021.

WANG, S. S.; DAVIDSON, B.; GILLESPIE, C.; HARRIS, L. R.; LENT, D S. Dynamics of enhanced protein ultrafiltration using an immobilized protease. **Journal of Food Science**, v. 45, n. 3, p. 700–702, 1980.

WANG, W.; HAN, X.; YI, H.; ZHANG, L.-W. The ultrafiltration efficiency and mechanism of transglutaminase enzymatic membrane reactor (EMR) for protein recovery from cheese whey. **International Dairy Journal**, v. 80, p. 52–61, 2018b.

WANG, W.; LIN, J.; CHENG, J.; CUI, Z.; SI, J.; WANG, Q.; PENG, X.; TURNG, L-S. Dual super-amphiphilic modified cellulose acetate nanofiber membranes with highly efficient oil/water separation and excellent antifouling properties. **Journal of Hazardous Materials**, v. 385, p. 121582, 2020.

WANG, Z.; JIANG, X.; CHENG, X.; LAU, C. H.; SHAO, L. Mussel-inspired hybrid coatings that transform membrane hydrophobicity into high hydrophilicity and underwater superoleophobicity for oil-in-water emulsion separation. **ACS Applied Materials & Interfaces**, v. 7, n. 18, p. 9534–9545, 2015.

WANG, Z.; JIN, J.; HOU, D.; LIN, S. Tailoring surface charge and wetting property for robust oil-fouling mitigation in membrane distillation. **Journal of Membrane Science**, v. 516, p. 113–122, 2016.

WANG, Z.; YANG, H-C.; HE, F.; PENG, S.; LI, Y.; SHAO, L.; DARLING, S. B. Mussel-inspired surface engineering for water-remediation materials. **Matter**, v. 1, n. 1, p. 115–155, 2019b.

WESCHENFELDER, S. E.; BORGES, C. P.; CAMPOS, J. C. Oilfield produced water treatment by ceramic membranes: bench and pilot scale evaluation. **Journal of Membrane Science**, v. 495, p. 242–251, 2015.

WONG, P. C. Y.; LEE, J. Y.; TEO, C. W. Application of dispersed and immobilized hydrolases for membrane fouling mitigation in anaerobic membrane bioreactors. **Journal of Membrane Science**, v. 491, p. 99–109, 2015.

XIANG, Y.; LIU, F.; XUE, L. Under seawater superoleophobic PVDF membrane inspired by polydopamine for efficient oil/seawater separation. **Journal of Membrane Science**, v. 476, p. 321–329, 2015.

XIE, H.; CHEN, B.; LIN, H.; LI, R.; SHEN, L.; YU, G.; YANG, L. Efficient oil-water emulsion treatment via novel composite membranes fabricated by $CaCO_3$-based biomineralization and TA-Ti(IV) coating strategy. **Science of The Total Environment**, v. 857, p. 159183, 2023.

XIE, S.; GUO, L.; ZHANG, M.; QIN, J.; HU, R. Durable hydrophobic ceramics of Al_2O_3–ZrO_2 modified by hydrophilic silane with high oil/water separation efficiency. **Journal of Porous Materials**, 2021.

YAN, Z.; ZHANG, Y.; YANG, H.; FAN, G.; DING, A.; LIANG, H.; LI, G.; REN, N.; VAN DER BRUGGEN, B. Mussel-inspired polydopamine modification of polymeric membranes for the application of water and wastewater treatment: a review. **Chemical Engineering Research and Design**, v. 157, p. 195–214, 2020.

YANG, H.-C.; PI, J-K.; LIAO, K-J.; HUANG, H.; WU, Q-Y.; HUANG, X-J.; XU, Z-K. Silica-decorated polypropylene microfiltration membranes with a mussel-inspired intermediate layer for oil-in-water emulsion separation. **ACS Applied Materials & Interfaces**, v. 6, n. 15, p. 12566–12572, 2014.

YANG, J.; MA, X.; ZHANG, Z.; CHEN, B.; LI, S.; WANG, G. Lipase immobilized by modification-coupled and adsorption–cross-linking methods: a comparative study. **Biotechnology Advances**, v. 28, n. 5, p. 644–650, 2010.

YANG, J.; WANG, L.; XIE, A.; DAI, X.; YAN, Y.; DAI, J. Facile surface coating of metal-tannin complex onto PVDF membrane with underwater superoleophobicity for oil-water emulsion separation. **Surface and Coatings Technology**, v. 389, p. 125630, 2020.

YANG, X.; DUAN, L.; RAN, X. Effect of polydopamine coating on improving photostability of polyphenylene sulfide fiber. **Polymer Bulletin**, v. 74, n. 3, p. 641–656, 2017.

YANG, Y.; WANG, H.; LI, J.; HE, B.; WANG, T.; LIAO, S. Novel functionalized nano-TiO_2 loading electrocatalytic membrane for oily wastewater treatment. **Environmental Science and Technology**, v. 46, p. 6815-6821, 2012.

YAO, S.; FANE, A. G.; POPE, J. M. An investigation of the fluidity of concentration polarisation layers in crossflow membrane filtration of an oil-water emulsion using chemical shift selective flow imaging. **Magnetic Resonance Imaging**, v. 15, n. 2, p. 235–242, 1997.

YEROSLAVSKY, G.; RICHMAN, M.; DAWIDOWICZ, L.; RAHIMIPOUR, S. Sonochemically produced polydopamine nanocapsules with selective antimicrobial activity. **Chemical Communications**, v. 49, n. 51, p. 5721–5723, 2013.

YI, S.; DAI, F.; ZHAO, C.; SI, Y. A reverse micelle strategy for fabricating magnetic lipase-immobilized nanoparticles with robust enzymatic activity. **Scientific Reports**, v. 7, p. 9806, 2017.

YU, L.; KANEZASHI, M.; NAGASAWA, H.; TSURU, T. Phase inversion/sintering-induced porous ceramic microsheet membranes for high-quality separation of oily wastewater. **Journal of Membrane Science**, v. 595, p. 117477, 2020.

YU, L.; HAN, M.; HE, F. A review of treating oily wastewater. **Arabian Journal of Chemistry**, v. 10, p. S1913–S1922, 2017.

YUJUN, W.; JIAN, X.; GUANGSHENG, L.; YOUYUAN, D. Immobilization of lipase by ultrafiltration and cross-linking onto the polysulfone membrane surface. **Bioresource Technology**, v. 99, n. 7, p. 2299–2303, 2008.

YUREKLI, Y. Layer-by-layer self-assembly of multifunctional enzymatic UF membranes. **Journal of Applied Polymer Science**, v. 137, n. 22, p. 48750, 2020.

ZARE, A.; BORDBAR, A-K.; RAZMJOU, A.; JAFARIAN, F. The immobilization of *Candida rugosa* lipase on the modified polyethersulfone with MOF nanoparticles as an excellent performance bioreactor membrane. **Journal of Biotechnology**, v. 289, p. 55–63, 2019.

ZARGHAMI, S.; MOHAMMADI, T.; SADRZADEH, M. Preparation, characterization and fouling analysis of in-air hydrophilic/underwater oleophobic bio-inspired polydopamine coated PES membranes for oily wastewater treatment. **Journal of Membrane Science**, v. 582, p. 402–413, 2019.

ZDARTA, J.; MEYER, A. S.; JESIONOWSKI, T.; PINELO, M. A general overview of support materials for enzyme immobilization: characteristics, properties, practical utility. **Catalysts**, v. 8, n. 2, p. 92, 2018.

ZHANG, D.; WANG, G.; ZHI, S.; XU, K.; ZHU, L.; LI, W.; ZENG, Z.; XUE, Q. Superhydrophilicity and underwater superoleophobicity TiO_2/Al_2O_3 composite membrane with ultra low oil adhesion for highly efficient oil-in-water emulsions separation. **Applied Surface Science**, v. 458, p. 157–165, 2018a.

ZHANG, D.-H.; YUWEN, L.-X.; PENG, L.-J. Parameters affecting the performance of immobilized enzyme. **Journal of Chemistry**, v. 2013, p. e946248, 2013.

ZHANG, H.; LUO, J.; LI, S.; WEI, Y.; WAN, Y. Biocatalytic membrane based on polydopamine coating: a platform for studying immobilization mechanisms. **Langmuir**, v. 34, n. 8, p. 2585–2594, 2018b.

ZHANG, H.; LUO, J.; LI, S.; WOODLEY, J. M.; WAN, Y. Can graphene oxide improve the performance of biocatalytic membrane? **Chemical Engineering Journal**, v. 359, p. 982–993, 2019.

ZHANG, H.; WAN, Y.; LUO, J.; DARLING, S. B. Drawing on membrane photocatalysis for fouling mitigation. **ACS Applied Materials Interfaces**, v. 13, p. 14844-14865, 2021a.

ZHANG, J.; ZHOU, F.; LI, S.; WAN, Y.; LUO, J. Surface functionalization of nanofiltration membrane by catechol-amine codeposition for enhancing antifouling performance. **Journal of Membrane Science**, v. 635, p. 119451, 2021b.

ZHAO, Q.; LIU, C.; LIU, J.; ZHANG, Y. Development of a novel polyethersulfone ultrafiltration membrane with antibacterial activity and high flux containing halloysite nanotubes loaded with lysozyme. **RSC Advances**, v. 5, n. 48, p. 38646–38653, 2015.

ZHOU, L.; LUO, X.; LI, J.; MA, L.; HE, Y.; JIANG, Y.; YIN, L.; GAO, L. Meso-molding three-dimensionally ordered macroporous alumina: a new platform to immobilize enzymes with high performance. **Biochemical Engineering Journal**, v. 146, p. 60–68, 2019.

ZHOU, R.; REN, P-F.; YANG, H-C.; XU, Z-K. Fabrication of antifouling membrane surface by poly(sulfobetaine methacrylate)/polydopamine co-deposition. **Journal of Membrane Science**, v. 466, p. 18–25, 2014.

ZHU, L.; CHEN, M.; DONG, Y.; TANG, C. Y.; HUANG, A.; LI, L. A low-cost mullite-titania composite ceramic hollow fiber microfiltration membrane for highly efficient separation of oil-in-water emulsion. **Water Research**, v. 90, p. 277–285, 2016.

ZHU, Y.; WANG, D.; JIANG, L.; JIN, J. Recent progress in developing advanced membranes for emulsified oil/water separation. **NPG Asia Materials**, v. 6, n. 5, p. e101–e101, 2014.

ZHU, Y.; CHEN, D. Novel clay-based nanofibrous membranes for effective oil/water emulsion separation. **Ceramics International**, v. 43, n. 12, p. 9465–9471, 2017.

ZHU, Z.; CHEN, Z.; LUO, X.; LIANG, W.; LI, S.; HE, J.; ZHANG, W.; HAO, T.; YANG, Z. Biomimetic dynamic membrane (BDM): fabrication method and roles of carriers and laccase. **Chemosphere**, v. 240, p. 124882, 2020.

ZIN, G.; WU, J.; REZZADORI, K.; PETRUS, J. C. C.; DI LUCCIO, M.; LI, Q. Modification of hydrophobic commercial PVDF microfiltration membranes into superhydrophilic membranes by the mussel-inspired method with dopamine and polyethyleneimine. **Separation and Purification Technology**, v. 212, p. 641–649, 2019.

ZUCCA, P.; SANJUST, E. Inorganic materials as supports for covalent enzyme immobilization: methods and mechanisms. **Molecules (Basel, Switzerland)**, v. 19, n. 9, p. 14139–14194, 2014.

ZUO, J.-H.; CHENG, P.; CHEN, X-F.; YAN, X.; GUO, Y-J.; LANG, W-Z. Ultrahigh flux of polydopamine-coated PVDF membranes quenched in air via thermally induced phase separation for oil/water emulsion separation. **Separation and Purification Technology**, v. 192, p. 348–359, 2018.